Molecular Neurogenetics of Eye Development in *Drosophila*

Thesis by

Patricia Jean Renfranz

In Partial Fulfillment of the Requirements

for the Degree of

Doctor of Philosophy

California Institute of Technology

Pasadena, California

1989

(submitted December 15, 1988)

For my parents

Acknowledgments

Although for many years I thought the time to write these acknowledgments would never arrive, it has now arrived. Firstly, I would like to thank my advisor Seymour Benzer for having me in his lab, for his keen interest and his finely honed wit, and for attempting to teach me how to be a scientist. He has provided me with a lot of room in which to grow, and although I may not always agree with his approach, it has resulted in my becoming more independent. I thank Paul Sternberg for reminding me that thinking about one's work can be fun, and the other members of my committee, David Anderson, Elliot Meyerowitz, and Mel Simon, for their interest and patience. For financial support, I would like to acknowledge the National Institutes of Health, the National Science Foundation, and the Lawrence A. Hanson Foundation, and Charles Brokaw and Nancy Gill, who always seemed to know from where everything was coming.

The Benzer Lab has changed much since the early days when space was plentiful, relatively, time was slow, and Gerald Rubin was but a figment of our imagination. I cannot thank Larry Zipursky enough, for his introducing me to the field of eye development by showing me that lovely picture of a MAb staining pattern on an eye disc, and for his encouragement over the years. There are so many members of the group whose friendship I cherish and who have been more help to me than they could ever imagine; words are inadequate. I list them here briefly, to insure that the memory can always be triggered: T. Venkatesh whose attitudes about life I shall try to remember; Dennis Ballinger for being thoughtful, always eager to help, and generous with his time; John Pollock for his expertise on the *sevenless in situ* hybridizations and darkroom techniques, and also for being a wonderful person; Roger Hackett, who spoke of alternatives and who taught me about Conan the Barbarian; Billy Leiserson for flowers, and him and Erich Schwarz for company, advice, and for falling into holes; and Nancy Bonini for being here at the end.

Utpal Banerjee I thank for everything: for introducing me to *sevenless*, inviting me

to join him, and sharing almost all the duties of cloning a gene. He was my second advisor, as well as my friend, always on the lookout for my interests even when I was not. On the *sevenless* project, I would also like to thank David R. Hinton for collaborating on the EM localization and Bruce Rabin for teaching me how to do Westerns.

Much of this thesis would not have been completed until the next decade without the help of the technicians. In particular, I would like to thank Eveline Eichenberger, who has always been so kind to me, for her diligent care of the fly stocks; Rosalind Young for her excellent EM techniques which we could not have done without, and Marika Anderson, Jenny Mao, Julia Chang, Christine Krause, Frances Aguirre and the others for everything else.

There are also the people who made my life out here a life: Paula Watnick, Tina Kramer, Chi-Bin Chien, and Mani Ramaswami among others. I wish that I had met Melinda Adams long before I did; I can't imagine what these years could have been like with someone like her around. Erika Simon, Anne Godfrey, and John Sidney I thank for their constant support; even when we are out of touch, I know we still think of each other. My sister Peggy I thank for instilling in me a love of the West, and for leading me to Canyon de Chelly and for all the feelings that memory engenders.

Lastly, I would like to thank David Blair, who tried his best to teach me to swim, who took me to the Devil's Punchbowl and back, and without whom this thesis would never have happened. He inspires in me so many feelings, about joy in science and whence it can come, and about life and whither it can go. He reassured me when the winds blew in the desert, went on hunts for the best whatever in the universe, brought me music, and became my best friend.

Abstract

The compound eye of *Drosophila melanogaster* begins to differentiate during the late third larval instar in the eye-antennal imaginal disc. A wave of morphogenesis crosses the disc from posterior to anterior, leaving behind precisely patterned clusters of photoreceptor cells and accessory cells that will constitute the adult ommatidia of the retina. By the analysis of genetically mosaic eyes, it appears that any cell in the eye disc can adopt the characteristics of any one of the different cell types found in the mature eye, including photoreceptor cells and non-neuronal accessory cells such as cone cells. Therefore, cells within the prospective retinal epithelium assume different fates presumably via information present in the environment. The *sevenless*$^+$ (*sev*$^+$) gene appears to play a role in the expression of one of the possible fates, since the mutant phenotype is the lack of one of the pattern elements, namely, photoreceptor cell R7. The *sev*$^+$ gene product had been shown to be required during development of the eye, and had also been shown in genetic mosaics to be autonomous to presumptive R7. As a means of better understanding the pathway instructing the differentiation R7, the gene and its protein product were characterized.

The *sev*$^+$ gene was cloned by P-element transposon tagging, and was found to encode an 8.2 kb transcript expressed in developing eye discs and adult heads. By raising monoclonal antibodies (MAbs) against a *sev*$^+$-β-galactosidase fusion protein, the expression of the protein in the eye disc was localized by immuno-electronmicroscopy. The protein localizes to the apical cell membranes and microvilli of cells in the eye disc epithelium. It appears during development at a time coincident with the initial formation of clusters, and in all the developing photoreceptors and accessory cone cells at a time prior to the overt differentiation of R7. This result is consistent with the pluripotency of cells in the eye disc. Its localization in the membranes suggests that it may receive information directing the development of R7. Its localization in the apical membranes and microvilli is

away from the bulk of the cell contacts, which have been cited as a likely regions for information presentation and processing. Biochemical characterization of the *sev*$^{+}$ protein will be necessary to describe further its role in development.

Other mutations in *Drosophila* have eye phenotypes. These were analyzed to find which ones affected the initial patterning of cells in the eye disc, in order to identify other genes, like *sev*, whose gene products may be involved in generating the pattern. The adult eye phenotypes ranged from severe reduction of the eye, to variable numbers of photoreceptor cells per ommatidium, to subtle defects in the organization of the supporting cells. Developing eye discs from the different strains were screened using a panel of MAbs, which highlight various developmental stages. Two identified matrix elements in and anterior to the furrow, while others identified the developing ommatidia themselves, like the anti-*sev* MAb. Mutation phenotypes were shown to appear at many stages of development. Some mutations seem to affect the precursor cells, others, the setting up of the pattern, and still others, the maintenance of the pattern. Thus, additional genes have now been identified that may function to support the development of a complex pattern.

Table of Contents

List of Illustrations

Chapter V

Epilogue

List of Tables

Chapter I

An Introduction:

Structure and Development of the Compound Eye

During nervous system development, a small population of stem cells gives rise to a great diversity of neurons and glia. Steps in the process of neurogenesis include the generation of a precursor cell population, the routing of daughter cells into appropriate developmental pathways, and the establishment of neural connections with specific spatial properties. Recent studies suggest that different types of neurons and glia of the vertebrate nervous system can be derived from a pluripotent precursor (Turner and Cepko, 1987; Holt et al., 1988; Wetts and Fraser, 1988). Multipotent nervous system precursor cells have also been demonstrated in insects by genetic and laser ablation studies (Ready et al., 1976; Lawrence and Green, 1979; Taghert et al., 1984). Thus in both vertebrates and invertebrates, the major determining factors for cell-type specification and pattern formation may lie in the particular location that a stem cell occupies, including its contacts with other cells and the extracellular matrix in which the cell is embedded. The environment may provide proliferative as well as determinative cues and may itself change in response to the developmental states of neighboring cells. The study of neural development in invertebrate systems allows for the identification of mutations that affect development, and therefore genes and gene products that may function in the determinative events. This thesis describes studies on the processes of controlled generation of diversity and establishment of ordered cellular arrays during development of the retina of *Drosophila melanogaster*. In this chapter, first the structure, then the morphogenesis, of the adult eye is discussed. In the latter sections, experimental manipulations of the developmental phenomena are described.

The adult visual system

The visual system of most dipterans consists of the compound eye (retina) and the underlying optic lobes, comprising the lamina (first optic ganglion), the medulla (second optic ganglion), the lobula and the lobula plate (for review, see Meinertzhagen, 1973; Kankel et al., 1980). The system also comprises the ocelli, three visual organs on the

dorsal aspect of the head and the interneurons thereof. A large amount of the extracellular surface of the head is made up of retinal facets (Fig. 1A and B). Each adult compound eye comprises approximately 800 facets, or ommatidia, and the external morphology of each of these units is remarkably conserved from one to another. As can be seen in Figure 1C, the internal structure of each ommatidium is also reiterative. Each ommatidium is made up of 22 cells of several different types: eight photoreceptor neurons (retinula, or R, cells), four non-neuronal cone cells, two primary pigment cells, three secondary and one tertiary pigment cells that are shared between neighboring ommatidia, and one hair-nerve group comprising four cells (Ready et al., 1976). Errors in the structure are rare, and are found almost exclusively at the perimeter of the eye (T.E. Hanson, unpubl. data).

Each R cell has a light-collecting organelle, the rhabdomere, which extends on a stalk into the interretinular space (IRS). In *Drosophila*, unlike some other dipterans, the rhabdomeres from the photoreceptors within each facet are not fused with each other, and their structural characteristics do not vary between ommatidia. It is likely that the opsins, the phototransduction enzymes of the R cells, are localized in the rhabdomeres, since the vertebrate rod photoreceptor cell opsin is localized in the rod outer segments (reviewed in Stryer, 1986). The six outer rhabdomeres arise from photoreceptor neurons R1-R6; these cells express the opsin Rh1 (O'Tousa et al., 1985; Zuker et al., 1985). Depending on the plane of section, the central rhabdomere arises from either R7 or R8. The R7 cell body and rhabdomere are distal to the R8 cell body and rhabdomere. Both R7 and R8 rhabdomeres extend into the center of the ommatidium. Therefore, in any one plane of section, one usually sees only the R7 cell and its rhabdomere extending between R1 and R6, or the R8 cell and its rhabdomere extending between R1 and R2. Each R7 cell expresses one of two unique opsins, Rh3 or Rh4 (Fryxell and Meyerowitz, 1987; Montell et al., 1987; Zuker et al., 1987). R8 is presumed to express a unique opsin but it has not yet been identified. The R cells can be divided into three groups, R1-R6, R7 and R8, on the basis of these opsin differences, on mutations that differentially affect each subset of

cells, and on different connectivity patterns of the different R cells in the optic lobe (see below).

The microvillar array that makes up the rhabdomeres of the *Drosophila* R cells is parallel to the stalk supporting them. In other dipterans, the morphology of the rhabdomeres can provide further visual specialization. For instance, in *Sympycnus lineatus*, an active predatory dipteran that lives and hunts on or near water, the illuminated facets vary in color from one row of ommatidia to another; the color alternates between red and yellow. Upon investigation of the internal structure of the retina, Trujillo-Cenóz and Bernard (1972) found that the R7 rhabdomere could have either of two microvillar orientations (polarities), which varied between rows. The R1-R6 rhabdomere microvilli were consistently parallel to the stalk, and the R8 microvilli lay in a plane perpendicular to the stalk. In rows that appeared red, the R7 microvilli were parallel to the stalk, and hence were orthogonal to the underlying R8 rhabdomere (termed Type A structure). In rows that appeared yellow (termed Type B), the R7 microvilli were perpendicular to the stalk, and hence were parallel to the R8 microvilli. The authors propose that this refinement in microvillar structure could confer a survival advantage by screening out horizontally polarized light from the surface of the water, and / or by providing enhanced color or polarization contrast.

The *Drosophila* eye is divided into dorsal and ventral halves by the equator, which runs from posterior to anterior across its center (Fig. 1C). On either side of the equator, the polarity of the ommatidia are in mirror symmetry to each other. On the dorsal side of the equator, the R7 rhabdomere, extending into the IRS from between R1 and R6, enters the ommatidium from the ventral aspect. Accordingly, on the ventral side of the equator, the ommatidia are arranged such that the R7 rhabdomere enters from the dorsal aspect. The equator is not found in all dipteran eyes; ommatidia from the "true bug" *Oncopeltus* all have the same polarity (Shelton and Lawrence, 1974).

In order for visual information to be processed, the response to light in the R cells

must be relayed to the optic lobes. The transfer occurs in a spatio-specific array called the optic cartridge (Braitenberg, 1967; Trujillo-Cenóz and Melamed, 1973; Meinertzhagen, 1973). As shown in Figure 1D, the axons of R1-R6 terminate in the lamina. The axons from R7 and R8 pass through this structure to terminate at different levels in the medulla. As described by Braitenberg (1967), the projection pattern of R1-R6 onto the lamina in flies is quite specific. Because of the curvature of the eye, the R1-R6 cells in one ommatidium do not receive light from the same point in space. However, in any trapezoidal array of six neighboring ommatidia, one R cell from each does receive light from the same point. This group of six R cells comprises an interommatidial set, in which each R1-R6 cell type is represented. The axons of one ommatidium leave the retina bundled together. Upon reaching the lamina, however, the R1-R6 axons each innervate a different lamina cartridge. Each lamina cartridge receives input from the interommatidial set of six photoreceptors that have the same point of view. Hence, the image of the outside world is reestablished by the connections of the R cells in the first optic ganglion.

Early development of the visual system

The adult visual system of holometabolous insects such as *Drosophila* develops from the two eye-antennal discs and optic lobe anlagen of the larva. Genetic marking data in *Drosophila* showed that each eye-antennal disc arises from approximately 23 cells set aside at the embryonic blastoderm stage (Garcia-Bellido and Merriam, 1969). These cells actively proliferate through the three larval instars. They appear to be committed to form the cell types found in the various head structures that develop from the eye-antennal disc, but are not committed to specific tissues until later in development. Clonal patches made early in the first larval instar (Morata and Lawrence, 1979) could give rise to both antenna and retina of the adult; they were not restricted to a single tissue. Later in first instar, clonal patches became restricted to the adult eye, and often had interesting patterns (Baker, 1978). The clones often had predominantly dorsal or ventral locations in the adult

eye, although the border did not adhere strictly to any morphological boundaries such as the equator (see also Ready et al., 1976). Another common clone shape was the sector, with the apex of the sector at the center of the eye and the rest radiating anteriorly from it. Baker rarely found clones in the extreme posterior of the adult eye, indicating that this region had already undergone or had yet to undergo mitoses during which the clones could be made. Since the retina develops in a wave of differentiation from posterior to anterior (see below), these data may indicate that mitoses occur in waves across the eye disc as early as the first larval instar.

Curiously, these clonal patches are remininscent of patches of position-effect variegation of the *white* (*w*) gene (Hazelrigg et al., 1984; Levis et al., 1985). In these experiments, the w^+ gene was transformed into a *white* mutant genome by P-element-mediated transposition. Generally, the transformants were fully rescued for eye color. However, in a few cases the expression of the w^+ gene was sensitive to cell position in the eye, and this sensitivity was dependent upon the site of integration of the construct into the chromosomes; i.e., the construct could be remobilized and could fully rescue the *w* phenotype. Often the patch boundary lay upon the dorsal-ventral median of the eye (again, not along the equator *per se*); sector clones were also found.

Although the patterns seen by the two techniques are very similar, variegation may not arise from clonal restrictions in the head. The clonal boundaries may reflect a pattern of daughter cell migration rather than a compartmental position restriction. However, the two sets of data do suggest that cells within the eye disc have mechanisms for determining their position within the epithelium, whether by clonal or non-clonal means.

In structure, the eye-antennal disc is a columnar epithelium, with cells arranged along the apical-basal axis. The apical surface of the cells is covered by microvilli extending into a dense, fibrous extracellular matrix (Waddington and Perry, 1960; Perry, 1968), which is ensheathed in a peripodial membrane.

Each eye-antennal disc is attached at its posterior end to the optic lobe by the optic

stalk (Fig. 2). Until the middle of the third larval instar, the axonal projections of the larval photoreceptor cells course through the optic stalk. The larval photosensitive organ, or Bolwig's organ, was first described by Bolwig in *Musca* (1946), and is located in the anterior of the larvae, in the pharangeal/mouth complex. In *Drosophila*, the larval photoreceptor system contains about twelve photoreceptor neurons. The axons from Bolwig's organ extend in a bundle from the cell cluster posteriorly along the antennal portion of the disc. Before reaching the eye portion, the bundle dives in between the peripodial membrane and the apical surface of the disc, where it continues to extend posteriorly. The bundle crosses from the eye disc and enters the optic lobe through the optic stalk. Innervation of the optic lobes by the axons from Bolwig's organ during development may be linked to the generation of the optic stalk (Steller et al., 1987). In their model, the point at which the axon bundle enters the optic lobe is the point at which the optic stalk will form. During development of the adult eye, the optic stalk becomes filled with a second population of axons, those from the developing photoreceptor neurons (discussed below).

Cellular differentiation in the eye disc

Cellular differentiation first becomes apparent in the eye disc during the middle of the third larval instar in *Drosophila*. Differentiation of the eye has been described in many insects, including *Drosophila*, in great detail (see Waddington and Perry, 1960; Melamed and Trujillo-Cenóz, 1975; Ready et al., 1976; Tomlinson, 1985). During middle-to-late third instar, a transverse groove divides the disc into anterior and posterior sections; this morphological landmark sweeps across the disc from posterior to anterior (Fig. 2). Autoradiographic studies have shown that anterior to the groove, prospective retinal cells, still indistinct from one another, continue to divide. When one of the epithelial cells divides, it detaches from the basal surface of the epithelium, and rounds up near the apical surface during the S phase. After cell division is complete, the two daughter cells reattach

to the basal surface of the disc.

At the groove, pattern formation and differentiation begin to occur; hence, this groove has been termed the morphogenetic furrow (Ready et al., 1976). Within the furrow, the cells begin grouping into what will be the ommatidia of the adult eye (Figs. 2B and C). At this stage, preclusters of five cells are found. Tracing these cells through development has shown that they correspond to presumptive R2, R3, R4, R5, and R8, with R8 at the center. Cells that are not grouped into the precluster undergo a final round of cell division just posterior to the furrow (Ready et al., 1976; Tomlinson, 1985). Since the final round of cell division occurs relatively synchronously in unpatterned cells at the furrow, the groove in the disc may be a result of individual cell morphological changes associated with cell division.

The last round of division generates the precursors of the rest of the cells of each ommatidium. First, the presumptive R1 and R6 are added to each cluster; then presumptive R7 joins to complete the photoreceptor complement. The four presumptive cone cells are added radially upon this basic unit, then the pigment cells, and finally, the hair-nerve group. Since morphogenesis occurs sequentially across the disc, one can see in any one disc many different stages of development of the retina. Newly developed preclusters are found in the row associated with the furrow, while increasingly mature clusters can be found in the more posterior regions of the disc. The furrow has been estimated to move at a rate of about one column every two hours (Campos-Ortega and Hofbauer, 1977), reaching the anterior border of the prospective retina about ten hours after pupation.

Cluster formation is accompanied by cell-type differentiation, including axon elongation by the presumptive R cells and the appearance and disappearance of antigens identified by monoclonal antibodies (MAbs) isolated in the Benzer lab (Fujita et al., 1982; Zipursky et al., 1984; Venkatesh et al., 1985; Banerjee et al., 1987b; see Chapter V). For example, MAb 3E1 identifies an element of the extracellular matrix located between the

apical surface of the epithelium and the peripodial membrane. The stain appears bright in the region of the disc anterior to the furrow. However, within the furrow, this stain is lost, and it does not reappear in the posterior region of the disc. Within the furrow, the presumptive photoreceptor neurons begin to express a neuronal phenotype. One of the earliest indications of expressing this fate is the elongation of an axon from the basal end of the cell. In sections across the optic stalk at early stages, bundles of five axons can be found crossing into the optic lobe (Trujillo-Cenóz and Melamed, 1973). Later, bundles of eight axons are found. The presumptive R cells also begin to express markers associated with assuming a neural identity. One of these is identified by the MAb 22C10 (see Fig. 2B), which labels peripheral nerves and their axons (Fujita et al., 1982; Zipursky et al., 1984). First, the epitope appears in the apical tips of the photoreceptors. As the photoreceptors mature, antigen is found more basally in the cells. After about ten hours of R cell differentiation, it is found exclusively in the axons of the photoreceptors.

The individual constituents of each ommatidium also do not differentiate at once; their differentiation also occurs in a "wave." Tomlinson and Ready (1987a) found that within the five-cell precluster, expression of the antigen defined by MAb 22C10 first occurs in presumptive R8. Following this, R2 and R5 begin to express it, then R3 and R4. After the presumptive photoreceptor complement is complete, R1 and R6, and finally, R7 express the antigen. A similar sequence of expression was seen for an epitope of horse radish peroxidase, and for the epitope of a neural nucleus-specific antibody.

Differentiation of the ommatidia behind the furrow is accompanied by movement of nuclei along the apical-basal axis of the epithelium (Tomlinson, 1985). The migration of nuclei reflects patterns of cell division, and also the requirement that the individual cells assume morphological and structural identities in the adult eye. The data suggest that the nucleus of a presumptive photoreceptor cell rises to the apical aspect of the cell before that cell extends an axon. Also, in the adult eye, the bulk of the cone cells lie distal to the photoreceptors, just under the crystalline cone. This arrangement is first elaborated in the

eye disc shortly after the presumptive cone cells have joined the cluster. The cone cell nuclei rise apically, so that in very apical sections of the eye disc tangential to the surface, most of the area of the cluster is occupied by the cell profiles of the four cone cells, although the eight photoreceptor cell tips can been seen. Accordingly, in less apical sections, the cone cell profiles are narrow processes. Photoreceptor nuclei are organized on a more complex pattern, but also show systematic changes along the apical-basal axis, such that different combinations of photoreceptor nuclei occupy the bulk of the cluster area.

Terminal differentiation of the ommatidium

Cell clustering and gross morphogenesis is accompanied by the terminal differentiation of the cells, beginning at the furrow, and continuing through pupation. Axon elongation is a cell-type-specific differentiation event initiated at the furrow. About 24 hours after the passage of the furrow, the presumptive photoreceptors begin to express a gene whose product was first identified by the MAb 24B10 (Zipursky et al., 1984). The protein is localized in the cell membranes of the photoreceptor cells and their axons. By genetic analysis of the gene encoding the antigen, called *chaoptic* (*chp*), it was found that the protein may function in the elaboration or maintenance of the rhabdomere microvilli (Zipursky et al., 1985; Van Vactor et al., 1988; Reinke et al., 1988). In the adult, large amounts of the protein encoded by chp^+ are found extensively in association with the rhabdomeres.

The equator results from a rotation of each cluster by 90°, in opposite directions in the dorsal and ventral halves of the eye. Rotation of the ommatidia begins after cell clustering is complete, but before puparium formation (Ready et al., 1976).

During pupariation, morphogenesis and terminal differentiation events occur in the different retinal cell types at different stages, as seen especially in the beautiful electron micrographic studies of Waddington and Perry (1960) and Perry (1968). By about 24

hours post-puparium formation, the epithelium is stretched thin. The four-cell, hair-nerve group is well displayed at the corners of the ommatidial units. By 48 hours, the arrangement of the main elements is complete, so that the bulk of the two primary pigment cells is distal to the cone cells, and the four cone cells are distal to the R cells. The sensory hair has been secreted by this time. Also, pigment granules can be found in the tertiary pigment cells, and pigment deposition has begun in the secondary pigment cells.

At about 48 hours post-puparium formation, the R cells elongate by about fivefold. The light-collecting organelle, the rhabdomere, begins to form along the central margin of each R cell, by infolding of the cell membranes. Adjacent to the folds, many microtubules collect, perhaps to form a scaffold to support the extensive membrane elaborations. At about 50 hours, the R cells begin to pull away from the center, and tight intercellular junctions (zonula adherens) form where the cell junctions are exposed to the IRS. Many small vesicles also collect in the region where the rhabdomere is forming. From this time on through emergence of the adult fly, the microvilli continue to be elaborated, lengthening and becoming hexagonally packed. Expression of genes closely associated with visual transduction appears to begin about 72 hours after puparium formation (Montell et al., 1985; O'Tousa et al., 1985; Zuker et al., 1985; Cowman et al., 1986; Fryxell and Meyerowitz, 1987; Montell et al., 1987; Zuker et al., 1987; Montell and Rubin, 1988).

Other components of the retina also continue to develop. The hair-nerve group migrates to the extreme distal retina in about 48 hour pupae. The cone cells are relatively dormant until about 40 hours. At this time, small electron dense patches appear on the apical tips of the cone cells, on the microvilli. Although the evidence is circumstantial, Waddington and Perry state with confidence that at this time the cone cells are secreting the corneal lens, because it appears coincidentally with and in close apposition to the cone cell microvillar patches. By 48 hours, each ommatidium is covered with a cuticle layer, and after 50 hours, the fibrous material of the corneal lens is laid down in a lamellar

fashion. In the interval between 72 and 96 hours, the cone cells retract from the lens to form the pseudocone cavity, the crystalline cone. The primary pigment cells migrate to cup the crystalline cone. In the adult, the cone cells become packed with microtubules.

As stated, pigment granule deposition begins at 48 hours in the basal retina. It continues up into the primary pigment cells as well. Interdigitated septate junctions form between the primary pigment cells and between the primary pigment and cone cells in the distal retina. Waddington and Perry (1960) and Perry (1968) also noted that the secondary and tertiary pigment cells contained granular masses of something ultrastructurally like lipid or myelin. Since the secondary and tertiary pigment cells are presumed to insulate electrically the ommatidia from one another, perhaps this deposition has some functional significance in that regard.

Development of the retina-lamina-medulla complex

One of the critical steps in the development of the visual system is the formation of the exquisite, precise connections between the retina and the optic lobes. It is known that while the eye can develop independently of the brain, the brain does not develop properly without the normal contact from the axons of the retina (Meyerowitz and Kankel, 1978; Fischbach, 1983). The process of innervation begins during cluster formation. Since the cellular machinery for phototransduction is not expressed until much later in development, innervation and induction of neural differentiation in the optic lobes may occur independently of photoreceptor activity.

Innervation of the optic lobe has been described by Trujillo-Cenóz and Melamed (1973) and Meinertzhagen (1973) for muscoid flies, and by Hanson (T. E. Hanson and S. Benzer, unpubl. data) for *Drosophila*. Before retinal development occurs in the eye disc, the optic stalk contains the axons from the larval photosensitive organ; in *Drosophila*, these number about 12. During the third larval instar, the optic stalk begins to be occupied by a second populations of nerve bundles. The new bundles are axons from

the developing retinal field; each bundle usually contains eight axons, although bundles of five can be found, originating from the preclusters. These eight axons arise from R1-R8 of each ommatidium, growing as a bundle from the basal end of the neurons. After passing through the basal lamina, they grow along the optic stalk, where they enter the anlage of the lamina. Cells in the optic lobe anlage have been actively proliferating. Symmetric and asymmetric divisions of neuroblasts have generated populations of ganglion mother cells, which in turn generate ganglion cells. The ganglion cells will differentiate into neurons. As reviewed in Meinertzhagen (1973), Hinke (1961) found that in *Drosophila* mutants in which the developing eye field is reduced or lacking, the size of the optic lobe upon innervation is initially greater than in the wild type. This evidence suggests that the initial effect of innervation of the optic lobes by R cells is to inhibit neuroblast proliferation. The data conflict on the question of whether any neural cell differentiation in the dipteran optic lobe occurs before innervation from the developing retina.

The various rhabdomeres in an ommatidium look at different points in space, and the visual information from groups of neighboring ommatidia is sorted in the lamina optic cartridge, as described above (Braitenberg 1967). The columnar organization of the optic cartridge found in the adult optic lobe is generated during the pupal stages. Initially, the axons of R7 and R8 have collateral branches in the lamina anlage. However, even at the earliest stages, they continue to grow through the anlage of the lamina, extending into the medulla neuropile, where they will eventually form synapses. In the developing lamina neuropile, the axons from R1-R6 in each bundle remain together for about the first 24 hours of pupation. Growth cones elaborated on the tips intermingle with those developing lamina neurons. Trujillo-Cenóz and Melamed (1973) note that this simple organization is similar to that found in more primitive insect groups with fused R1-R6 rhabdomeres. After 24 hours, the axons form a collateral process extending radially from the bundle center, and each axon twists 180° relative to its original orientation (Braitenberg, 1967).

This marks the start of the organization of the optic cartridge. The growth cones from other bundles and from the lamina targets intermix extensively. After another 24 hours of development (48 hours post-puparium formation), the growth cone contacts from the interommatidial set of R1-R6 condense onto one set of lamina monopolar neurons; there is a pair of neurons, L1 and L2, per lamina cartridge. The other growth cone contacts are eliminated. At this time, each cartridge now receives input from the interommatidial set of R1-R6, forming the mature lamina cartridge. It is not for another 24 hours (in 72 hour pupae) that synapses begin to form, as seen by synaptic vesicles and synaptic T-bars. Interestingly, this corresponds approximately to the time at which the genes that function in phototransduction are first expressed. Of course, the optic lobe structure and cell-type composition are very complex, containing more than just lamina cartridges. These more complex features will not be discussed here, but are reviewed in Strausfeld (1976) and Kankel et al. (1980).

Innervation of the optic lobes by the retina is probably required for optic lobe cell differentiation. Several investigators (Meyerowitz and Kankel, 1978; Fischbach, 1983; Fischbach and Technau, 1984) have shown that without innervation or with abnormal innervation, the optic lobes are either extremely reduced in size or disorganized, respectively, in the adult. Meyerowitz and Kankel (1978) analyzed this effect in mutants of *Drosophila* with severely rough eyes; these mutants also had disorganized optic lobes. In genetic mosaics in which patches of eye tissue were genotypically mutant while the optic lobes were most likely genotypically wild-type, the underlying optic lobes were still in disarray. In mosaics with genotypically wild-type patches in the retina and genotypically mutant optic lobes, the part of the optic lobes receiving innervation from the wild-type patch could acquire a morphology approximating that of the wild type. Hence, it appears that innervation is necessary for optic lobe differentiation; the retina may serve as an organizing force on the optic lobes. Since mutants in which the eyes are not functional in the adult nevertheless had approximately wild-type optic lobe structure

(Meyerowitz and Kankel, 1978), the requirement does not appear to rely on the activity of the cells.

This requirement for innervation could result from a phenomenon described in vertebrate neural development (for review, see Cowan et al., 1984). Innervation-dependent cell survival has been demonstrated in vertebrate systems. It has been suggested that after contact between the innervating and target cells, target neurons that have not been innervated are eliminated, and may degenerate. This mechanism insures that the sizes of the two neuronal populations match. It is unknown if a similar mechanism operates during innervation of the optic lobe by the retina in insects. If so, the abnormal innervation in mutants could result in greater than normal cell degeneration in the optic lobes. The experiments discussed above would support this, especially in light of the exquisite precision of the projection pattern.

Development of the eye: commitment

Thus far, morphogenesis of the eye and optic lobe of the insect has been described. By experimental manipulation, including invasive and genetic techniques, its development has been investigated in many insects. Although the eyes among the different insects vary, the similarities between them are quite remarkable. Comparative studies of the experimental results may lead to testable models of development.

A common sequence of eye development occurs in most insect systems studied. The compound eyes of both holo- and hemimetabolous insects develop from a retinal epithelium; development occurs in a wave from the posterior to the anterior of the epithelium, and is accompanied by proliferation. In hemimetabolous insects, i.e., ones that do not metamorphose, the eye usually grows by addition to or enlargement of the existing eyes through the larval nymph stages. The eyes of the nymph usually function also as the eyes of the adult. The eyes of *Oncopeltus* (Shelton and Lawrence, 1974; Green and Lawrence, 1975) and *Periplaneta* (Hyde, 1972; Nowell and Shelton, 1980) develop

in this manner. The eyes of holometabolous insects usually develop extensively in the latter larval instars. The eyes can develop externally on the head epidermis, as in *Lepidoptera* (for example, Nardi, 1977), or internally on epithelial discs, as in *Drosophila*, other flies, and the honey bee, *Apis* (for example, Eisen and Youssef, 1980). These insects usually have a lateral larval eye, such as Bolwig's photosensitive organ in flies. Mosquito larvae have independent lateral eyes (lateral ocelli), and specific cell-type differentiation occurs in the last larval stage. However, competence to differentiate occurs overtly during earlier larval stages (White, 1961, 1963).

In order for the eye to develop, the prospective retina must be capable of differentiation. The compound eye of the mosquito *Aedes aegypti* has been extensively studied in this regard, along with the eye of *Oncopeltus* and the cockroach *Periplaneta.* As described by White (1961, 1963), the mosquito eye develops from the lateral head epidermis. During the first larval instar, some of the epidermal cells at the posterior of the head condense to form the optic placode. The placode expands anteriorly by an advancing wave of proliferation. However, until the fourth larval instar, the placode is otherwise undifferentiated. During the fourth instar, the wave of proliferation is followed by a wave of differentiation, and is marked by extensive pigmentation. White (1961) determined that the lateral head epidermis could differentiate only after passage of the wave of optic placode formation, and that condensation relies on contact with previously condensed placode. Transplants of non-retinal epithelium onto the potential field could block condensation. Also, at early stages, head epidermis that does not usually form the retina could be made to do so if it was placed in contact with optic placode. The origin of the optic placode was then investigated (White, 1963). Prior to optic placode formation, lesions were made in the posterior region of the lateral head epidermis approximately where condensation of the placode was expected to be initiated. In one-third of the cases, an eye did not develop, but eye development could be rescued by transplanting in a piece of optic placode from another larva. Even as late as the third instar, optic placode from a

red-eye mosquito strain could be introduced into a black-eye strain, into the posterior region of what would have formed black-eye tissue, and adult eyes with red facets adjacent to black facets could be found. White was able to conclude that the prospective eye region in the host was intact and competent to respond to developmental cues, but it was not able to do so without optic placode formation, and that optic placode formation could be inititated only at a specific place on the head epidermis. Optic placode formation, or competence, appears to traverse the prospective retinal epithelium as a wave where competent cells induce neighbors to assume a similar state. Also, a region in the posterior of the prospective eye region is, in a sense, a morphological and physiological differentiation center, perhaps producing or first being able to respond to a factor that initiates the ability to differentiate.

Bodenstein (1939, 1962), Gateff and Schneiderman (1975), and Campos-Ortega and Gateff (1976) have performed complementary experiments with *Drosophila* discs, by investigating the developmental capacity of eye discs during the different larval stages. Eye discs at different stages were transplanted into late third instar larvae (the stage at which differentiation of the retina occurs), and allowed to develop and undergo metamorphosis, to find the stage at which adult head structures, e.g., eye facets, could form in spite of the immaturity of the discs. They found that at a stage past midsecond instar, the discs were capable of generating ommatidia, even though these discs were much smaller than late third instar discs. The resulting eye had fewer facets. However, when discs from earlier stages were used, no adult retina components could be found. Differentiation seems not to rely simply on counting rounds of cell division. Rather, the ability of cells in the morphogenetic field to respond to differentiation stimuli may be determined sometime around midsecond instar; once this state is attained, cells in the eye disc are fully competent to respond to a midthird instar-specific differentiation "signal." It is possible that in *Drosophila*, during second instar, a wave of competence passes across the developing disc, readying the cells for differentiation. Given the similarities between

Drosophila and the mosquito, such is likely to be the case. Until the middle of second instar, the eye disc could be like the prospective eye tissue of the mosquito; in the absence of experimental perturbation, it will form an eye. However, competence to assume this fate, which can be uncovered only through experimental manipulation, is assumed later, perhaps as a wave of some agent across the eye disc.

Development of the eye: initiation and propagation of morphogenesis

Once cells of the prospective retinal epithelium are competent to form adult retina, differentiation can be initiated. For many years, it has been known that *Drosophila* eye discs grown *in vitro* do not differentiate unless cultured in the presence of the larval ring gland (reviewed in Bodenstein, 1962). Humoral factors might therefore be involved in the initiation of eye development. Eye mutants in *Drosophila* that lack compound eyes may be useful for identifying such factors. For instance, the adult compound eyes of the *Drosophila* eye mutant *eyes absent* (*eya*) (Sved, 1986; Hackett, Leiserson, and Benzer, unpubl.) are completely lacking. There is never any evidence of adult compound eye ommatidia; the larval photosensitive organ and the adult dorsal ocelli appear normal. Hackett found that *eya* eye discs appear normal through the second larval instar and perhaps into the early third. However, beginning in the midthird instar larva, the eye disc cells appear to degenerate. The degeneration seems to precede differentiation; no markers or morphological characteristics indicative of differentiation are expressed (see Chapter V). Perhaps cells in the *eya* eye disc develop normally until the time of differentiation. If development is initiated by a humoral factor(s), perhaps *eya* cells are unable to respond to or do not produce this factor. Degeneration could be explained by the lack of alternate programs of differentiation past the time of compound eye commitment. It is not known whether the *eya* function is produced autonomously by eye disc cells; further work on this gene is currently in progress.

Several conflicting studies have been published on the issues of recruitment and

induction in terms of the initation and propagation of the developmental wave. Initial experiments on *Periplaneta* (Hyde, 1972) and *Oncopeltus* (Shelton and Lawrence, 1974; Green and Lawrence, 1975) indicated that cells were recruited along the developmental front to form ommatidia. Grafting experiments on the roach (Nowell and Shelton, 1980; Nowell, 1981) have now demonstrated that the recruitment step is preceded by active proliferation, and that there is a zone of proliferation along the growing eye margin from which daughter cells are pushed out anteriorly.

Lebovitz and Ready (1986) attempted similar analyses on the *Drosophila* eye disc to determine if the morphogenetic furrow was a recruitment margin along which clusters were formed. In these experiments, fragments from the anterior of developing eye discs, cut so that they did not include the furrow, were transplanted ectopically into similarly staged host larvae. Cluster formation occurred in about two-thirds of the fragment samples. This indicated that cluster formation did not depend upon the presence of the original morphogenetic furrow, although new cluster formation was accompanied by formation of a transverse groove. They concluded that the furrow is not an inductive front but rather is a consequence of development. Furthermore, the eye field grew in size, indicating that the anterior of the disc may contain a source of cells whose progeny are committed to form retina. Given the complications of disc fragment regeneration, it is difficult to conclude, as the authors do, that the data indicate a budding zone in the anterior of the disc.

By comparing the data from different species, the following speculations about initiation of *Drosophila* eye development can be made. It seems that young discs become capable of differentiating during midsecond instar, in a manner similar to the optic placode stage in mosquito, although they do not actually differentiate until midthird. There may be a competence-inducing center in the posterior, as White (1961, 1963) hypothesized for mosquito, required for the initiation and propagation of the competent state. Overt differentiation, however, seems not to require contact with previously differentiated

tissue, as the recruitment hypothesis would claim. If proliferation, determination and differentiation occur in waves from posterior to anterior across the eye disc, differentiation may begin in the posterior solely because cells there are able to respond to differentiation cues before the less mature, more anterior cells in the disc are able. If this is the case, the disc fragments (Lebovitz and Ready, 1986) could support differentiation of ommatidia because the anterior cells had already become capable of differentiation. It could be predicted that if disc fragments were taken from early second instar discs, they would not be able to respond to differentiation cues present in the late third instar stage. They should, however, be capable of rescue from this state of limbo by direct contact with posterior eye disc tissue from midsecond instar.

The non-clonal origin of ommatidia

Within the furrow, cells are clustered and begin to assume specific cell identities. From the work of Shelton and Lawrence (1974) and Ready et al. (1976), it became clear that the constitutents of an insect ommatidium were not necessarily clonally related. Ready et al. (1976) showed that mosaic clones could cross the equator as well, indicating that the dorsal / ventral halves do not arise in response to clonal restrictions of fate. By inducing recombination with irradiation during the late third larval instar, clones could be marked during the final rounds of cell division; each of the two daughters could develop into any cell type in the adult eye that could be marked (Lawrence and Green, 1979). Therefore, it appears that any cell in the eye disc, once it is committed to forming retina, can generate and / or differentiate into any of the possible cell types comprising the adult eye, including at least the three different types of neuron and the three types of pigment cell. The cells anterior to the morphogenetic furrow therefore seem to comprise an equivalence group.

The concept of the equivalence group arose from studies on the nematode *C. elegans* (Kimble et al., 1979), and has also been used to describe equipotent cells in the leech (for review, see Sternberg, 1988a). Several equivalent groups of cells have been

described in the nematode. The number of cells and the number of possible fates vary between groups. Some equivalence groups are characterized by an initial bias of the cells towards different fates, and others are not. There is often a primary fate, defined as the fate one of the cells will assume if all the other cells in the group are destroyed (usually always by laser ablation). For instance, in the vulval equivalence group, comprising six equipotent cells, there are three possible fates: type 1, 2 or 3. In the wild type, one cell assumes the type 1 fate, two the type 2 fate, and three the type 3 fate. The fates appear to be directed by yet another cell, the anchor cell, because they seem to depend on the distance of an equipotent cell from the inducing cell (Sternberg and Horvitz, 1986). In the absence of the anchor cell, the primary fate is type 3. The analysis of mutations that affect cell-type decision making indicates that a cell-to-cell signalling system operates to stabilize the pattern of differentiation, perhaps via positive and negative feedback loops. For example, in the mutant *lin-15*, the type 1 and type 2 fates can occur independently of the presence of the anchor cell. Study of this mutant (Sternberg, 1988b) has revealed that a cell assuming the type 1 state may inhibit neighboring cells in the equivalence group from assuming the type 1 fate. Neighboring cells assume the type 2 fate.

In the eye disc, it is not really known if any one cell in a specific position is capable of assuming each type of cell found in the adult eye. It is possible that although the daughters generated during the final round of cell division can assume one of a number of fates, the fates they assume are influenced somehow by the position of the precursor cell in the retinal epithelium. The precursor cell in position x,y could always generate a "type a" daughter cell and a "type b" daughter cell. Given the small size of the eye disc and the lack of means to identify a specific precursor cell, this possibility is difficult to test.

The equipotent nature of differentiating cells in the eye disc seems the more likely possibility, though. Interactions among neighboring cells could provide a mechanism for generating the initial array. Stimulatory factor(s) may play a role in initiating differentiation, but, imposed upon the positive effect of the factor, could be an inhibitory

mechanism for regulating the spacing, and therefore the number, of nascent ommatidia in a row. In the alga *Anabaena* (Wilcox et al., 1973), an inhibitory mechansim seems to be used for regulating the number and spacing of the specialized heterocyst cells. They occur at a frequency of about one out of every 12, at a spacing of about 40 μm. A gradient of inhibitor concentration may spread from a differentiating heterocyst; only at a concentration below a certain threshold may another cell adopt this fate. The differentiating cell also seems to have a mechanism for reinforcing its own identity. In this gradient model, it is also assumed that there is some means by which the non-heterocysts block the flow of the inhibitor, e.g., by binding it or destroying it. In insect systems, it has been suggested that the regular spacing of sensory bristles on the cuticle may result from a graded inhibitory signal (Wigglesworth, 1940; Moscoso del Prado and Garcia-Bellido, 1984).

Cells in the eye disc that form the "nucleation site" at which the nascent ommatidia condense could be using a similar mechanism to space themselves. At the furrow, the presumptive ommatidia are regularly spaced at a distance of about 12-15 μm from center to center. Once a cell, or group of cells, begins to differentiate, an inhibitor could be released. The inhibitor could be displayed on the cell surface, or could diffuse through the epithelium or through the extracellular matrix. Given the fibrous structure of the apical extracellular matrix and the extensive elaboration of microvilli into this region, it is a potential site for inhibitor action. The fibrous structure of the matrix could limit the flow of diffusible substances in certain directions, and could also slow the rate of diffusion such that it became a process of molecular percolation through a matrix rather than free diffusion through an aqueous medium. The effective range of the inhibitor could then be limited more readily to a few microns laterally. Lateral inhibition could therefore control the number of ommatidia seeded in a row. The identification of mutations that affect the spacing of clusters in the eye disc (see Chapter V) might allow the elucidation of the

mechanism.

Intraommatidial cell-type determination could occur in an analogous manner, although here the system would become increasingly complex, since each cell seems to have the capacity to differentiate into at least eight cell types (R1-R6, R7, R8, cone cell, primary, secondary, or tertiary pigment cells, hair nerve group). Many workers in the field of eye development have therefore proposed that the information needed for "microheterogeneity" of cell types within a cluster is found on the cell surface of neighboring cells. In this model, the fate that a cell assumes is controlled by its position within the developing pattern. Perhaps pattern formation is initiated by environmental cues, and initial spacing of pattern elements controlled by percolating factors. Once those steps occur, though, the patterned cells may begin to express molecules that influence the fate of cells that join the cluster at a later time. As discussed above, Tomlinson and Ready (1987a) have shown that cells within developing clusters non-synchronously express certain gene products, indicating that the cells make developmental decisions sequentially beginning with R8 first and ending with R7. Although the markers they used are eventually expressed in all the R cells, the delay between the expression of these genes in the different cell types could be sufficient time for the cells to express position-specific genes as well.

Local cell interactions have been demonstrated to function in both the ventrolateral, neurectodermal region of the *Drosophila* and grasshopper (*Schistocerca americana*) embryo, as described by the use of molecular genetics and laser ablation (reviewed by Campos-Ortega, 1988; Taghert et al., 1984; Doe and Goodman, 1985a,b). An early step in neurogenesis is the segration of neuroblasts (NBs) and epidermoblasts (EBs) from the initially undifferentiated ventrolateral epithelium. During neurogenesis, about one-quarter of the cells in the neurectoderm assume the NB fate, and three-quarters the EB fate. It appears that any cell in the neurectoderm is capable of differentiating into either type, and that interactions among the uncommitted cells may cause them to assume different

properties during segregation. Although a stochastic mechanism may bias a cell towards the NB fate, the evidence suggests that a cell moving down the NB pathway inhibits neighboring cells from assuming the NB fate, or promotes them to assume the EB fate.

Mutations in *Drosophila* have been identified that affect the neurogenesis pathway (for review, see Campos-Ortega, 1988; Vässin et al., 1985). The neurogenic loci comprise at least seven complementation groups. In a loss-of-function mutation at a neurogenic locus, all neurectoderm cells in the mutant embryo assume the NB fate. Six of the loci, e.g., *Notch* (*N*), have been shown to be non-autonomously required for EB differentiation, while one, *Enhancer of split* [*E(spl)*] is autonomously required for the EB fate. For example, an N^- cell transplanted to an N^+ neurectoderm is capable of assuming an EB fate, while an N^+ cell transplanted into an N^- neurectoderm can promote the EB fate in neighboring N^- cells. Thus, a set of gene products has been identified that are important for neuroepidermal stem-cell determination in *Drosophila*, involving local cell-to-cell interactions. Interestingly, molecular analysis of *N* (Wharton et al., 1985; Kidd et al., 1986) has shown that it encodes a gene product remarkably similar to that of the *lin-12* locus of *C. elegans*, which functions in cell-type determination in the vulval equivalence group discussed above (Greenwald, 1985; Yochem et al., 1988). Both proteins may have membrane-spanning domains, with the extracellular domain comprising repeats similar to those found in epidermal growth factor, and the intracellular domain comprising repeats similar to the yeast cell cycle control genes *cdc10* and *SW16*. A similar mechanism could be used in the eye disc for segregation of neural and non-neural cell types (*cf* discussion of the *N* and *E(spl)* loci, below; Chapter V).

Tomlinson and Ready (1987b; Tomlinson, 1985) have proposed that cell type in the *Drosophila* eye disc could be determined by the extent of the contact made between a differentiating cell and the presumptive R8. Sets of cells appear to differentiate at about the same time, in terms of migration of their nuclei and their antigen expression. The sets are R2 and R5, R3 and R4, R1 and R6, and the unpaired R7. The sets also have in

common their amount of contact with R8, as well as their contacts with other pairs. Tomlinson and Ready suggest that cell-type determination is controlled by location in which a post-mitotic, undifferentiated cell finds itself within the developing ommatidium, and that specific proteins will be expressed on specific faces of the differentiating cells. For example, a cell that is located on the anterior aspect of a cluster, between an R2 and an R5, and sharing a face with R8 will always differentiate into an R3/4 class photoreceptor neuron. Whether the symmetry of the developing cluster contributes towards cell identity or whether it is a consequence of the close packing of the cells, remains to be seen. The hypothesis that it is cause rather than effect is difficult to test for several reasons. Firstly, cell position and cell identity are equivalent in meaning; in the eye disc there is as yet no way of telling cell type, independent of cell position. Secondly, because of the present lack of experimental means of physically reshuffling the cells, one cannot alter the contacts between differentiating cells. Thirdly, there are no known morphological or functional distinctions between R1-R6 cells even in the adult. All proteins or genes that have been shown to function in R1-R6 appear equally required by all members of the R1-R6 class.

Mutations that affect the eye of *Drosophila*

The analysis of mutations in *Drosophila* that affect the morphology of the eye is expected to be critical for our eventual understanding of development of the pattern and cell-type determination. Many mutations that affect the morphology of the compound eye have been identified (see Lindsley and Grell, 1967). The phenotypes range from defects in eye pigmentation, e.g., *white*, to complete lack of the compound eyes, e.g., *eyes absent*. Presumably, mutations could be identified that affect each step in differentiation, maintenance, and function of the eye. Although many of these would be expected to be specific to the eye, some of them may have more global functions, for instance, in proliferation, epidermal versus neural cell-type differentiation, and development of

patterns. Characterization of some of these mutants during development of the eye is the focus of Chapter V.

As discussed in the previous section, several neurogenic loci seem to function in determination of neural versus epidermal cell type, and as such may function in eye development. Eye specific alleles at the *N* and *E(spl)* loci have been identified. At the *N* locus, the eye specific mutations, *split* (*spl*) and *facet* (*fa*), are recessive and result in severe roughening and some reduction of the adult eye (see Chapter V). While *N* may function in the neurectoderm region as an inhibitor of neuroblast differentiation, or alternatively as a promoter of epidermoblast differentiation, its function during eye development is unknown. As the name indicates, the *E(spl)* locus was first described as a dominant, gain-of-function mutation that enhances the rough eye phenotype of *spl* flies. The null phenotype of this gene is recessive lethal because of neural hyperplasia at the expense of the epidermoblasts, a defect that is autonomous to the epidermoblast cells. Molecular analysis of this gene is under way. Thus, genes that affect cell-type determination in the ventral neurectoderm may function during segregation of cell type in the retinal epithelium. Perhaps the neurogenic gene products function in neural (photoreceptors) and non-neural (cone cells, pigment cells) cell-type determination during development of the eye. In any event, the results indicate that gene products that function in other developmental processes in the fly may also play a role in development of the eye. There are a number of mutants with no adult compound eye ommatidia (*eya*; Sved, 1986) or severely reduced eyes (*Bar*; Lindsley and Grell, 1967), or with the converse phenotype, supernumerary eyes (*extra eye*; Marcey and Stark, 1985; Baker et al., 1985). The gene products of the genes identified by such mutations may function in retina precursor cell proliferation, viability and / or competence. Mutants have also been described with more subtle defects in the adult eyes; the external morphology of the eye is often roughened. Some of these, such as *Star* and *Rough eye*, are recessive lethals, indicating that the genes are required elsewhere during development. However, many of

them, like *rough*, *roughened eye*, and *glass* seem to be eye-specific. The phenotypes and characteristics during development of many of these mutations are discussed in Chapter V.

The *sevenless* mutation

Mutations at the *sevenless* (*sev*) gene lead to one of the most subtle phenotypes in the adult compound eye. The mutant was first identified by Harris et al. (1976) by a defect in fast phototaxis. Wild-type flies, when given a choice between ultraviolet and visible light, choose ultraviolet at a frequency of about 10:1 ; *sev* mutant flies, when given the same choice, prefer to phototax towards visible light at a frequency of about 25:1. In *sev* mutants, each of the ommatidia lacks one of the elements of the patterned array, namely, photoreceptor cell R7. The gene was mapped to the proximal edge of the 10A1-2 band of the X chromosome (Harris et al., 1976; Zhimulev et al., 1981). By genetic mosaic analyses (Harris et al., 1976; Campos-Ortega et al., 1979), it was shown that sev^{+} gene activity is required in R7 in order for an R7 to be present; the phenotype cannot be rescued by the presence of sev^{+} gene product in any or all of the other R cells and / or pigment cells. Therefore, sev^{+} gene product in presumptive R7 is both necessary and sufficient for the presence of an R7 in the adult eye.

Examination of the third instar eye disc by electron microscopy (Campos-Ortega et al., 1979) showed that the *sev* phenotype does not result from degeneration of cell R7 during pupal stages. Clusters of cells in the posterior of sev^{+} eye discs show eight R cells, while in the mutant sev^{LY3}, there are only seven R cells per cluster. The developmental requirement of the sev^{+} gene product was confimed by making genetic mosaics of sev^{+} and sev^{LY3} clones in the third instar larva stage. In these studies, Campos-Ortega et al. (1979) demonstrated that sev^{+} activity is required autonomously in cell R7 during development of the eye. They also added an interesting twist to the autonomous requirement of R7 for sev^{+} activity. By making clones of *sev* mutant cells

0-12 hours before pupariation, *sev*^{LY3} R7 cells, as indicated by the linkage of markers, could be recovered. The perdurance effect occurred in almost 30% of the clones, and was estimated to last through one to three divisions. Therefore, although *sev*$^{+}$ activity is required autonomously in R7, this activity may be inherited through at least one division from a *sev*$^{+}$ precursor cell.

The developmental characteristics of *sev* mutant eye discs were compared to those of *sev*$^{+}$ eye discs using techniques of electron microscopy (Tomlinson and Ready, 1986). In the wild type, as discussed above (**Cellular differentiation in the eye disc**), preclusters of five cells form within the morphogenetic furrow; these five cells will form R2, R3, R4, R5 and R8. To each precluster is added presumptive R1 and R6; then presumptive R7 completes the group. The construction of the ommatidium is accompanied by the migration of the presumptive cell nuclei; as a cell joins a cluster, its nucleus rises apically; cells that are destined to form neurons subsequently elongate an axon, and the nucleus migrates to a slightly less apical position. After the rise of the presumptive R7 nucleus, the nuclei of the presumptive posterior and anterior cone cells make their apical migration, the posterior cone cell adjacent to the differentiating R7, and also contacting R1 and R6; the anterior presumptive cone cell contacts R3 and R4. Tomlinson and Ready (1986) examined the sequence of events in *sev* mutants. According to their data, a cell in the position of presumptive R7 is found in the mutant at early stages, before and during the presumptive R7 nucleus migration stage. This cell, however, does not elongate an axon, and its nucleus does not sink basally. Rather, their data suggest that the nucleus of the cell in the position of presumptive R7 assumes the position of the nucleus of a posterior cone cell; however, there is no resulting duplication of the posterior cone cell in *sev* mutant ommatidia. The data presented are limited, but if the interpretation is correct, it suggests that a *sev*$^{-}$ cell in the position occupied by presumptive R7 is unable to interpret the cues presented that promote differentiation into an R7 neuron. This interpretation preserves the cell-autonomous developmental

requirement of *sev*$^{+}$ function.

Predictions

The developing compound eye of *Drosophila* as discussed in the preceding sections provides a system at the confluence of many different areas of study, including pattern formation, the concepts of cell commitment and competence, cell-cell interactions during development, and neural differentiation. The developmental characteristics of the eye allow for speculation regarding what types of molecules will be involved in its development, from molecules required on the cell surface to intracellular machinery for effecting differentiation.

Growth factors and growth factor receptors have often been implicated in development of the vertebrate nervous system. Factors that affect cell proliferation and differentiation of vertebrate neurons have been identified, as have factors with neurotrophic effects (see, for example, Hanley, 1988; Morrison et al., 1987; Walicke, 1988; DiCicco-Bloom and Black, 1988). The concentration of the factor is reflected intracellularly by the enzymatic activity of its corresponding receptor; thus, the factor-receptor system can serve as a means of transmembrane communication between cells or between cells and the extracellular matrix.

Several genes with similarity to vertebrate proto-oncogenes, growth-factor receptors, and growth factors have been cloned from *Drosophila*. Many of them appear to be expressed in the eye disc, especially posterior to the morphogenetic furrow. The transcript of the *Drosophila* homolog to the proto-oncogene c-*src* is expressed in this region (Simon et al., 1985), as well as a protein similar to the human insulin receptor (Piovant and Léna, 1988). The N^{+} protein, which plays a role in eye development, has regions of similarity to epidermal growth factor (Wharton et al., 1985; Kidd et al., 1986). Mutations at the *Drosophila* Abelson proto-oncogene (*abl*) homolog often have pupal lethal effects, but flies that survive have pattern defects in the adult compound eye. These

ommatidia have varying numbers of photoreceptor cells, abnormal rhabdomeres, and irregular pigment cell formations (Henkemeyer et al., 1988). The proteins c-*src*, insulin receptor and *abl* have been shown to possess protein tyrosine kinase activity (for review, see Yarden and Ullrich, 1988).

The proteins encoded by the family of *ras* proto-oncogenes bind guanine nucleotides, have GTPase activity and are membrane-associated; they are presumed to behave similarly to G-proteins (for review, see Barbacid, 1987). The *Drosophila ras* gene was cloned, and a dominant allele (putative constitutively active) of the gene was constructed under control of the heat shock promoter (Bishop and Corces, 1988). A shift to the inductive temperature to permit manifestation of the dominant effect was often lethal, but brief, one-hour shifts performed during the mid-to-late third instar stage resulted in a prominent scar across the adult compound eye. The scar consisted of unpigmented, irregular and fused ommatidia. The developmental effects were not described in detail, but the evidence strongly suggests that GTP-binding proteins, in addition to tyrosine kinases, may function in eye development.

Classical second messenger systems may be acting intracellularly for information processing. The possibilities include differential phosphorylation of protein substrates and variable cyclic nucleotide concentrations, both of which can have profound effects upon a cell by changing Ca^{2+} concentrations and phospholipid make-up of cell membranes. Since differentiation in the eye disc involves changes in the expression of epitopes (Zipursky et al., 1984; Venkatesh et al., 1985), it also may require the molecular machinery for inducing changes in gene transcription, which are expected to occur during differentiation. Therefore, receptors linked to a transcriptional cascade are likely to form a central part of the mechanism used by the retina precursor cells to control their differentiation.

Goals

The goals of my graduate research in this area were many. The foremost was to become familiar with the system and with the techniques necessary to analyze the development of the *Drosophila* compound eye. The second was to make some contribution to the field, to answer some questions, if also to raise new ones.

This thesis concerns the detailed study of one of the genes involved in formation of the adult compound of eye of *Drosophila*. Mutations in the *sev* gene have a subtle, reproducible and fully penetrant effect upon development of the reiterative pattern. With Dr. Utpal Banerjee, a postdoctoral fellow in the Benzer group, the molecular characterization of the sev^{+} gene was undertaken. The goals were to clone the sev^{+} gene, determine its pattern of expression and its localization during development of the retina. These results are discussed in Chapters II-IV. The second part of the work involved the characterization of other genes that, when mutated, give rise to adult eyes with altered morphology. Late third instar eye discs from 20 eye mutants were stained with monoclonal antibodies that highlight various patterns in the developing array. The eye disc phenotypes were then compared with adult eye phenotypes. The goal in this part was to identify genes, like *sev*, that function during the development of the eye. The results are presented in Chapter V. It is the hope that these studies have opened up new avenues of research, which investigators can follow in order to understand better the complex molecular events governing the development of the adult compound eye.

Figure 1. The morphology of the adult visual system.

(A) Scanning electron micrograph of the adult head. The compound eye of *Drosophila* comprises approximately 800 facets, or ommatidia, in a precise, reiterative array. Anterior is to the right.

(B) At closer study, each facet is hexagonal, and has a sensory bristle extending from the anterior corner of each facet. Anterior is to the right.

(C) Transmission electron micrograph of a tangential section through an eye. The precise array of facets reflects the internal structure of the ommatidium. Each ommatidium comprises eight photoreceptor neurons (R1-R8) as well as other non-neuronal cells. The rhabdomeres of the R cells extend into the interretinular space. In this section through the distal retina, the rhabdomeres of R1-R6 have a trapezoidal arrangement around the central R7 rhabdomere, which extends in between R1 and R6. The opposite polarity of the R7 rhabdomere entrance into the interretinular space reflects the equator, as seen across the center of the photograph. In more proximal planes of section, one would see the rhabdomere of R8 rather than R7; it enters the IRS from between R1 and R2. Anterior is to the right.

(D) A horizontal section through the adult head stained with the MAb 24B10, which is specific for photoreceptor cells and their axons. The axonal projections of R1-R6 terminate in the lamina, the first optic ganglion, while the axons of R7 and R8 terminate at different locations in the medulla, the second optic ganglion.

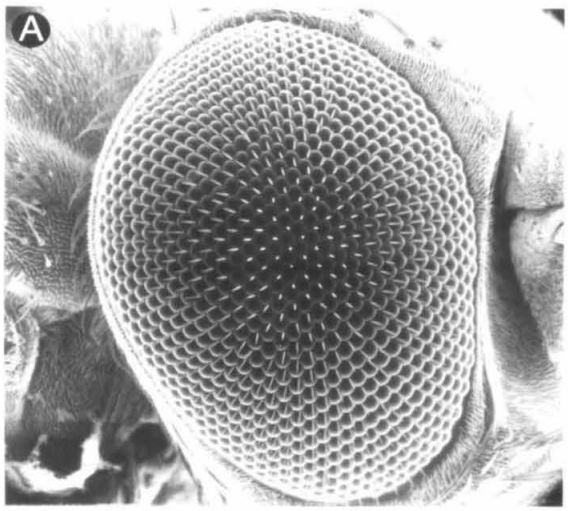
A

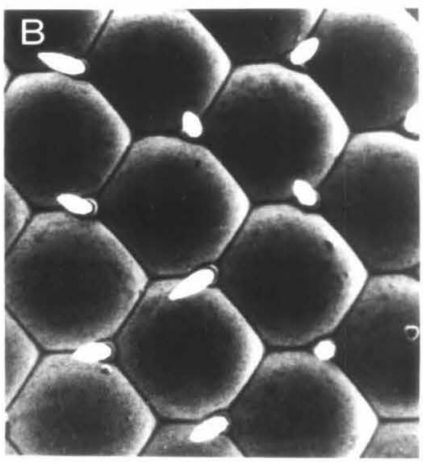
B

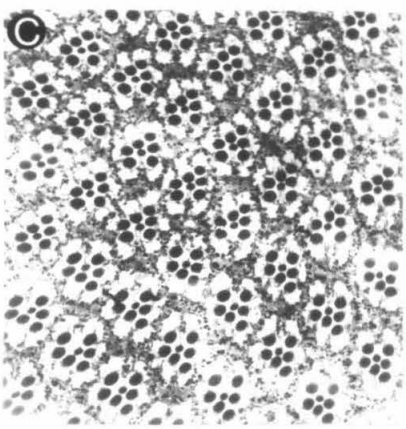
C

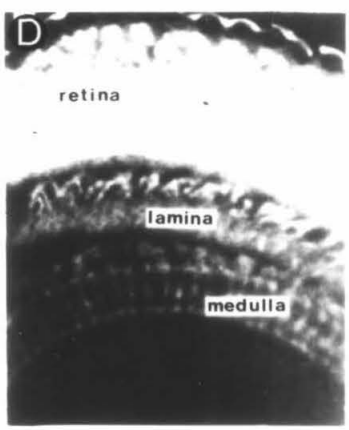
D
retina
lamina
medulla

Figure 2. The eye-antennal disc and optic lobe.

(A) A scanning electron micrograph of a late third instar eye-antennal imaginal disc attached by the optic stalk to the optic lobe. The arrow head marks the displacement of the morphogenetic furrow, which indicates the anterior limit of differentiation. Anterior is to the right.

(B) A similarly staged preparation as in part A is stained with the MAb 22C10, which stains peripheral neurons and their axons. The developing photoreceptors in the eye disc are stained, beginning just posterior to the morphogenetic furrow (arrowhead). Their axons extend posteriorly through the optic stalk, and into the developing optic lobe. Anterior is to the right.

(C) Schematic representation of the developmental events occurring in an eye disc during the late third instar. Ahead (anterior) of the furrow, undifferentiated precursor cells divide. At the morphogenetic furrow, preclusters of five cells form; they are presumptive neurons R2, R3, R4, R5, and R8. Cells that are not clustered divide, and their daughters join the preclusters. Presumptive R1 and R6 are added first; then R7 completes the photoreceptor complement per cluster. Upon this cluster will be added the presumptive cone cells, presumptive pigment cells, and the cells that will comprise the hair-nerve group. Anterior is to the right.

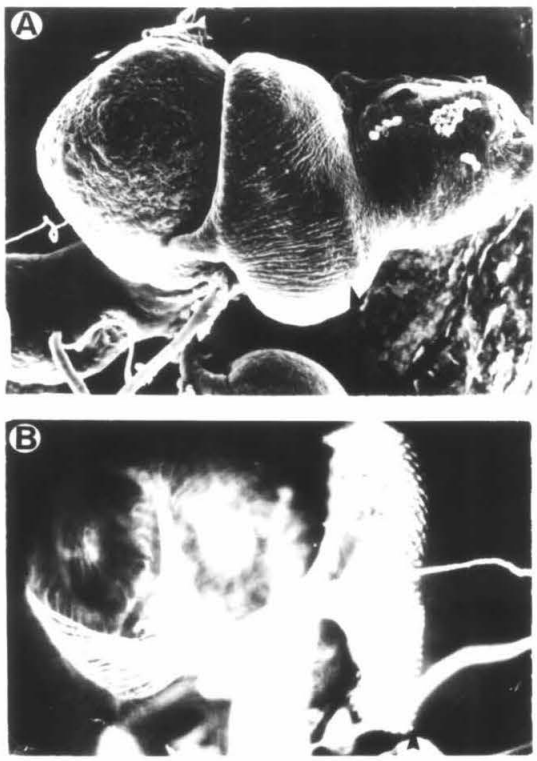
A
B
C
Posterior
Anterior
Morphogenetic Furrow
Mature 8 cell clusters
5 cell preclusters
Unpatterned cells

Chapter II

Molecular Characterization of *sevenless*, a Gene Involved in Neural Pattern Formation in the *Drosophila* Eye

Introduction

In this chapter, the molecular characterization and expresson of the *Drosophila sevenless* (*sev*) gene is described. The data were published in the following manuscript:

Banerjee, U., Renfranz, P.J., Pollock, J.A., and Benzer, S. (1987a). Molecular characterization of *sevenless*, a gene involved in neural pattern formation in the *Drosophila* eye. *Cell* **49**, 281-291.

A review of the *sev* phenotype and our experimental rationale are illustrated in Figure 1. Cell clustering occurs in the wake of a morphogenetic furrow that sweeps from posterior to anterior on the larval eye-antennal imaginal disc (Ready et al., 1976). At a given time, the various developmental stages can be observed in a single disc. Just behind the furrow, preclusters of five cells develop (photoreceptor cells R8, 2,5,3,4). Later, cells R1 and R6 join; then R7 completes the group. As shown in Figure 1B, each bundle of axons in the optic stalk (one bundle from each cluster in the eye disc) contains eight axons, one from each photoreceptor. In the fully developed adult eye (Fig. 1C), the outer positions in the trapezoidal pattern in each ommatidium are occupied by cells R1-6. R7 and R8 are central, R7 being directly above R8.

In the *sev* mutant, R7 specifically is absent in each ommatidium (Figs. 1D and 1F). The bundles through the optic stalk consist of only seven axons (Fig. 1E). This X-linked mutation maps to the 10A1-2 band of the X-chromosome at map position 1-33.2$\pm$ 0.2 (Harris et al., 1976; Zhimulev et al., 1981). Harris et al. (1976) and Campos-Ortega et al. (1979) demonstrated that the *sevenless* phenotype is cell autonomous. The sev^+ gene therefore appears to assist a developmental decision in the precursor of R7, at a specific time.

To explore the mechanism, certain basic information is needed, such as the nature of the sev^+ gene product, the time in development when the gene is expressed, and the

relation of that time to the other events occurring in the disc. It is also important to know whether the gene is expressed uniquely in the putative R7 cell, in other cells, or in both. Does it continue to be needed at all stages of development, or is its action needed only to scale one hurdle in a developmental sequence? To obtain such information, we undertook the cloning of the gene, the characterization of its expression, and the identification of its product. [Hafen et al. (1987) also isolated the *sev* gene, using a different method.]

Results

P-Element induced alleles of *sev*

Three new alleles of *sev* were created by hybrid dysgenesis (Engels and Preston, 1979; Bingham et al., 1982; Rubin et al., 1982), in crosses mating males of a "P cytotype" strain with females of an "M cytotype." In such a cross, the P-transposable elements in the germline of the progeny are mobilized, and frequent mutations result.

Two screening techniques were used. The first was to adapt the optical phenomena of pseudopupil and deep pseudopupil (Franceschini and Kirschfeld, 1971a, 1971b) to rapid screening of large numbers of flies. The deep pseudopupil technique (Figs. 1G and 1I) was employed for the primary screen since it could be used on live, etherized flies. Mutant candidates were mated pairwise to attached-X females, and their phenotypes confirmed by the pseudopupil method (Figs. 1H and 1J).

A second screening method was behavioral, based on the color choice difference in phototaxis between *sev* and wild-type flies (Harris et al., 1976 ; Heisenberg and Buchner, 1977; Gerresheim, 1981). Cell R7 is a strong UV receptor. In the T-maze paradigm we used, wild-type flies, when given a choice between ultraviolet (350 nm) and green light (550 nm), chose UV over green 25:1, while *sev* mutants typically made the reverse choice 10:1.

Using the deep pseudopupil screening method on 12,500 male progeny from

dysgenic crosses, two P-element induced alleles, *sev*^{P1} and *sev*^{P2}, were isolated. Another 22,400 male and female flies were screened by the color-choice paradigm. This gave rise to a third P-allele, *sev*^{P3}. These three mutants fully expressed the sevenless phenotype and were stable in a P-background.

EMS-induced alleles

When this work was started, two alleles, *sev*^{LY3} and *sev*^{dr1}, were available, having been induced in our laboratory by treatment of wild-type flies with ethylmethane sulfonate (EMS). Using the color-choice paradigm to screen 30,000 EMS mutagenized chromosomes, we isolated five new alleles, *sev*^{E1} - *sev*^{E5}. Five additional alleles isolated by Dr. F. Gerresheim (1981) and three alleles from the laboratory of Dr. D. Ready were kindly sent to us. All of the EMS- and P-element induced alleles were fully recessive and failed to complement the original mutant *sev*^{LY3}. All were checked anatomically in plastic sections, and ten were examined by electron microscopy. All showed the same phenotype, i.e., the lack of cell R7.

Transposon tagging of the *sev* gene

The P-element-induced mutant *sev*^{P1} was chosen for further characterization. To locate the P-elements in its genome, radioactively labelled P-element DNA was hybridized *in situ* to salivary gland chromosomes from *sev*^{P1} larvae. Approximately fifty P-element insertion sites were identified, including one at band 10A1-2, the location of the *sev* gene. A clone corresponding to this latter insert was isolated from a library constructed with *sev*^{P1} DNA and was designated λ-sev^{P1}. Figure 2A shows the localization of this clone on the X chromosome. A central 5.9 kb SalI fragment of the clone hybridized to P-element DNA (Fig. 2B).

Previous genetic mapping has shown that *sev* is located between the deficiency break points of Df(1)^{vM6} and Df(1)*ras-v*^{17Cc8} (Zhimulev et al., 1981). Mapping of

clone λ- sev^{P1} by chromosomal *in situ* hybridizations to these deficiencies localized the clone to this position (data not shown).

Genomic DNA map of the *sev* region

Genomic DNA clones overlapping with clone λ-sev^{P1} were isolated by screening genomic libraries constructed from wild-type (Oregon-R and Canton-S) flies. Figures 2B and 2C show a map based on these clones. By mapping clones, covering over 120 kb of DNA from the region, we found that the clone λ-sev^{P1} reflects a deletion of 53 kb of DNA from the genome of the mutant sev^{P1}. This is best illustrated in Figure 3A, where a Southern blot of genomic DNA from mutant sev^{P1} showed no cross hybridization when those fragments of clone λ-4G(5) were used as the probe. Thus, this segment of DNA is deleted from the genome of sev^{P1}. Figure 3A also highlights the restriction fragment differences detected by this probe between the genomic DNA of mutant sev^{P3} and the parental strain $25A^{var}$. Mapping showed that the DNA rearrangement in sev^{P3} was also a deletion, but of only 11 kb (Fig. 2C). This mutant thus affords a finer localization of the *sev* gene. The genomic clone λ-11H(1) spans most of the latter deleted region.

Restriction fragment polymorphism in an EMS-induced *sev* allele

Genomic DNA was prepared from each of 18 alleles of *sev* and cut with two different sets of restriction enzymes. These digests were all probed on Southern blots with genomic clone λ-11H(1). The EMS-induced allele sev^{f1} was found to differ in its restriction fragment pattern from the others (Fig. 3B), including sev^{d2}, which was isolated by Gerresheim in the same mutagenesis and shares the same parental background with sev^{f1} (Gerresheim, 1981). The same restriction-site polymorphism was seen in sev^{f1} when compared with three other mutant alleles of identical genetic background (not shown). Finer mapping showed that although sev^{f1} is EMS-induced, it is not a point

mutant. As can be seen in Figure 3B, a 3.7 kb band is missing in this allele, and two additional bands at 5.7 kb and 2.3 kb arise. Mapping showed that this was due to an insertion into the 3.7 kb SalI-XhoI fragment, the left border of which is found at position 0 in Figure 2C. As will be seen below, this insertion disrupts only a single transcription unit in genomic clone λ-11H(1). This strongly suggested that this region of DNA corresponds to the *sev* gene.

Identification of the *sev* gene transcript

By Northern blot analysis, seven regions of transcription were identified within or flanking the 53 kb deletion of the mutant sev^{P1}. These are listed in Table 1. Among them, only three were located in the 11 kb deleted in the mutant sev^{P3}, and so were considered as candidates for the sev^{+} gene transcript. Restriction fragments of the genomic clone λ-11H(1) (Fig. 2C), which mapped to the region deleted in the sev^{P3} genome, were used to probe Northern blots of poly(A)$^{+}$ RNA isolated from wild-type imaginal discs, adult heads and adult bodies.

The 12 kb SalI fragment in the center of clone λ-11H(1) identified an 8.2 kb transcript in poly(A)$^{+}$ RNA from mass-isolated late third instar imaginal discs, as well as in adult heads, but not from adult body (note: however, see Chapter III). This fragment was used to isolate nine cDNA clones from head cDNA libraries. The longest, c2(3), was 4.7 kb.

The cDNA clones recognized the same 8.2 kb transcript in the wild type as did the corresponding genomic DNA used to isolate them. The tissue specificity of this transcript is shown in Figure 4. It was detected in late third instar imaginal discs, 5-12 hr whole pupae, and adult heads. It was not detected in 22-30 hour pupae, nor in adult body. This transcript was not detected by genomic DNA probes outside and flanking clone λ-11H(1). To test for possible effects of *sev* mutations on transcript expression, Northern blots were also done on the *sev* alleles sev^{P3} and sev^{LY3} using poly(A)$^{+}$ RNA prepared from

imaginal discs and adult heads. In the P-induced deletion mutant *sev*^{P3}, the 8.2 kb transcript was not detected in either imaginal discs or adult heads. Instead, two altered transcripts of 7.4 and 6.6 kb were found in both tissues when the cDNA clone c2(3) was used as probe. However, these altered transcripts were not recognized by a shorter cDNA clone c2(6), nor with the leftmost 6 kb SalI fragment of λ-11H(1), since this DNA is deleted in the genome of *sev*^{P3}. Thus, the right breakpoint of the deletion in mutant *sev*^{P3} is within the transcribed region, as illustrated in Figure 2C.

In the EMS-induced allele *sev*^{LY3}, the 8.2 kb transcript was present in approximately normal abundance, size and tissue specificity as in the wild type. Since this mutant was EMS-induced, it could produce a transcript containing missense or nonsense codons translated into a defective product. As will be seen below, some of the EMS-induced alleles produced transcripts detectable by *in situ* hybridization on tissue, while others apparently did not.

Using other DNA probes within the 11 kb span of genomic DNA that is deleted in the mutant *sev*^{P3}, two other transcripts were detected in poly(A)$^+$ RNA derived from various larval, pupal, and adult tissues. Both hybridized to the leftmost 6 kb SalI fragment of clone λ-11H(1). Neither of these transcripts, 0.7 kb and 3.2 kb in length, was detected in wild-type third instar larval imaginal disc poly(A)$^+$ RNA. The first was expressed in whole pupae, in adult head, and in adult body, while the second was expressed only in 5-12 hour pupae. The *sev* mutation is cell-autonomous (Campos-Ortega et al., 1979); *sev*$^+$ activity in cell R7 should occur at or before the crucial time of decision in the eye disc. It has also been shown by genetic mosaic experiments (Campos-Ortega et al., 1979) that the time of action of the *sev* gene is in the third instar larva. This ruled out the 0.7 kb and 3.2 kb transcripts as candidates for the *sev* gene, since they were transcribed only at later stages, after the furrow has traversed the disc and the *sev* phenotype is manifest. The 8.2 kb transcript, on the other hand, was expressed in third instar larval discs. The genomic DNA corresponding to this transcript contains an

insertion in the EMS-induced allele sev^{f1}, affecting only this transcript and producing the sevenless phenotype. The evidence thus indicates that this is the transcript of the *sev* gene.

Localization of *sev* gene transcripts in wild-type tissue

cDNA clone c2(3) and corresponding gel-isolated restriction fragments from genomic DNA clones were ^{3}H-labelled and used for *in situ* hybridization to eye discs from late third instar larvae and prepupae. As shown in Figures 5A and 5B, a whole mount eye-antenna disc, probed with the c2(3) insert fragment, revealed sev^+ transcripts from just behind the morphogenetic furrow to the posterior end of the disc.

When seen in cross section (Figs. 5C and D), the sev^+ signal extended through a large part of the thickness of the disc immediately behind the furrow. More posteriorly, corresponding to later stages of development, the signal condensed to the apical surface of the disc. Clustering of silver grains could be discerned in the posterior region of the disc, both in the whole mount preparation and in sectioned discs (Figs. 5A-D).

The level of hybridization becomes quite apical in the posterior region of the disc, as shown in Figures 5C and 5D. As development continued, and the morphogenetic furrow completed its traversal of the disc, the sev^+ transcript remained restricted to the apical region. This is illustrated in Figures 5E and 5F for the eye disc of a 6-9 hr old white prepupa. For comparison, Figures 5G and 5H show the localization, in a similarly staged disc, of the transcript of the 24B10 gene that is expressed in all the photoreceptor cells (Zipursky et al., 1984; Zipursky et al., 1985; Van Vactor et al., 1988; Reinke et al., 1988). The 24B10 signal extended through a thicker layer, the apical two-thirds of the disc. The difference in the observed patterns is striking. It could represent expression of sev^+ in a subset of cells whose perikarya are apically positioned.

Figure 6 shows the scenario of sev^+ transcription at later stages of prepupal development. The robust, tissue-specific signal found in early disc development continues

through prepupation, then fades prior to pupation, as the eye disc everts. This is consistent with the Northern blot results (Fig. 4).

Northern blots clearly indicated that the *sev* transcript is expressed, albeit at a low level, in the adult head [probably at a level of one out of every four- to five-hundred thousand RNA species (see Experimental Procedures)]. We have not yet been able to determine the exact tissue localization by *in situ* methods. The level of expression was lower than our limit of detection. The significance of this transcription in the adult is currently unknown.

Transcription in *sev* mutants

All the mutant alleles were tested by *in situ* hybridization, the cDNA clone c2(3) as probe. Examples of the results are illustrated in Figure 7. In the case of the *sev*^{P1} allele, where the entire gene is deleted, no *in situ* hybridization signal was apparent. In *sev*^{P3}, where part of the gene is deleted, and abnormal transcripts were found in Northern blots (above), *in situ* hybridization showed a signal with essentially normal tissue specificity, but of lower intensity. While the majority of the EMS-induced alleles gave normal hybridization signals, *sev*^{E3} gave a reduced level of signal, and *sev*^{elm} and *sev*^{fig} gave none that were detectable with the c2(3) cDNA clone used as probe. The occurrence of EMS-induced mutants lacking the transcript corresponding with cDNA clone c2(3) is further evidence of the correct identification of the *sev* gene by this cDNA probe.

As will be discussed in Chapter III, poly(A)$^+$ RNA from adult heads of each of the *sev* alleles was probed with cDNA clone c2(3). For the most part, the data concur with the *in situ* studies, and indicate that seven of the alleles produce a stable transcript, albeit a defective one, and three have a reduced level of transcript.

Localization of *sev* protein

The cDNA clone c2(6) was isolated from a λ-gt11 expression library. It was found

to contain a 1.8 kb insert, and expressed a 180 kDa fusion protein. About 60 kDa was from the carboxyl terminus of the *sev* gene; the rest was bacterial β-galactosidase. The SDS- polyacrylamide gel-isolated fusion protein was injected into a mouse and an immune serum was obtained. This produced a specific staining pattern that commenced immediately behind the furrow in the eye disc (Fig. 8A). This pattern was absent in the mutant sev^{P1} (Fig. 8B), confirming that the antigen is a product of the sev^{+} gene.

Figure 8C shows the posterior region of a wild-type disc at higher magnification, in phase contrast. Rows of roughly square clusters are readily discernible, each cluster covering an area of about 100 μm^2. The antibody staining in each cluster of the same disc (Fig. 8D) was restricted to an area of about 15 μm^2. The staining had a flattened toroidal shape, with a weakly stained center, and was located near the apical surface of the epithelium. A wild-type disc stained with a different antibody (MAb 6B11), which highlights the membranes of the photoreceptor cells is shown in Figure 8E. This disc was photographed at the same magnification, providing a scale for comparison. The ringlike staining of the sev^{+} protein is clearly much smaller than a whole cluster, and compared with the membrane stain, the staining is more diffuse.

Discussion

To obtain P-element-induced mutants, we started with a stock that already contained a P-element cytologically close to the map position of the *sev* gene, and that showed variable expression of the sevenless phenotype (see Experimental Procedures). The expectation was that mobilization of this P-element might excise parts of the *sev* gene. Indeed, the two stable P-alleles that have thus far been analyzed, sev^{P1} and sev^{P3}, both show deletions of different amounts of genomic DNA from this region.

An 8.2 kb trancript, mapping to the regions deleted in the mutants and to genomic clone λ-11H(1), was expressed in the developing eye imaginal disc, posterior to the morphogenetic furrow. Since the *sev* mutation is cell-autonomous, and since neuronal

differentiation of the photoreceptor cells occurs immediately behind the furrow (Ready et al., 1976; Tomlinson, 1985), this was the best candidate for the *sev*$^{+}$ transcript. The 8.2 kb transcript was not detected by genomic segments outside the span of clone λ-11H(1). Tissue *in situ* hybridization experiments showed it to be absent in strain *sev*^{P1}, and Northern blots showed it to be altered in size in *sev*^{P3}. The latter mutant showed, instead, two smaller transcripts recognized by a longer cDNA clone, but not by a shorter one, suggesting that the deletion in *sev*^{P3} cuts into the transcribed region of the *sev* gene. Since the 3' end of the gene is deleted, the occurrence of two transcripts could be due possibly to weak termination signals. Three of the EMS-induced alleles tested by tissue *in situ* hybridization showed weak or no expression of the 8.2 kb eye disc RNA. Also, one EMS allele (*sev*^{f1}) showed restriction fragment changes because of an insertion into the transcribed region. The *sev*^{f1} allele nevertheless produces a transcript of approximately normal size (data not shown). However, comparison of our data with those of both Basler and Hafen (1988) and Bowtell et al. (1988) shows that there are three introns within the restriction fragment that is polymorphic in this allele.

Taken together, the evidence indicates that the 8.2 kb trancript is the product of the *sev* gene, and that genomic clone λ-11H(1) contains the entire gene. The possibility cannot be excluded that there are microexons outside the clone.

sev^{P1} is a null allele

In the P-element-induced mutant *sev*^{P1}, the *sev* gene appears to be completely deleted, and the 8.2 kb transcript is absent. This should therefore present the null phenotype. Male flies in this stock are viable and fertile in the hemizygous condition, and their eye structure is like those of other alleles. Thus, lack of R7 and altered photochoice behavior seems to be the null phenotype of *sev*. Females homozygous for this deletion are viable and lack R7, but are sterile. However, the deletion is large and is known, by the production of different transcripts (Table 1), to cover other genes, so this sterility may not

be related to the *sev* gene. No such sterility was observed for any of the other alleles, including sev^{P3}, which contains an 11kb deletion. Note that all the screening techniques used to isolate the current *sev* alleles were designed to isolate mutants that lacked cell R7 but were hemizygous-viable. This automatically selected against other possible phenotypes or lethality that could be associated with certain mutations in the gene.

From the region in and around that deleted in sev^{P1}, at least seven transcription units were identified. The tissue and stage specificity of the transcripts varied (Table 1). Zhimulev et al. (1981) performed a fine cytogenetical analysis of the region of the X chromosome where the *sev* gene maps. In the bands covering 9F12-10A7, eleven complementation groups have been identified, covering about 0.89 map units of recombination. Six of the groups are essential loci; i.e., mutations in them are lethal. The two groups that immediately flank *sev* are *ms(1)BP6* distal and *slm* proximal. The distal gene, when mutated, has a male sterile phenotype, and *slm* a semilethal phenotype. Since sev^{P1} males are fertile and appear fully viable, it is unlikely that these two flanking loci are disrupted by the 53 kb deletion. Therefore, we are left with six transcripts around the *sev* locus with unknown functions; some of them show interesting patterns of expression. The data indicate that this region of the X chromosome by no means has been saturated for mutations.

The size of the haploid *Drosophila* genome is estimated at 165 million basepairs (see Kornberg, 1980). If the *sev* region were at all representative in terms of number of transcription units per kilobasepair (approximately one per 10 kb), it would indicate that there are approximately 16,500 unique transcripts in the *Drosophila* genome. Levy and Manning (1981) estimated, by RNA sequence complexity studies, that there are approximately 16,000 transcripts expressed in larvae, pupae and adults. Interestingly, in 1947, Muller estimated by genetic data, e.g., frequencies of mutations and cross-overs, that the number of genes in *Drosophila* could be 10,000.

Tissue and stage specificity of *sev*$^{+}$ gene expression

In the eye disc, *sev* transcript was seen immediately behind the furrow and in the more fully differentiated posterior portion of the disc. In sections of the disc perpendicular to the furrow, the signal immediately behind the furrow was seen in the entire cross section of the disc, while more posteriorly, it became restricted to the apical level. Antibody staining confirmed that the protein product is also apically localized. The cells in the eye disc form an epithelium, with processes attached to the apical and basal surfaces, with each cell body widest in the region of its nucleus. Tomlinson (1985) described the movements of the various photoreceptor cell nuclei. Immediately behind the furrow, the nucleus of the presumptive cell R7 is positioned basally, about 50 μm below the apical surface. More posteriorly, it rises to within 8 μm of the apical surface. The nuclei of cells R1, R6, and the cone cells follow a similar pattern, the time and extent of rise varying with each cell type. In contrast, the nuclei of the other photoreceptor cells (R2,3,4,5,8) occupy the apical half of the layer, both immediately behind the furrow and more posteriorly. The observed expression seen of the *sev*$^{+}$ gene shifted to the apical surface, as would be expected for the perikarya of cells R7, R1 and R6 and the cone cells. However, apical expression was also seen just behind the furrow, as would be expected if transcription occurred in some or all of the other cell types.

Transcription in mutants

While some of the EMS-induced alleles lack the transcript, others did express it. This is not surprising, since EMS-induced mutants could express transcripts that are ineffective as a result of a single codon change. In *sev*^{LY3}, the transcript was identical in length to the one in the wild type, and its tissue and temporal specificity were also normal. Similarly, in the P-allele *sev*^{P3}, although the transcripts were altered in size, they were expressed in the correct tissue and at the correct time. The fact that expression can occur in *sev* mutants, especially in the adult head, is an important point, since mature R7

cells do not develop in the eye discs of any of the *sev* alleles and the mutation is cell autonomous, indicating that expression is not unique to presumptive and / or mature R7.

Mechanisms of *sev* action

While the exact link between the sev^+ gene product and differentiation of cell R7 is as yet unknown, two extreme models can be discussed in light of our results.

In the first model, all or most postmitotic cells could be expressing a sev^+ product, but only a cell that receives the correct cues, e.g., from its neighbors, utilizes or activates this protein. In this model, the cues *per se* do not turn on the sev^+ gene but only help one of several expressing cells to differentiate and display the R7 phenotype. The expression seen in mutants lacking R7 would be due to the expression in these other cells.

In the second model, positional cues help turn the sev^+ gene on in a specific precursor cell that eventually differentiates to become R7. In this scenario, expression of the gene is limited to cell R7 and the expression seen in mutants is then from the presumptive R7 cell which, although it fails to undergo neuronal differentiation, continues to make a transcript.

Both models preserve the requirements of pluripotency of undifferentiated cells and cell autonomy of the *sev* mutation that requires sev^+ activity in cell R7. Both models also recognize the need for positional information that determines which cell assumes the fate of R7.

At this stage of the study, it was not possible to rule out either of these models based upon the initial protein localization by the mouse tail serum, although transcription in the *sev* alleles would indicate that the former possibility is more likely. The matter is discussed again in Chapter IV.

With this study of the *sev* gene, we only began to answer some of the basic questions about its function. We learned that the gene encodes a rather long transcript, which is expressed posterior to the furrow, in a morphogenetically important area, at a

time when the photoreceptor clusters are being assembled. The *sev* protein is expressed similarly. The cloning of the gene and the localization of its products are, however, only a first step in solving an intriguing problem of determination in an individual neuron. The molecular studies described provide further insights into the problem and materials with which to attempt to find its solution.

Experimental Procedures

Strains and materials

Flies were raised on standard cornmeal-yeast-agar at 25 °C and 40% humidity in a 12 hr light-dark cycle. Strain Df(1)$^{v\text{M6}}$ and Df(1)*ras-v*$^{17\text{Cc8}}$ were obtained from Zhimulev et al. (1981). The P-type stocks were obtained from W. Benz in W. Engels' laboratory. Five alleles of *sev* (x1, d2, f1, f3IE, and x3) were isolated and kindly sent to us by Dr. F. Gerresheim, three alleles (elm, fig and bb) were gifts of Dr. D. Ready, and the remaining alleles (P1-P3, E1-E5, LY3, and dr1) were isolated in our laboratory.

Mutagenesis

The P-type stocks already contained P-elements in the vicinity of the 10A1-2 band of the X chromosome, where the *sev* gene maps. Close examination revealed that in one of them (stock 25A), some sevenless ommatidia occurred in about one per thirty eyes. The number of sevenless ommatidia in a variegated eye varied from as few as two to several hundred, with no obvious spatial pattern. Since this suggested the possibility of the presence of a P-element close enough to be affecting the *sev* gene, such a variegated male was mated to "P-type" attached-X females to set up a stock designated 25A$^{\text{var}}$. This stock showed variegation similar to the original 25A stock, i.e., some sevenless ommatidia in about one per thirty eyes. Chromosomal *in situ* hybridization of P-element DNA showed the presence of a P-element insertion site near the 10A1-2 band. This stock was used as a

source for male P-type flies in the dysgenic crosses, the idea being that mobilization of the P-element causing the variegation could produce a heritable and fully expressed *sev* phenotype.

For dysgenic crosses, the following mating scheme was used:

$25A^{var}/Y$ (P) x XX/Y (M)

↓

F1 (P/M) mated *inter se*

↓

F2 screened for *sevenless* phenotype.

Male mutants isolated from the screen were mated to attached-X/Y females of P-cytotype and the stocks were maintained as such, or were homozygosed using an FM7 balancer stock with a P-background.

EMS-induced mutagenesis was done according to Lewis and Bacher (1968).

Screening for *sev* mutants

A. Optical methods

We used the following modifications of the methods of Franceschini and Kirschfeld (1971a, b) for rapid screening and characterization of *sev* mutants.

Deep pseudopupil: An inverted microscope was used. On a strip of double-stick tape attached to a glass slide, etherized flies were placed ventral side up, wings down and proboscis at an angle of about 40° upward. A condenser focussed a bright light source, from above, through a 1mm aperture and a heat filter, onto the front of the head. With this antidromic illumination, the deep pseudopupil was observed from below by focussing a

10X objective at the center of curvature of the eye.

Pseudopupil: For closer examination of mutant candidates, the pseudopupil method was used. A 1 X 3 cm^2 plexiglass piece, 0.16 cm thick, was bevelled and polished at a 40° incline along the 1 cm edge, and glued to a glass microscope slide. Using nail polish, fly heads were attached so that they lay on the incline, eyes upward. A drop of immersion oil was placed on the eye, thus optically neutralizing the cornea. The pseudopupil pattern was observed in a microscope by passing light antidromically from below, using a condenser with a small aperture, and viewing with a 100X Zeiss oil-immersion objective. This method was used only for secondary testing, after a stock of a putative mutant had been set up.

B. Behavioral method

A T-maze apparatus was used for the color-choice phototaxis test. Flies were placed in a middle chamber that could be slid into position between two transparent plastic tubes, each illuminated from the end, one with green light, the other with UV. A fiber-optic tungsten source was used for green, and a 25 Watt germicidal lamp for UV, filtered, respectively, with interference filters peaked at 550 nm and 350 nm. For each trial, about 25-50 flies were light adapted under diffuse white fluorescent light for 15 minutes, then tested in the maze. The apparatus was lightly tapped during the 20 second test period. The intensity of light was empirically adjusted such that sev^{LY3}, the original allele, chose green over UV 10:1, while wild-type Canton-S flies chose UV over green 25:1. In screening for mutants, flies that consistently chose green in four trials were examined by the optical methods for the sevenless phenotype.

Histology

Tissue was fixed in 1% formaldehyde and 1% glutaraldehyde and postfixed with 1% osmium tetroxide, stained in uranyl acetate (for EM only), dehydrated in ethanol and propylene oxide, and embedded in Epon 812. For light microscopy, 1μm thick sections

were stained with 1% toluidine blue. Thin sections (800-900 Angstroms) were made for electron microscopy.

Isolation of clone λ-sev^{P1}

DNA from *sev*^{P1} flies was partially digested with MboI. Fragments larger than 15 kb were selected by sucrose gradient and ligated to EMBL3 phage that had been digested with BamHI and EcoRI. An Amersham Corporation packaging kit was used, and the library was screened without amplification. Twenty-five thousand phages (corresponding to about 2.5 *Drosophila* genomes) were screened with labeled P-element DNA, and 133 positives were isolated. Plate lysates of these phages were combined into fourteen pools of about ten each. DNA from each pool was hybridized *in situ* to wild-type chromosomes, thus identifying the pool containing the band 10A1-2 insert. The ten clones constituting that pool were then tested individually, yielding the clone λ-sev^{P1} that hybridized to the 10A1-2 band.

Cloning and mapping

Phage library screening, nick translation, subcloning, Southern blots, isolation of DNA fragments, and restriction mapping were by standard methods (Maniatis et al., 1982). DNA hybridizations were carried out at 68 °C in 6X SSC, 5X Denhardt's solution, 0.4 mg/ml salmon sperm DNA, 10 mM EDTA, 0.5% SDS, and 10^6 cpm/ml of nick-translated DNA. Filters were washed at high stringency in 0.1X SSC and 0.5% SDS at 60 °C.

Labeled fragments of clone λ-11H(1) were used to probe cDNA libraries made from wild-type adult head poly(A)$^+$ RNA. Two million plaques were screened from a library constructed in the λ-gt11 system (Itoh et al., 1986), kindly provided for us by Dr. P. Salvaterra. This screening yielded four cDNA clones.

A second library, constructed in the λ-SWAJ vector system, from adult head

poly(A)$^+$ RNA, was kindly given to us by Dr. M. Palazzolo (Palazzolo and Meyerowitz, 1987). Two million plaques were screened, and five cDNA clones were isolated. From these data, we estimate that in the adult head, the *sev*$^+$gene is expressed at a level of one out of every four- to five-hundred thousand species (0.00025 to 0.0002% of cloned species).

Chromosomal *in situ* hybridization

Salivary gland chromosome squashes (Gall and Pardue, 1971) were hybridized at 37 °C with ^{3}H- or ^{35}S- labelled DNA in 10% dextran sulphate, 2X SSC, 50% formamide, and 1 mg/ml salmon sperm DNA. Two hundred thousand cpm of labelled probe were used for each slide. Slides were washed extensively in 2X SSC at room temperature, dehydrated in ethanol, coated with Kodak NTB2 emulsion (1:1 in water), and developed in D19 (1:1). Squashes were stained with 5% Giemsa to visualize bands.

Mass isolation of imaginal discs

The method of Eugene et al. (1979) was used with some modifications. In a population cage containing 20,000-40,000 Oregon-R flies less than two weeks old, eggs were collected on cornmeal agar and yeast paste in plexiglass boxes (10 X 13 X 30 cm^3). Three boxes at a time were put in the cage for 2-3 hr collections and were maintained at 25 °C in 80% relative humidity on a 12 hr light-dark cycle. Late third instar larvae were collected on day 5. Nine boxes yielded approximately 700 ml of larvae. They were chilled, passed through a meat grinder, sieved, and allowed several rounds of sedimentation for 30 minutes to 1 hr. The sedimented material was separated on a Ficoll step gradient and fractions enriched for discs were purified over glass.

Isolation of RNA and northern blot hybridization

Pupal and adult tissues were ground to powder in liquid nitrogen in a mortar and pestle,

but this step was omitted for discs. The first extraction was with a hot mixture of water-saturated phenol and 2X NETS (200 mM NaCl, 2 mM EDTA, 20 mM Tris HCl pH 7.5, 1% SDS). Four ml of phenol and 2 ml of 2X NETS were used per gram of tissue. The aqueous layer was re-extracted with phenol at least three times. Nucleic acids were twice precipitated at -20 °C with ethanol. Poly(A)$^+$ RNA was selected with oligo-dT cellulose, as described by Maniatis et al. (1982).

RNA was separated on 1% agarose-formaldehyde gels and blotted onto nitrocellulose paper as described by Maniatis et al. (1982), except that the gels were blotted immediately after electrophoresis. After baking, filters were prehybridized and hybridized at 42 °C, in 5X SSPE, 50% formamide, 0.1% SDS, 0.1mg/ml of salmon sperm DNA and 9.2% dextran sulphate. Nick-translated probe was added at 10-20 ng/ml solution (1-5 x 10^5 cpm/ng). After hybridizing overnight, filters were washed briefly at room temperature, then 4 X 20 min at 60 °C in 0.1X SSC and 0.1% SDS.

In situ hybridization to tissue

Third instar larvae were collected after they climbed out of the food. Older animals were staged as follows (Mitchell and Petersen, 1982): White prepupae at 0-3 hr of age sink in 1M NaCl, at 3-5 hr float in 1 M NaCl but sink in water, and at 5 hr float in water. Pupation begins at 11-12 hours.

For sectioning, whole larvae or prepupae were frozen in Tissuetek OCT compound on a block of dry ice and allowed to equilibrate at -20 °C. Some pupae were dissected from their cases prior to embedding. Frozen sections were cut at 6 μm. Serial section ribbons were placed on subbed microscope slides (Gall and Pardue, 1971), heated on a 50 °C hot plate for 2 min, and dried at room temperature over silica gel for at least one hour. In some cases, eye discs were dissected from migrating third instar larvae or prepupae and specifically oriented in OCT prior to sectioning.

Whole mount discs were either mass-isolated or individually excised, and fixed for

hybridization following Kornberg et al. (1985).

Nick-translated, ^{3}H-labelled DNA probes were prepared with all four nucleotides labelled to a specific activity of about 5 x 10^{7} cpm/μg. Tissue sections were processed for hybridization following Hafen et al. (1983), omitting the pronase step. For whole mount disc preparations, the pronase step was included. Background and null levels of hybridization signal were established by using labelled genomic fragments from outside the region of the *sev* gene.

Isolation of antibody

Lysogens of clone c2(6) were prepared, grown in 2 liter cultures, and induced essentially as described by Young and Davis (1983). Harvested cells were resuspended in 2x Laemmli sample buffer, boiled for 5 min, and centrifuged in an SS34 rotor at 18 K for 30 min. The supernatant was run on preparative gels; the fusion protein band was exciesd and electroeluted. One hundred μg of protein per injection were used for each mouse. Standard immunization procol was followed (Fujita et al., 1982). The staining procedure with tail serum was as described (Zipursky et al., 1984).

The fusion protein ran on gels at a different molecular weight (180 kDa) than β-galactosidase (120 kDa), was recognized on protein immunoblots by anti-β-galactosidase antibodies, and was recovered on anti-β-galactosidase columns.

Figure 1. *Comparisons* of wild-type and *sev* mutant.

(A) Schematic representation of photoreceptor cluster formation in wild-type third instar larval eye disc. Cluster formation follows the movement of the morphogenetic furrow from posterior to anterior. Behind the furrow, clusters of five are formed, followed by addition of R1, R6 and R7 to form mature clusters of eight. Cell R7 is the last to join. (Differentiated cell types other than the photoreceptor cells are not shown.)

(B) Section through the optic stalk. Eight axons can be seen in the bundle from each cluster of photoreceptor cells.

(C) Section tangential to the adult eye. The trapezoidal pattern in each ommatidium arises from the rhabdomeres of outer cell R1-R6. R7 is central. R8 is more proximal and is not seen at this level of section.

(D) In *sev* mutants R7 does not form.

(E) In *sev*, there are only seven axons in each bundle.

(F) In *sev* mutant eye, R7 is absent.

(G-J) Optical methods of deep pseudopupil and pseudopupil used in the isolation of *sev* mutants. Anterior is to the right in all the photographs.

(G) Deep pseudopupil of a wild-type eye. The virtual image at the center of curvature of the eye is due to superposition of rays from a set of neighboring ommatidia. The outer spots arise from R1 through R6; the smaller central one is from R7. R8 is deeper in the eye and does not participate in this image. Bar = 200 μm.

(H) Pseudopupil of a wild-type eye. The cornea of the fly is optically neutralized with oil, and an oil immersion objective used to observe the real image at the tip of each rhabdomere. Each ommatidium shows the typical trapezoidal pattern. Bar = 10 μm.

(I) Deep pseudopupil of a *sev* mutant eye. The central R7 is missing in every ommatidium, and hence is absent from the superposition image. This pattern can be observed in live, etherized flies and serves as a screening technique for defects in retinal anatomy.

(J) Pseudopupil of a *sev* mutant eye. Each ommatidium lacks the central cell R7, resulting in some disorientation of the trapezoidal arrangement of R1-R6

wild type
sevenless
A
mature clusters
5-cell preclusters
unpatterned cells
B
optic stalk
C
adult eye
G
H
FURROW
FURROW
D
E
F
I
J
POSTERIOR
ANTERIOR

Figure 2. The *sev*$^{+}$ gene region.

(A) *In situ* hybridization of labelled DNA to larval salivary gland polytene chromosomes. Labelled genomic clone λ-sev^{P1} hybridized to wild-type (Canton-S) chromosomes, which carried no detectable P-elements. Only one site of hybridization was detected, at the 10A1-2 band. This signal was due to the genomic DNA flanking the P-element in the clone λ-sev^{P1}.

(B) Genomic map of the *sev* region. Clone λ-sev^{P1} was isolated first. The hatched region in this clone contains P-element-homologous DNA. The flanking DNA segments map 53 kb from each other, indicating a deletion of that amount of DNA from the genome of the mutant *sev*^{P1}. Solid bars represent clones isolated from wild-type DNA. Only a few representative clones covering the 120 kb walk are shown. A restriction map of the wild-type genome is also shown. S: SalI, X: XhoI, E: EcoRI.

(C) Location of cDNA clones on the restriction map of wild-type DNA covered by genomic clone λ-11H(1). The consistent termination of the various sized oligo(dT) primed cDNA clones within a single restriction fragment suggests that these are 3' ends; hence, the direction of transcription is from right to left. Zero is set at the SalI restriction site nearest to the 3' end. The 11 kb span of DNA deleted in the mutant *sev*^{P3} is also shown.

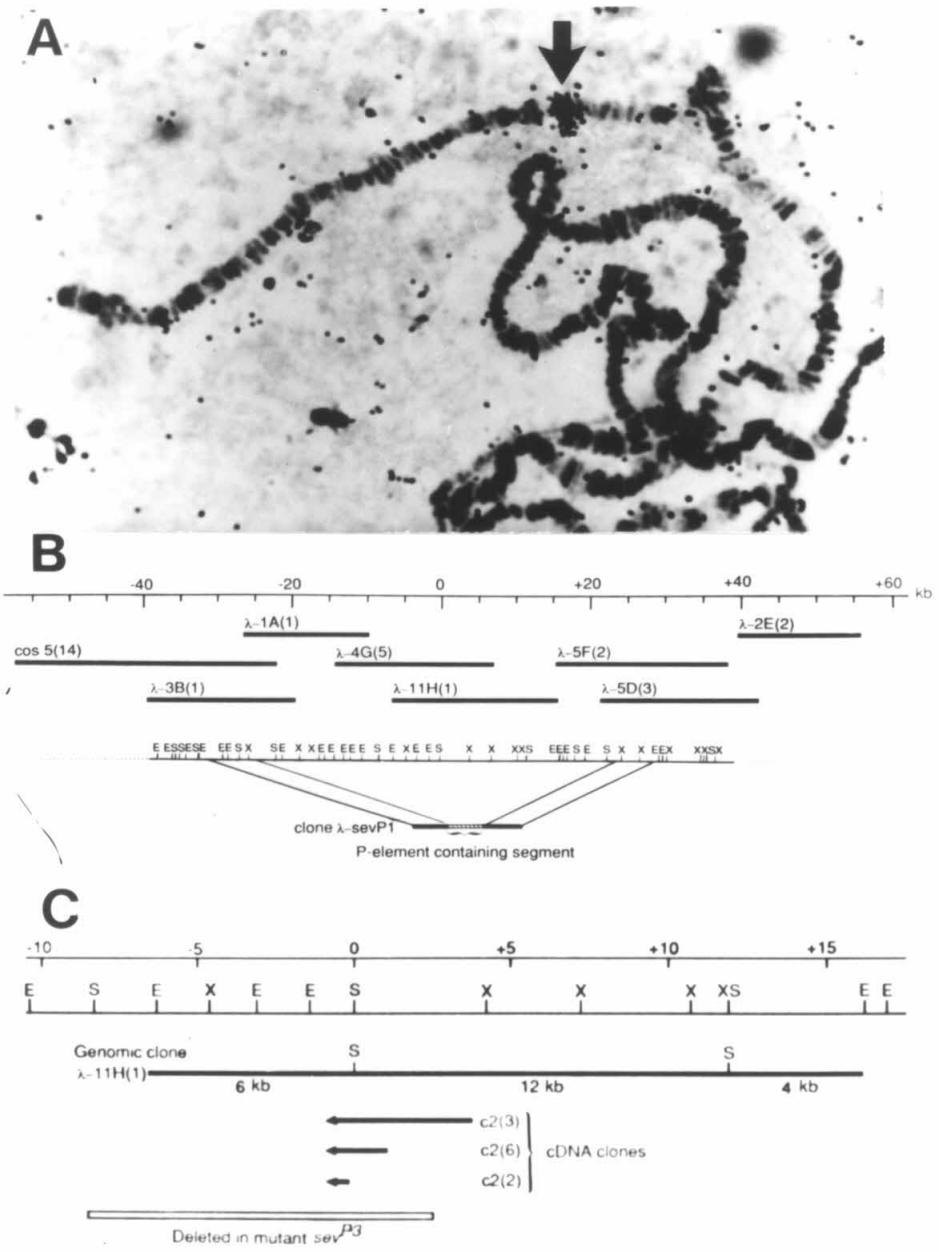
A
B
-40
-20
0
+20
+40
+60
kb
λ-1A(1)
λ-2E(2)
cos 5(14)
λ-4G(5)
λ-5F(2)
λ-3B(1)
λ-11H(1)
λ-5D(3)
clone λ-sevP1
P-element containing segment
C
-10
-5
0
+5
+10
+15
Genomic clone
λ-11H(1)
6 kb
12 kb
4 kb
c2(3)
c2(6)
c2(2)
cDNA clones
Deleted in mutant sev^P3

Figure 3. Genomic Southern blots.

(A) P-alleles *sev*^{P1} (lane 1) and *sev*^{P3} (lane 3) are compared with their parental strain 25A^{var} (lane 4) and with the Oregon-R wild-type strain (lane 1). Genomic DNA from each strain was digested with SalI and run on a 0.5% agarose gel. The probe was a nick-translated mixture of cloned genomic DNA fragments from region -7.5 to +8.0 kb in the map (Fig. 2). In the mutant *sev*^{P1}, these fragments have been deleted. In *sev*^{P3}, they have been altered. The same filter has been probed with other regions from the walk, showing that each lane has an equal amount of intact DNA.

(B) EMS-induced *sev* alleles are compared with wild-type stocks Oregon-R (lane 1) and Canton-S (lane 5). Genomic DNA from each strain was digested with SalI and XhoI, and run on a 0.5% agarose gel. The probe was a nick-translated mixture of insert fragments from clone λ-11H(1). Mutants *sev*^{d2} (lane 2) and *sev*^{LY3} (lane 3) showed no differences. Mutant *sev*^{f1} (lane 4), a sister allele to *sev*^{d2}, showed changes in the restriction pattern.

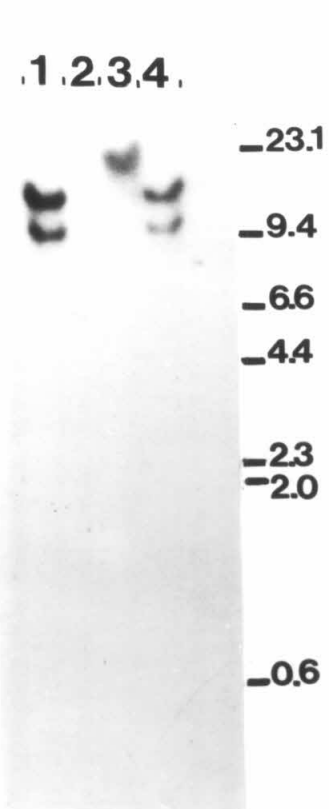
1 2 3 4
23.1
9.4
6.6
4.4
2.3
2.0
0.6

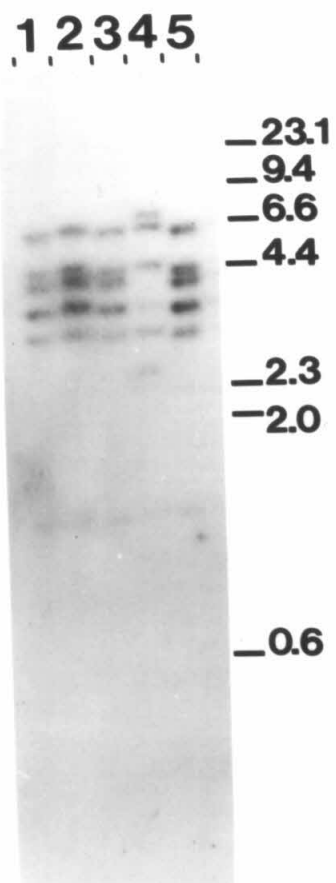
1 2 3 4 5
23.1
9.4
6.6
4.4
2.3
2.0
0.6

Figure 4. Northern blot probed with cDNA clone c2(3).

All RNA species are poly(A)$^+$ RNA, except if noted. Lane 1, Oregon-R adult head poly(A)$^-$ RNA. Lane 2, Oregon-R adult body. Lane 3, Oregon-R 22-30 hr pupal. Lane 4, Oregon-R 5-12 hr pupal. Lane 5, Oregon-R adult head. Lane 6, *sev*^{LY3} adult head. Lane 7, *sev*^{P3} adult head. Lanes 8 and 9, Oregon-R late third instar mixed imaginal disc (two separate preparations; lane 8, discs purified over glass, lane 9, discs not glass-purified). Lane 10, *sev*^{LY3} late third instar mixed imaginal discs. Lane 11, *sev*^{P3} late third instar mixed imaginal discs. Ten micrograms of RNA was loaded in each lane, except for lanes 3 and 4, which contained 20 μg. Molecular weight markers shown are HindIII fragments of phage l DNA. Size of wild-type transcript was estimated at 8.1 +/- 0.2 kb and 8.3 +/- 0.2 kb from two independent gels. The same blot was probed with other clones from the region, showing that all lanes had comparable amounts of RNA.

The results show the presence of the 8.2 kb transcript in discs, early pupae and adult heads, but not in late pupae, adult bodies, or poly(A)$^-$ RNA. Mutant allele *sev*^{LY3} expresses a transcript of normal size and abundance in both discs and adult heads. Mutant allele *sev*^{P3} shows altered transcripts (7.4 and 6.6 kb) in both discs and adult heads. The altered transcripts of *sev*^{P3} are not detected by cDNA clone c2(6) (data not shown).

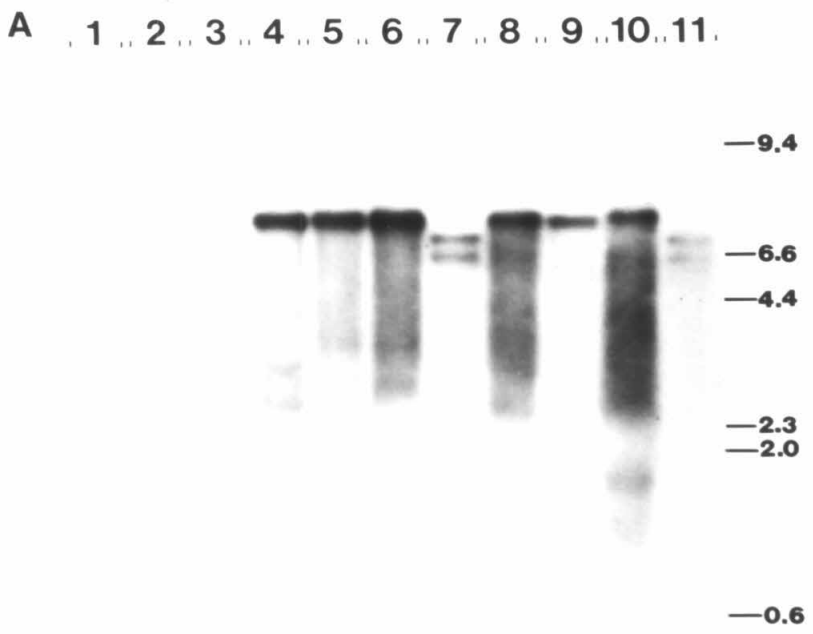
A
1
2
3
4
5
6
7
8
9
10
11
9.4
6.6
4.4
2.3
2.0
0.6

Figure 5. The *sev*$^+$ gene transcript *in situ.*

(A-D) *sev*$^+$ gene transcript in whole mount eye-antenna discs and sectioned wild-type eye-antenna discs. Anterior to the right. Bars = 50 μm. Arrows: morphogenetic furrow. Autoradiogram of discs probed with cDNA clone c2(3).

(A) Bright and (B) dark field. The *sev*$^+$ transcript appears only posterior to the morphogenetic furrow.

(C-D) Apical shift of *sev*$^+$ transcript as development proceeds. (C) Bright and (D) dark field photographs of disc sectioned perpendicular to the furrow. Arrows: morphogenetic furrow. Note vertical spread of transcript immediately behind the furrow, condensing to the apical surface in the posterior, more mature region of the disc.

(E-H) *sev*$^+$ transcript in eye disc of a 6-9 hr pupa, as compared with the 24B10 transcript. Discs sectioned perpendicular to the furrow. At this stage, the furrow has traversed the entire disc. Silver grains for *sev*$^+$ are highly apical, in contrast to 24B10, where they are more widely spread through the thickness of the disc. ap = apical and ba = basal. Anterior is to the right. Bars = 20 μm.

(E and F) *sev*$^+$ in bright field and in dark field, respectively.

(G) and (H) Eye disc of comparable age probed with 24B10 DNA.

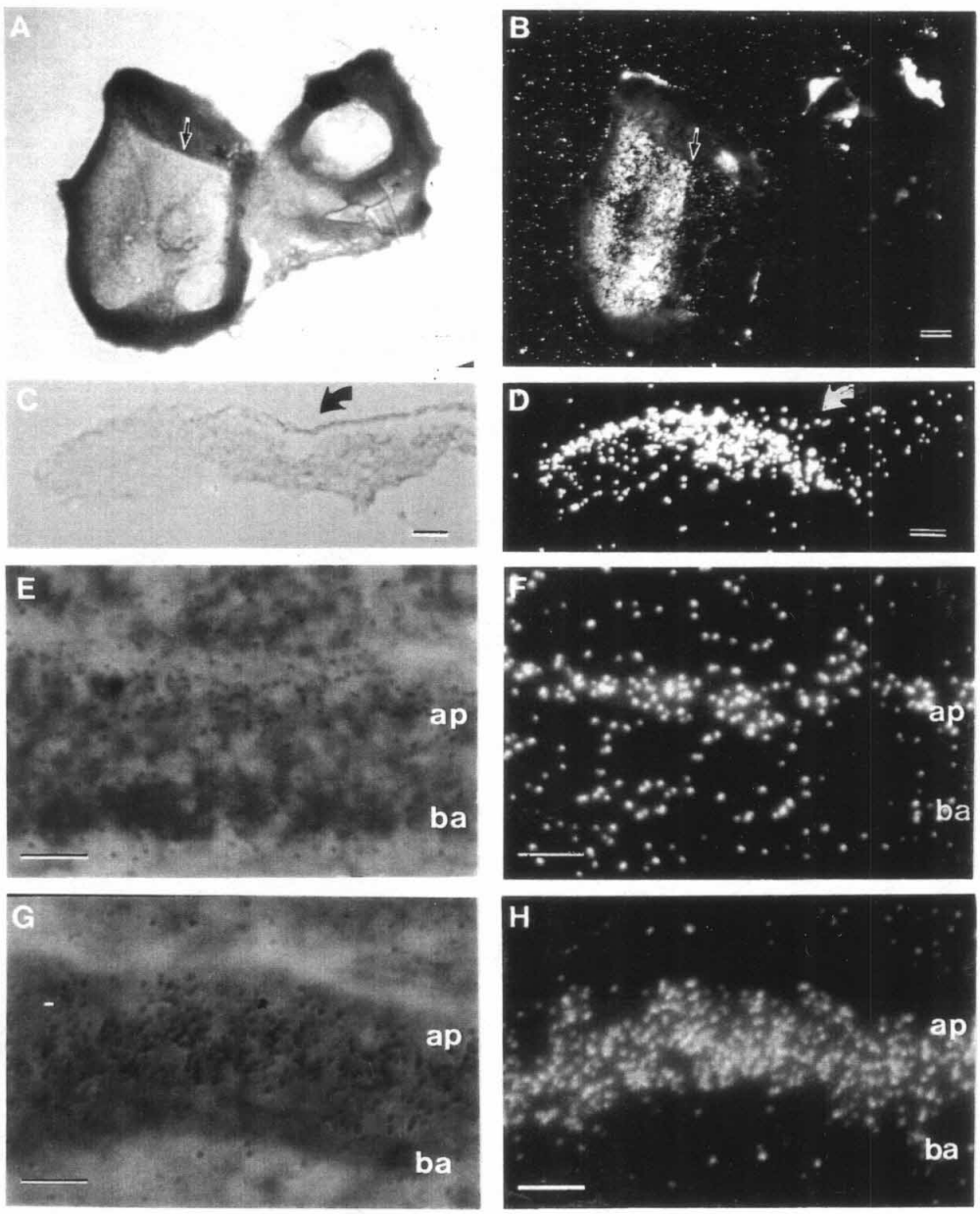
A
B
C
D
E
ap
ba
F
ap
ba
G
ap
ba
H
ap
ba

Figure 6. *sev* $^{+}$ transcripts in sections of prepupae at various ages.

All were hybridized at the same time, with the same ^{3}H-labelled cDNA clone c2(3) used as probe, and exposed for the same duration. Each section is shown above in bright field and below in dark field. (A,B) Age 0-3 hr after cessation of crawling. (C,D) 5-7 hr. (E,F) 7-9 hr. (G,H) 11-12 hr. The results indicate that the copy number of the transcript diminishes as the eye develops.

The eye disc undergoes major movements during pupal development (Steinberg, 1943). As seen here, there is a rotation of the disc at about 4 hr, and later a counterclockwise rotation as the eye disc assumes its final position at the head surface. The orientation is the same in all of the figures, the anterior of the animal pointing to the right. Anterior (a) and posterior (p) ends of the eye disc (ED) are indicated in each case. Br = brain, OL = optic lobes. Bars = 100 μm.

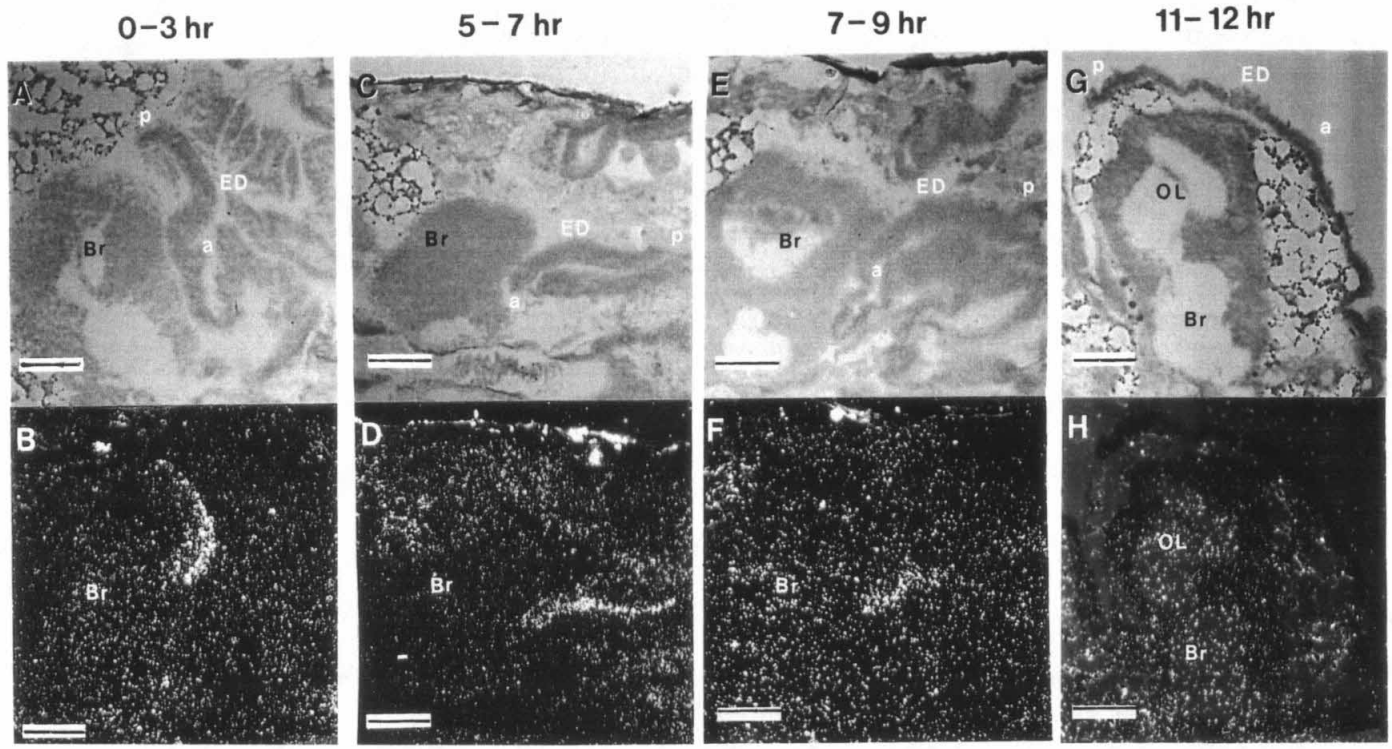
0–3 hr
5–7 hr
7–9 hr
11–12 hr
A
B
C
D
E
F
G
H
p
ED
a
Br
OL

Figure 7. *Expression of transcripts in* ***sev*** *mutant alleles.*

The cDNA clone c2(3) was used as probe. White pre-pupae (age 0-3 hr) of seventeen different mutant alleles were sectioned and processed simultaneously. Three examples of the results are shown in bright and dark field. Bars = 100 μm.

(A,B) EMS-induced mutant sev^{f1}, which is positive for transcription.

(C,D) Mutant sev^{E3}, an EMS-induced mutant that is negative.

(E,F) Mutant sev^{P1}, in which the entire *sev* gene is deleted.

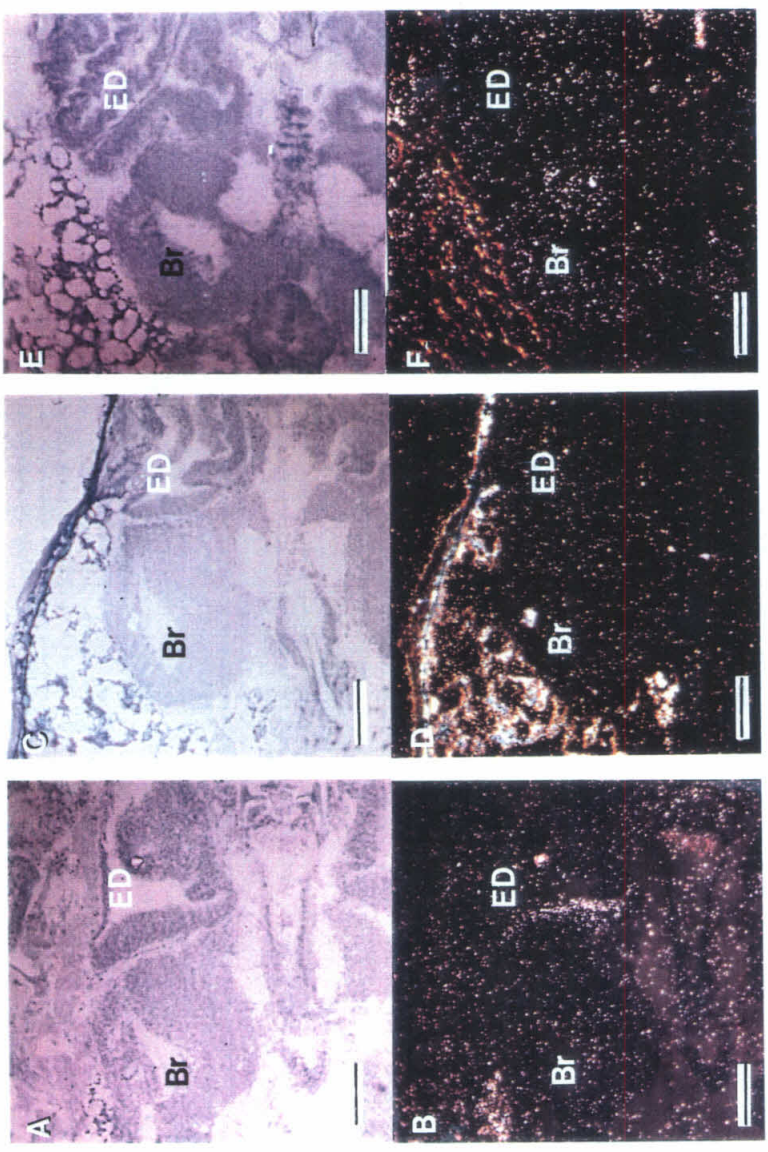
A
ED
Br
B
ED
Br
C
ED
Br
D
ED
Br
E
ED
Br
F
ED
Br

Figure 8. Eye-antennal imaginal disc stained with a mouse polyclonal serum directed against the fusion translation product of cDNA clone c2(6).

(A) Whole mount fluorescence on wild-type disc. Bar = 25 μm. Arrow: morphogenetic furrow. Disc is slightly distorted because of folding of edges.

(B) Whole mount fluorescence on *sev*^{P1} disc. Bar = 25 μm. Arrow: morphogenetic furrow.

(C) High magnification phase-contrast view of clusters in a wild-type disc. Bar = 10 μm.

(D) Fluorescence photograph of the same disc as in (C). Bar = 10 μm.

(E) Disc stained with MAb 6B11 that highlights photoreceptor cell membranes. Bar = 10 μm.

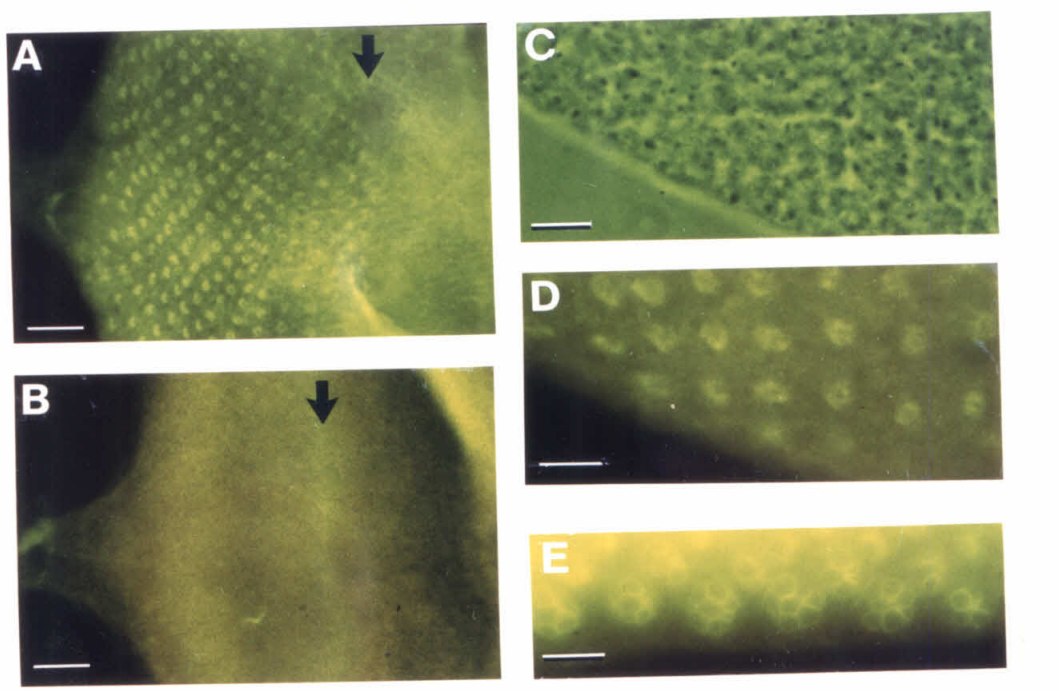
A
B
C
D
E

Table 1. Transcripts Identified in the Region of the *sev* Gene

Region (kb) (Figure 4)	Transcript Size (kb)	Tissue: Late Third Instar Disc	5-12 Hr Pupa	22-30 Hr Pupa	Adult Head	Adult Body	Maps to sev^{P3} Deletion
-27 to -19	2.5	-	-	-	+	-	No
-19 to -10	1.0	-	-	-	+	+/-	No
-14 to -1	3.2	-	+	+	-	-	Yes
-6.5 to -1	0.7	-	+	+	+	+	Yes
-1.2 to +16	8.2	+	+	-	+	-	Yes
+16 to +26	1.5	+	+	+	+	+	No
	2.5	+	+	+	+	+	No
	0.8	-	+	+	+	-	No
+37 to +43	2.4	+	nt	nt	+	+	No

nt = not tested

Chapter III

Biochemical Studies of the *sevenless*$^{+}$ Protein

Introduction

During development of the *Drosophila* compound eye, cells within the eye disc assume different fates, presumably via information present in their environment (see Chapters I and II for discussion). It appears that any cell in the eye disc can adopt the characteristics of any one of the different cell types found in the mature eye (Ready et al., 1976; Lawrence and Green, 1979). The *sevenless*$^+$ (*sev*$^+$) gene product appears to play a role in the expression of one of these possible fates. As a means of better understanding the information transduction mechanisms used during cell differentiation in the developing disc, as well as describing other tissues where the gene may be expressed, initial experiments were conducted to characterize the protein product of the *sev*$^+$ gene.

As discussed in Chapter II, the *sev*$^+$ gene was cloned by P-element transposon tagging, and found to encode an 8.2 kb transcript, expressed in the developing eye disc and adult heads. A polyclonal serum was raised against a fusion protein of bacterial β-galactosidase with the carboxy-terminus of the *sev*$^+$ protein, encoded by the 1.8 kb cDNA clone c2(6). This serum stained the developing eye disc in a pattern associated with the developing clusters; this staining was absent in the null allele *sev*^{P1}. In this chapter, the isolation and characteristics of monoclonal antibodies (MAbs) is described, along with their use in characterization of the protein.

The *sev*$^+$ gene was also cloned by Hafen et al. (1987). By DNA sequence analysis, they demonstrated that the predicted translation product of the 3' end of a *sev*$^+$ cDNA clone shows marked homology to protein tyrosine kinases, such as the viral transforming proteins v-*src* and v-*ros*, as well as to the intracellular domains of the growth factor receptors for epidermal growth factor and insulin. The region of the *sev*$^+$ gene we used in raising MAbs is the region encoding the putative protein tyrosine kinase domain. Basler and Hafen (1988) have also recently demonstrated, by site-directed mutagenesis, that the lysine residue conserved among various protein tyrosine kinases, the putative ATP-binding site, is necessary for the enzyme to function in R7 determinination.

Results

Isolation of mAbs directed against the *sev*$^{+}$ protein

As described in Chapter II, the λ-gt11 cDNA clone c2(6), encoding the C-terminus of the *sev*$^{+}$ protein, allowed the production of a fusion protein of bacterial β-galactosidase and the carboxy-terminus of the *sev*$^{+}$ protein. This fusion protein was used as immunogen, and hybridomas were made from mice whose tail-serum showed *sev*$^{+}$-specific staining on eye discs. The regular pattern of staining produced by the polyclonal tail serum on eye discs was used as the criterion for screening cloned cell line supernatants. Over 700 cell lines were screened by staining late third instar eye discs with each supernatant. Fourteen anti-*sev* MAb producing lines were established.

Eye disc protein immunoblot analysis

First, one Mab showing the *sev*$^{+}$ staining pattern, MAb 150C3, was chosen for initial analysis of the protein expressed in eye discs, to verify that it identified the *sev* protein. Subisotyping showed that this monoclonal antibody is an IgG1.

Figure 1 shows a Western blot stained with MAb 150C3 of homogenates prepared from late third instar larval eye discs. In eye discs from wild-type flies, the MAb identifies two bands that are missing in the *sev* deletion allele *sev*^{P1}, and the EMS-induced allele *sev*^{d2}. These have molecular masses of about 250 kDa (band A) and 60 kDa (band B). Band A is approximately the size expected of a translation product encoded by the 8.2 kb *sev*$^{+}$ RNA. Band B is possibly due to a cleavage product. Its intensity relative to band A varies in different preparations of normal discs, but it is consistently absent in mutants lacking band A. In the EMS-induced allele *sev*^{LY3}, which produces a transcript of normal size (Chapter II; Banerjee et al., 1987a), the *sev*$^{+}$ protein is present and is not measurably altered in size. Curiously, in repeated experiments, the intensity ratio of band A to band B was greater in *sev*^{LY3} than in the wild type, although the ratio is always less

than 1, suggesting that the protein in *sev*^{LY3} may have altered cleavage properties.

Other bands identified by MAb 150C3 in wild-type discs are also present in all the *sev* alleles, including the null allele *sev*^{P1} in which the entire gene is deleted. These presumably correspond to other proteins sharing epitopes with the product of the *sev* gene. This is not surprising in light of the strong homology at the 3' end of the *sev* gene with several other tyrosine kinase genes (Hafen et al., 1987), and because the fusion protein used as the immunogen was derived from a 3' cDNA fragment.

All of the MAbs were tested for their ability to identify the two *sev*$^{+}$ proteins on protein immunoblots. The same 250 kDa and 60 kDa protein species were identified in adult head tissue by MAb 150C3 (see below); since this tissue is more easily obtained, it was used in this experiment. Of the fourteen anti-*sev* producing lines that were established, 9 of them stained the *sev*$^{+}$ protein on blots, four of these strongly. All the MAbs that did stain the *sev*$^{+}$ proteins on immunoblots cross-reacted with other proteins, i.e., proteins present in the null allele *sev*^{P1}, to varying degrees. The original MAb tested, Mab 150C3, was the most consistent and strong of these. Therefore, it was used as the primary antibody in all further protein immunoblot experiments.

Expression of the *sev*$^{+}$ protein in different tissues

It was previously reported, based on Northern blot results, that the *sev*$^{+}$ gene is transcribed in the adult head (Chapter II; Banerjee et al., 1987a). Therefore, MAb 150C3 was used to probe the expression of the *sev*$^{+}$ protein in this and other tisssues (Fig. 2a). Expression was compared between late third instar eye-antennal imaginal discs, late third instar optic lobes and ventral ganglion, adult heads, adult heads from the mutant *eyes absent* (*eya*) that lack the compound eyes (Sved, 1986), adult heads from the mutant *sine oculis* (*so*) that lack the compound eyes and dorsal ocelli (Fischbach, 1983), and adult bodies. Also, various staged embryos were tested for expression (data not shown). The data demonstrate that *sev*$^{+}$ expression is not restricted to the developing eye-antennal

imaginal disc, nor is it specific to the retina. The protein product of the *sev*$^+$ gene is also expressed in the optic lobes, at a time when development of the adult optic system is occurring. [Expression can also be demonstrated in larval optic lobes alone, without the ventral ganglion (data not shown)]. The protein is found in the adult head and is also expressed in heads in which the retina and the dorsal ocelli are not present. Surprisingly, the protein also appears to be expressed in the body. Because of problems with overloading the capacity of the gel, only the more abundant 60 kDa protein (band B) could be detected; the band A protein could not be detected. Basler and Hafen (1988) now have data that confirm that the *sev*$^+$ mRNA is expressed in the body; the transcript is expressed at a level below the limit of detection of our Northern blots (Chapter II). There is no obvious difference in the relative abundances of the band A and band B *sev*$^+$-specific proteins in the different tissues.

Head extracts were also separated under non-reducing conditions and the protein immunoblot was probed with MAb 150C3 (Fig. 2B). Under these conditions it became more difficult to identify the proteins. However, both protein species, band A and band B, were identified, indicating that these two species are not linked by disulfide bridges.

Expression of the protein in alleles of *sev*

Two approaches were used to determine which alleles of *sev* produce a protein, albeit defective. One was the staining of late third instar imaginal discs from the different alleles, and the other was the staining of protein immunoblots from *sev* mutant heads. An example of the latter is shown in Figure 3, and the results are summarized in Table 1, along with transcript expression as determined by Northern blots and eye disc *in situ* hybridizations (Chapter II; Banerjee et al., 1987a; P.J.R. and J. Pollock, data not shown). Most of the EMS-induced alleles did produce a transcript of approximately wild-type size. However, only about a quarter of them encoded detectable protein. The immunoblot technique seemed to be slightly more sensitive than *in situ* detection of

transcript, as weak expression can be seen on immunoblots in the alleles sev^{fig} and sev^{X3}. These data provide further verification that the gene and proteins identified do correspond to sev^{+}. The P-element-induced allele sev^{P2}, like the allele sev^{LY3}, shows an altered ratio of band A to band B.

Immunoprecipitation of the sev^{+} proteins

Different conditions for the solubilization of the sev^{+} protein were investigated. Given the difficulty of obtaining large amounts of late third instar eye discs, and the ease of obtaining large amounts of adult heads, it was thought that the latter tissue would be preferable for the purification of useful amounts of the protein.

The ability of the fourteen different MAbs to precipitate the sev^{+} proteins from adult heads depended on the extraction conditions used to solubilize the tissue. Heads were homogenized in detergent buffer, the supernatant incubated with the MAb, and the antigen-antibody complex recovered on Protein A beads. This complex was directly mixed with Laemmli gel-loading mix, separated by SDS-Polyacrylamide gel elelectrophoresis (SDS-PAGE), and the products visualized with Mab 150C3 (see Experimental Procedures). At relatively low detergent concentrations (0.25% N-P40 and 0.1% Na Lauryl Sarcosine), only MAb 147H2 precipitated the 250 kDa and 60 kDa sev^{+} proteins (Fig. 4). However, it also precipitated cross-reacting species; the three major ones migrate at approximately 280 kDa, 220 kDa, and 97 kDa. At higher detergent concentrations, e.g., 1% CHAPS, all fourteen MAbs precipitated the 250 kDa and 60 kDa proteins (data not shown). None precipitated only the sev^{+} bands; all of them cross reacted to varying degrees with the three other major bands. Some seemed to precipitate the 97 kDa species preferentially rather than the sev^{+} proteins.

These experiments were repeated with total late third instar larvae. The results were essentially identical: although more quantitative release of the protein occurred at higher detergent concentrations, more specific immunoprecipitation occurred at lower

concentrations. Despite the presence of protease inhibitors, these bulk larval preparations often were marred by protein degradation, presumably because of the inclusion of the larval gut.

Enzymatic activity present in the immunoprecipitate

Given the results of Hafen et al. (1987), many attempts were made to demonstrate protein tyrosine kinase activity in the immunoprecipitate, to be used as an assay for future experiments, including protein purification. The proteins were precipitated from late third instar imaginal discs, from late third instar developing optic lobes, or from adult heads. Results from wild-type immunoprecipitates were always compared with immunoprecipitates from the allele sev^{P3}, which completely lacks the cDNA region used as immunogen (because of this, we are unable to determine if protein products are translated from the truncated transcripts. Even if this were so, these proteins would not be immunoprecipitated, and in any case would lack the putative tyrosine kinase domain).

An example of one of these experiments is shown in Figure 5. The sev^{+} and cross-reacting proteins were precipitated with MAb 147H2. After thorough washing of the Protein A-antibody-antigen beads, the immunoprecipitates were incubated in various known protein tyrosine kinase enzymatic assay conditions with or without the substrate enolase and 10 μCi of (γ-^{32}P)-ATP (protocols from Cooper and Hunter, 1982; Wang and Baltimore, 1983; Honegger et al., 1987; C. Shores, University of North Carolina, pers. comm.). Part of each sample was reserved for protein immunoblot analysis (Fig. 5A). In all cases, to varying degrees, there was evidence of protein kinase activity in the immunoprecipitates, while no detectable kinase activity was present in antibody-Protein A complex alone (Fig. 5B). Levels of substrate phosphorylation varied with divalent cation type and concentration. If no enolase was added to the reaction mixtures, the antibody heavy chain was usually labelled. If enolase was present, it was usually phosphorylated in addition. Phosphorylation of sev^{+} protein was not observed. Any phosphorylated

proteins were usually present in both the wild-type and *sev*^{P3} control lanes. Phosphates on tyrosine are known to be less sensitive to hydrolysis by base treatment than those on serines or threonines; it is often used as a method of differentiating between the presence of different phospho-amino acids (for example, see Bautch et al., 1987). Alkaline treatment of the gel did not remove all the phosphates and did not reveal any differences in kinase activity between the wild type and mutant (Fig. 5C). However, it does indicate that non-*sev*$^{+}$ associated tyrosine kinase activity may be present in the immunoprecipitate.

Since the kinase activity in the immunoprecipitates of endogenous protein was not different in the wild type and the mutant, attempts were made to demonstrate protein tyrosine kinase activity of the c2(6) fusion protein expressed in *E. coli*. Fusion proteins expressed in bacteria have been shown to be capable of enzymatic activity (for example, see Desplan et al., 1985). The tyrosine kinase viral-transforming protein v-*abl* is active in bacteria (Wang et al., 1982; Wang and Baltimore, 1985); its activity can be detected in crude sonicates of induced fusion protein, and in induced colonies growing on agar. The latter characteristic has been used as a method to screen for temperature-sensitive tyrosine kinase mutants of v-*abl* (Kipreos et al., 1987). In our cDNA construct, lack of the putative ligand-binding domain, which in other tyrosine kinases may inhibit kinase activity in the absence of ligand, obviates the need of ligand, a potential problem in the wild-type immunoprecipitates.

In the crude sonicates of c2(6) and the control samples cDNA clone c1(3), which does not express a *sev*$^{+}$-β-gal fusion protein, and parent *E. coli* strain Y1089, kinase activity could be detected. However, when immunoprecipitation was performed with either an anti-β-galactosidase antibody or the anti-*sev* Mab 147H2, no *sev*$^{+}$-specific activity could be found (data not shown). Therefore, it does not appear that the kinase domain as represented by cDNA clone c2(6) has tyrosine kinase activity when expressed in *E. coli*.

Antiserum against phosphotyrosine reveals a pattern on developing eye discs

Other protein tyrosine kinases may indeed be active during eye development. To explore this possibility, antiserum against phosphotyrosine was used to stain eye discs of wild-type and various mutant alleles of *sev*. This antiserum was a generous gift of Mark P. Kamps at the Salk Institute and University of California, San Diego. As shown in Figure 6, the staining patterns of the wild-type and the null allele sev^{P1} do not appear to be significantly different. The stain was quite strong in the morphogenetic furrow along cell membranes, as clusters form. More posteriorly, as clusters matured, the stain was apically localized and centered over each cluster.

Discussion

In this part of the study, several steps were completed that provide a framework for analysis of sev^{+} function. The isolation of fourteen monoclonal antibody-producing lines against the sev^{+} protein was an important first step, and, as seen in Chapter IV, will allow for the subcellular localization of the sev^{+} protein in developing eye discs.

Each of these MAbs was isolated on the basis of its ability to identify the sev^{+} proteins *in situ* on developing eye discs. Most of them stain the proteins on immunoblots, four of them strongly. The MAbs identify two protein species in wild-type eye discs that are not present in the null allele sev^{P1}. These have apparent molecular weights of 250 kDa and 60 kDa, with the 60 kDa species more abundant than the 250 kDa species. It has been reported (Basler and Hafen, 1988; Bowtell et al., 1988) by DNA sequence analysis that the sev^{+} gene could encode a protein of approximately 280 kDa. This protein has two potential membrane-spanning domains, resulting in an N-terminal intracellular domain of about 100 amino acids, a large extracellular domain of about 2000 amino acids, and an intracellular domain, including the region with homology to tyrosine kinases, of about 425 amino acids. Bowtell et al. (1988) suggest that cleavage at a putative Endopeptidase

cleavage site of arginine repeats just N-terminal to the second hydrophobic domain would result in two species, one of about 57 kDa. The smaller species would contain the tyrosine kinase domain. This is interesting in light of our protein immunoblot analysis. The MAbs were directed against a fusion protein generated by the terminal 1.8 kb of the mRNA. This message would correspond to about 60 kDa of the C-terminus of the protein. Therefore, if the protein is cleaved, any of these MAbs would identify the smaller cleavage product, as well as the non-cleaved protein, but would not recognize the other putative 190 kDa cleavage product. Such cleavage products of protein tyrosine kinases have been noted in a family typified by the insulin receptor (Ebina et al., 1985; Ullrich et al., 1985; reviewed in Yarden and Ullrich, 1988), in which the precursor protein is cleaved into α and β subunits, and the two α and two β subunits of each receptor are linked by disulphide bridges. The two sev^+ proteins identified by MAb 150C3 do not appear to be linked. Whether band A and band B exist *in vivo* and whether they are subunits or an artefact have yet to be determined.

The sev^+ proteins were found expressed in other tissues besides the developing eye disc. It is also expressed in late third larval instar developing optic lobes, in adult heads, and weakly in adult bodies. The expression in adult heads cannot be limited to the optic lobes, since roughly equivalent amounts of protein are found in the adult heads of the mutants *eya* and *so*. In the former, the adult compound eyes do not develop, and there is a corresponding lack of compound eye optic lobe tissue. In the latter, none of the adult visual system (compound eye and dorsal ocelli) is present; the adult optic lobes are therefore rudimentary (Fischbach and Technau, 1984). Therefore, sev^+ is most likely expressed in other parts of the brain. Preliminary *in situ* hybridization results (J. Pollock, pers. comm.) indicate that the transcript is expressed in the cortex of all of the adult brain.

The results of Ballinger and Benzer (1988) also indicate that the sev^+ protein has a function in the adult brain. As described in Chapters I and II, *sev* mutants have altered photochoice behavior. When flies are given a choice between green and ultraviolet (uv)

light, wild-type flies choose uv at a ratio of 10 to 1. When *sev* mutants are given the same choice, they choose green light at a ratio of 25 to 1. This behavioral abnormality had previously been ascribed to the lack of R7 from the ommatidia. However, Ballinger and Benzer noted that *sev* mutants are able to perceive uv light; when they are given a choice between uv and darkness, *sev* mutants choose uv in a manner much like the wild-type strain. They sought to understand better this complicated photochoice behavior. Mutagenizing the allele sev^{LY3} and using green / uv photochoice as a screening method, they identified an allele-specific dominant suppressor of the behavioral phenotype, *Photophobe* (*Ppb*). In sev^{LY3} ; *Ppb* double mutants, cell R7 is still lacking. It appears that the *Ppb* mutant is repelled by bright light, and that the defective protein encoded by sev^{LY3} serves to enhance further the increased sensitivity to light. Although the mechansim of this interaction is unknown, this is the first evidence demonstrating a function of sev^{+} other than its role in the differentiation of R7.

Most *sev* alleles do not appear to express a protein recognized by the Mabs (see Table 1). The four that do express wild-type levels of mutant protein may be useful for isolating suppressors of *sev*, since they are likely to result from a single amino acid change in the protein. Allele-specific suppressors could identify other genes that function in the pathway of R7 determination. It is interesting to note that two of the *sev* alleles that express protein show altered ratio of the 250 to 60 kDa species. It is possible that the altered residues affect the cleavage. Perhaps more interesting is the possibility that the cleavage process may be activity-dependent, since the tyrosine kinase activity of the defective proteins is presumed to be lacking or inappropriate. The generation of MAbs that can discriminate between the two putative cleavage products will be useful in investigating this phenomenon.

The results have also shown which detergent extraction conditions and MAb are most appropriate for partial purification of the proteins. However, since all immunoprecipitations contain cross-reacting proteins, it may be necessary to generate

additional antibodies with *sev*$^+$-specific immunoprecipitation profiles. Our data suggest that at least one of the cross-reacting proteins is a kinase, possibly a tyrosine kinase. At either the transcript, protein or phenotype level, several protein tyrosine kinases have been shown to be expressed in the developing eye disc. These include *Drosophila* c-*src* (Simon et al., 1985) and a protein similar to the human insulin receptor (Piovant and Léna, 1988). Since Mab 150C3 appears to precipitate the 97 kDa cross-reacting species in preference to the *sev*$^+$ species, additional protein tyrosine kinases might be isolable by the use of homologous epitopes.

The staining pattern of the antiserum against phosphotyrosine, which should reveal the location of protein tyrosine kinases activity in the eye disc, does not differ at the light microscope level between wild-type and the null allele *sev*^{P1}. The stain increased sharply in intensity at the morphogenetic furrow, and was distributed apically posterior to it. The localization of the *sev*$^+$ protein in the eye disc, which was demonstrated in Chapter II and is the topic of Chapter IV, is quite similar to this. Other protein tyrosine kinases may be active during eye development, with *sev*$^+$ probably not being the predominant one. Interestingly, the staining pattern indicates that other kinases are located in the apical regions of the cells.

In this chapter, initial characterization of the *sev*$^+$ proteins has been described; it should prove useful in any future studies of *sev*$^+$ function. It also raises many questions regarding the possible multifunctional roles of *sev*$^+$ in the developing brain and perhaps ventral ganglion, as well as its role in visual information processing as indicated by the *Ppb* mutation.

Experimental Procedures

Strains

The *sev* mutant and wild-type strains have been described (Chapter II; Banerjee et

al., 1987a). The *eya* mutant is described in Sved (1986), and *so* in Fischbach (1983) and Fischbach and Technau (1984).

Monoclonal antibodies to sev^+ protein

Fusion protein was isolated from lysogens of cDNA clone c2(6) as described (Chapter II; Banerjee et al., 1987a). Mice were immunized three times with 100 μg of fusion protein per injection, and hybridomas were made (Fujita et al., 1982) using myeloma cell line HL-1 (Ventrex). Of the 768 wells plated, 705 showed colonies that covered half the well. Supernatants from these were screened by immunofluorescent staining of whole-mount, late third instar, wild-type eye discs (see Chapters IV and V). Thirty lines revealed the sev^+ toroidal pattern associated with the developing ommatidia. These hybridoma lines were cloned by limiting dilution. Of these, only fourteen survived subcloning or continued to produce the sev^+ Mab staining pattern, for reasons unknown.

Immunoblot analysis

Late third instar wild-type or mutant eye discs or brains (50 pairs each) were dissected in TBS (100 mM Tris base pH 7.5, 130 mM NaCl, 5 mM KCl, 5 mM NaN_3, 1 mM EGTA); adult heads (n=20) or adult bodies (n=5) were severed with a razor blade. Embryos of different stages were collected onto plates. The tissues were homogenized immediately and boiled in sample buffer (Laemmli, 1970), with or without 5% β-mercaptoethanol. Proteins were separated on a 5-15% gradient SDS-polyacrylamide gel and electrophoretically transferred overnight to nitrocellulose. The nitrocellulose membrane was incubated with blocking buffer (50 mM Tris-HCl pH 8.0, 150 mM NaCl, 1 mM EGTA, 2% BSA, 0.1% Gelatin, 0.02% NaN_3, 0.05% Tween 20) and reacted with the primary antibody for 1-2 hours at room temperature; MAb supernatants were diluted 1:2 in blocking buffer. Immunoreactive bands were visualized by the alkaline phosphatase

method, using the Proto-Blot kit (Promega Biochemicals).

Immunoprecipitation

For larval tissues (eye discs or brains), the tissues were dissected in TBS, then homogenized in the detergent extraction buffer. All of the buffers contained 10 mM NaPhosphate pH 7, 100 mM NaCl, 1 mM EDTA, 1 mM EGTA, and the protease inhibitors 0.5 μM antipain, 0.5 μg / ml leupeptin, 0.1 mM PMSF, 0.1 μg / ml pepstatin and 5 μg / ml aprotinin. The final detergent conditions were either 0.25% N-P40 and 0.1% NaLauryl Sarcosine or 1% CHAPS (many different conditions were tested initially). Adult heads were collected in LN_2 by standard methods (Zipursky et al., 1984), pulverized in a mortar and pestle and Dounce-homogenized on ice with the detergent buffers. Adult heads were homogenized at a concentration of 0.5 g of heads per ml of buffer, while about 50 pairs of discs or brains were homogenized in 0.1 ml of buffer. After homogenization, the supernatant was recovered by centrifugation at 10,000 x g for 15 minutes. By immunoblot analysis, about half of the amount of the *sev* protein was not solubilized and therefore was lost in the pellet.

The supernatants were clarified by preincubation with Protein A beads for 1 hr at 4 °C. The supernatants were then allowed to mix with the primary antibody at a concentration in excess of antigen concentration for 1-12 hr. The antigen-antibody complex was collected by Protein-A beads (Bio Rad), using the manufacturer's directions for at least 1 hr at 4 °C. The pellets were washed five times with a 40 fold excess of buffer to bead volume. For protein immunoblot analysis, the Protein A beads-antibody-antigen complex was then mixed with Laemmli gel-loading buffer and treated as described above.

Kinase activity

To demonstrate kinase activity, many different conditions were tried. In the example shown in Figure 5, the reaction conditions were variations of those described for the epidermal growth factor receptor in Honegger et al. (1987). The following conditions were used: Immunoprecipitations were performed after homogenization of 0.25 g of wild-type or *sev*^{P3} heads per ml of the 0.25% N-P40 / 0.1% NaLauryl Sarcosine detergent buffer as described above. The pellets were washed twice in this buffer, and twice with a Hepes-Triton X-100 buffer (20 mM Hepes pH 7.5, 100 mM NaCl, 0.1% Triton X-100, 1 mM EDTA, 1 mM EGTA plus the protease inhibitors). The pellets were washed once in the appropriate kinase buffer reaction mix without (γ-^{32}P)-ATP and without protease inhibitors. The pellets were then resuspended in the kinase mix without protease inhibitors [0.1 M Pipes pH 6.8, 100 mM NaCl, 15 μM ATP, 50 μM $NaVO_4$, 0.1% Triton X-100, either 5 mM or 20 mM $MnCl_2$, and 10 μCi of (γ-^{32}P)-ATP (5000 Ci/mmol, Amersham)] that also could include 5 μg of acid-treated enolase (Sigma) as prepared in Cooper and Hunter (1982). The samples were prepared at three times the usual amount so that the same sample could be treated in three different ways, incubated at 25 °C for 20 min, divided into three aliquots, then separated by SDS-PAGE on a 5 - 15% gradient gel. For one third, the gel was immediately vacuum-dried onto Whatman 3MM paper. For another, the gel was stained for 30 min at 42 °C in Coomassie Blue R250 in 50% Methanol and 7% Acetic acid, destained for about 20 min, then dried. This facilitated the identification of enolase and the antibody chains, and appeared not to affect the number of labelled proteins. The gel on which the final third of the samples were separated was treated with alkali (Bautch et al., 1987): The gel was fixed for 15 min in 30% Methanol and 7% acetic acid, then incubated in 1 N KOH for 1 hour. Upon this treatment, the gel expanded by about one-half its size. After neutralization, the gel was rinsed in 30% methanol and then dried as above. In all cases, prestained molecular weight

markers were used because they could be identified independently of the treatment. The gels were then autoradiographed at room temperature.

Immunohistochemistry

Late third instar eye discs were stained by a modification of the procedure of Zipursky et al. (1984) presented in Chapter V except for the following modifications: Discs were incubated for 2 hours in purified antiphosphotyrosine antibodies diluted to a concentration of 2 μg per ml of TBS. This antiserum was a gift from M. P. Kamps and B.M. Sefton at the Salk Institute and University of California, San Diego. The rabbit immunoglobulins were detected with fluorescein-conjugated goat anti-rabbit IgG, IgA, and IgM.

Figure 1. *Western blot of protein homogenates from late third instar eye discs, probed with MAb against the* sev^{+} *protein.*

Wild-type (strain isoA C-S) is compared with three *sev* mutants. Lane 1: wild-type; lane 2: sev^{P1}; lane 3: isoA sev^{d2}; and lane 4: isoA sev^{LY3}. Proteins from 100 eye-antennal discs were loaded onto each lane and the blot was reacted with MAb 150C3. Two protein bands (arrowheads), one at 250 kDa (band A) and one at 60 kDa (band B), are missing in the null allele sev^{P1} and the EMS-induced allele isoA sev^{d2}. The molecular weight of the larger band was arrived at by comparison with high molecular weight markers thyroglobulin (330 kDa) and ferritin (220 kDa) (Pharmacia).

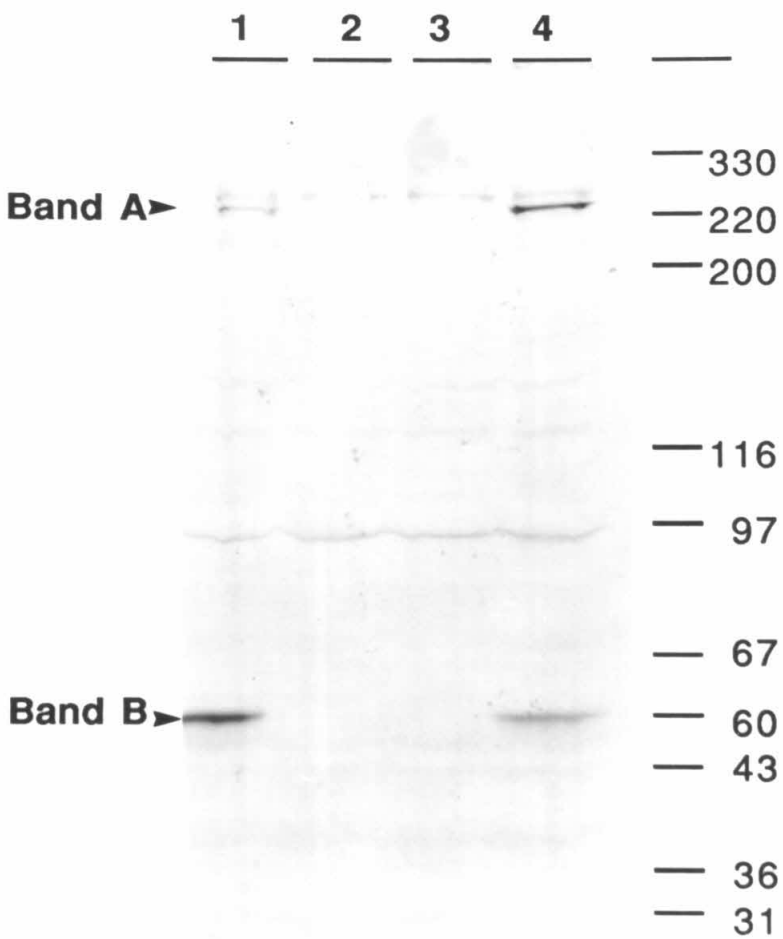
1
2
3
4
Band A
Band B
330
220
200
116
97
67
60
43
36
31

Figure 2. *Western* blot analysis of proteins from different tissues under A) reducing or B) non-reducing conditions, as probed with MAb 150C3.

(A) Expression of the *sev*$^{+}$ proteins are compared between wild-type larval eye discs, *sev*^{d2} larval eye discs and other tissues. Lane 1: wild-type adult body, n=5; Lane 2: *sev*^{d2} adult body, n=5; Lane 3: wild-type adult head, n=20; Lane 4: *sev*^{d2} adult head, n=20; Lane 5: *eya* adult head, n=20; Lane 6: *so* adult head, n=20; Lane 7: wild-type, late third instar, eye-antennal imaginal discs, n=100; Lane 8: *sev*^{d2} late third instar eye-antennal imaginal discs, n=100; Lane 9: wild-type, late third instar, optic lobes with ventral gangion attached, n=100.

The band A 250 and band B 60 kDa *sev*$^{+}$-specific proteins (arrowheads) can be identified in wild-type eye-antennal discs and heads, but also in late third instar optic lobes and ventral ganglion, in adult heads lacking compound eyes (lane 5), and in adult heads lacking compound eyes and ocelli (lane 6). The band B can be detected, albeit weakly, in wild-type adult bodies (lane 1).

(B) Under non-reducing conditions, the band A and band B *sev*$^{+}$ species can still be identified. Lane 1: wild-type adult heads, n=20; Lane 2: *sev*^{d2} adult heads, n=20.

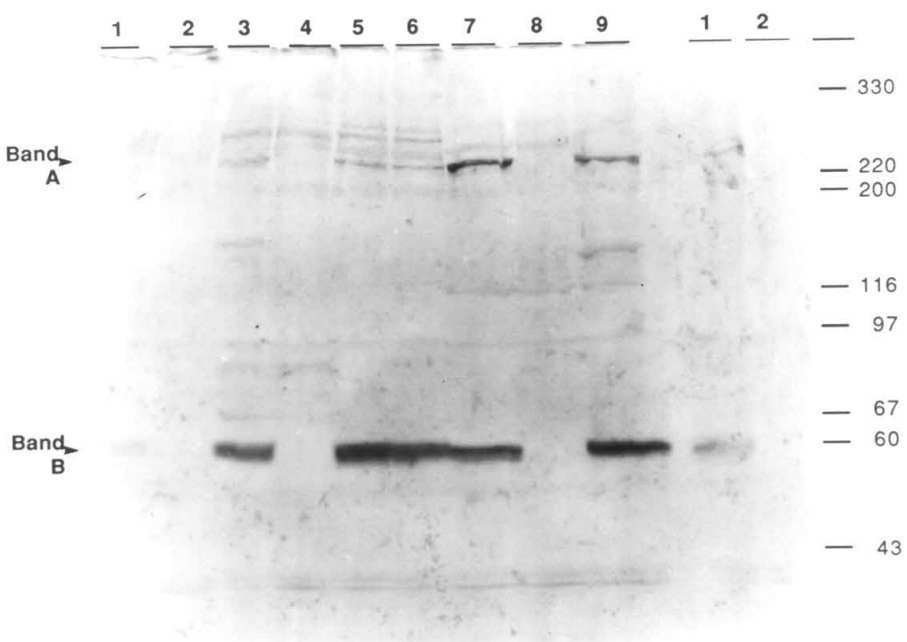
1
2
3
4
5
6
7
8
9
1
2
330
220
200
116
97
67
60
43
Band A
Band B

Figure 3. Western blot analysis of expression of the *sev* proteins in *sev* alleles. Protein homogenates from adult heads (n = 20) of wild-type and various *sev* alleles were probed with MAb 150C3. Arrows identify the *sev* - specific protein species, band A and band B. Lane 1: wild-type strain Canton-S; Lane 2: sev^{E1}; Lane 3: sev^{E2}; Lane 4: sev^{E3}; Lane 5: sev^{E4}; Lane 6: sev^{E5}; Lane 7: sev^{P1}; Lane 8: sev^{P2}; Lane 9: sev^{P3}; Lane 10: Wild-type strain $25A^{var}$.

In comparing the EMS-induced alleles $sev^{E1\text{-}E5}$ with the parent strain Canton-S, the alleles sev^{E2} and sev^{E4} do appear to express immuno-reactive protein, albeit defective, whereas the others do not. In comparing the P-element-induced alleles $sev^{P1\text{-}P3}$ with the parent strain $25A^{var}$, only the allele sev^{P2} appears to express immuno-reactive protein. The allele sev^{P1} is completely deleted for the *sev* gene, while the allele sev^{P3}, which encodes two altered transcripts, is deleted for the region used as immunogen for the MAb.

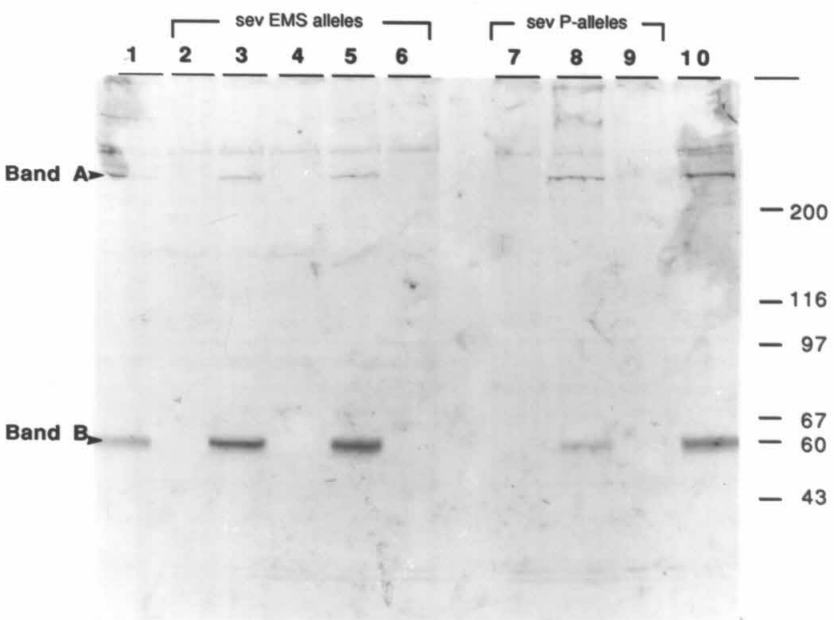
sev EMS alleles
sev P-alleles
1
2
3
4
5
6
7
8
9
10
Band A
Band B
200
116
97
67
60
43

Figure 4. Immunoprecipitation with MAb 147H2.

Adult heads from either wild-type or mutant were homogenized in the N-P40 / sarcosine detergent buffer, the *sev* reactive proteins were immunoprecipitated by MAb 147H2, and the complex collected withe Protein A beads. The equivalent of about 20 heads was loaded onto each lane. The products were probed with MAb 150C3. Lane 1: wild-type adult head homogenate; Lane 2: sev^{P3} adult head homogenate.

Both sev^{+}-specific proteins band A and band B (250 and 60 kDa; arrowheads) are precipitated. Also precipitated, i.e., present in the allele sev^{P3}, are protein species that migrate to about 280 kDa, 220 kDa, and 97 kDa. Antibody reactive bands from the Protein A beads immune complex are also identified (large arrows): Protein A (42 kDa), antibody heavy chain (about 52 kDa), and antibody light chain (about 27 kDa). Bands that are not reproducibly precipitated are noted by the small arrows.

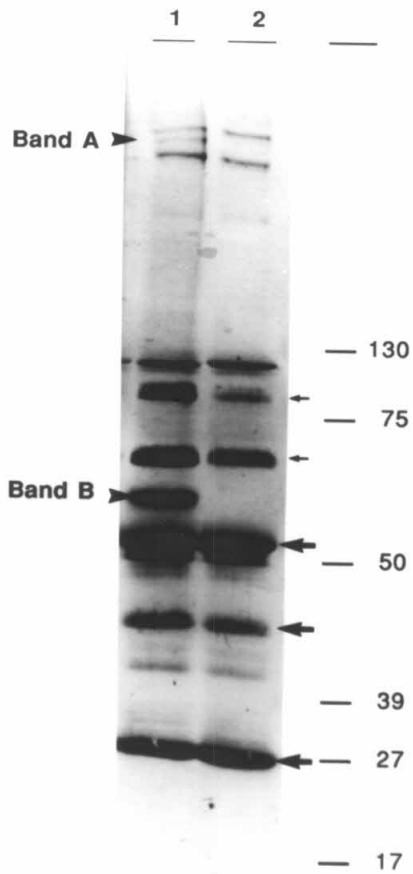
1
2
Band A
Band B
130
75
50
39
27
17

Figure 5. Kinase activity in the immunoprecipitates.

Immunoprecipitates from wild-type and mutant adult heads were prepared as described, then incubated with kinase reaction buffers with or without enolase (see Experimental Procedures), and with or without subsequent alkali treatment. Kinase activity is demonstrated by the transfer of the γ-phosphate, labelled with ^{32}P, of ATP.

(A) The *sev*$^{+}$ and other proteins are immunoprecipitated, as identified with MAb 150C3. Lane 1: wild-type heads, n=20; Lane 2: *sev*^{P3} heads, n=20; Lane 3: wild-type head immunoprecipitate; Lane 4: *sev*^{P3} head immunoprecipitate. Bands A and B (arrowheads) and immune complex (filled arrows) as in Figure 4.

(B) Kinase activity in the immunoprecipitates. Lane 1: wild-type head and Lane 2: *sev*^{P3} head immunoprecipitates incubated in kinase reaction buffer containing 5 mM $MnCl_2$ with enolase (open arrowhead) added; Lane 3: wild-type head and Lane 4: *sev*^{P3} head immunoprecipitates incubated in kinase reaction buffer containing 20 mM $MnCl_2$ with enolase added. Lane 5: wild-type head and Lane 6: *sev*^{P3} head immunoprecipitates incubated in kinase reaction buffer containing 20 mM $MnCl_2$ without added enolase. Lane 7: MAb 147H2 and Protein A beads incubated in kinase reaction buffer containing 20 mM $MnCl_2$ without added enolase.

(C) Alkali treatment of the samples does not remove phosphates. Lane 1: wild-type and Lane 2: *sev*^{P3} head immunoprecipitates incubated in kinase reaction buffer containing 5 mM $MnCl_2$ with enolase (open arrowhead) added; Lane 3: wild-type head and Lane 4: *sev*^{P3} head immunoprecipitates incubated in kinase reaction buffer containing 20 mM $MnCl_2$ with enolase added. After electrophoresis, the gel was incubated with KOH as described in Experimental Procedures. Compare with same lanes as in part B.

Part A, the immunoprecipitate control lanes, demonstrate that the *sev*$^{+}$ and cross-reacting bands were immunoprecipitated. Part B shows that radio-labelled antibody heavy chain

(filled arrow) and, if present, enolase (open arrow) are present in both wild-type and mutant lanes. Therefore, an active protein kinase is precipitated by MAb 147H2, but this activity is not *sev*$^{+}$-specific. Part C shows that the phosphates applied are resistant to elevated pH. The identity of other phosphorylated proteins is unknown.

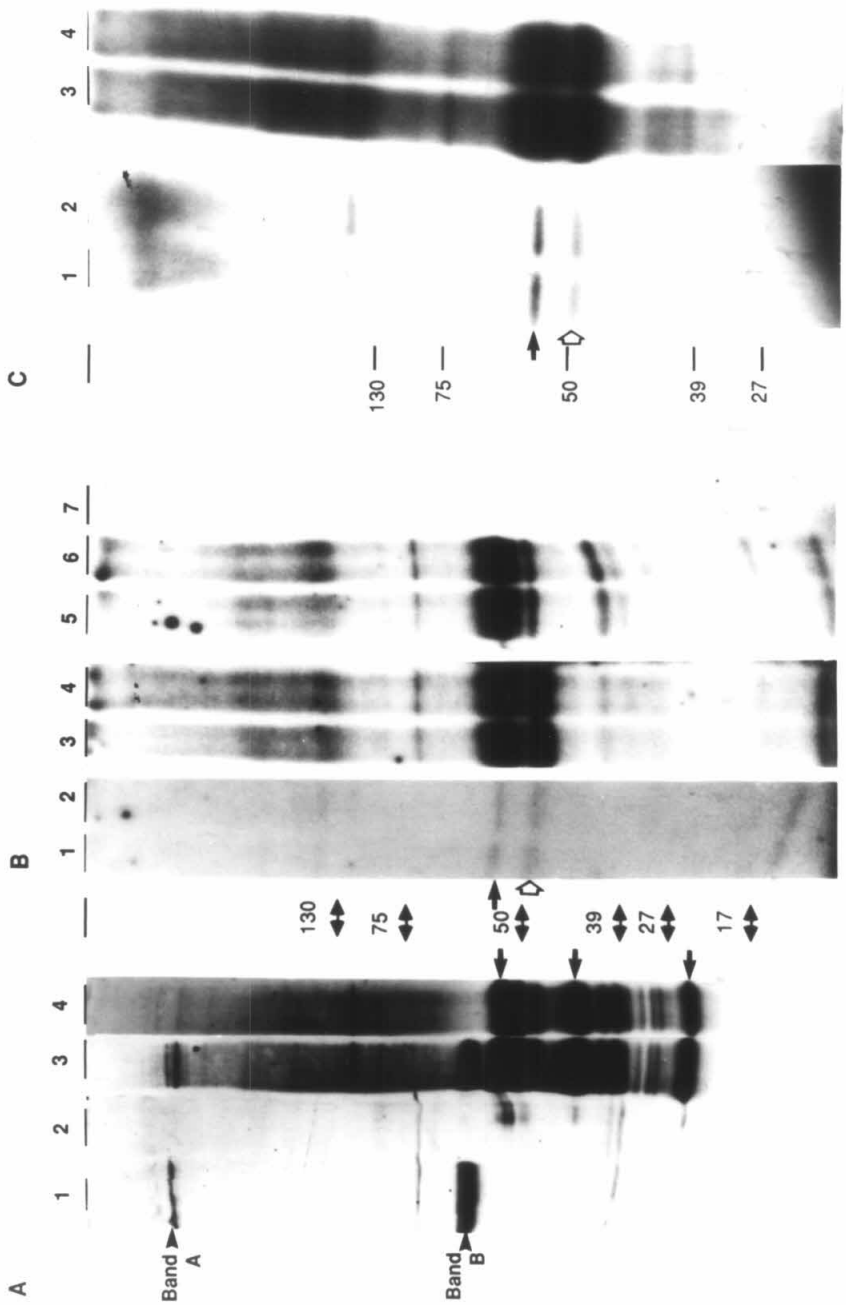
A
1
2
3
4
Band A
Band B
B
1
2
3
4
5
6
7
130
75
50
39
27
17
C
1
2
3
4
130
75
50
39
27

Figure 6. Localization of phosphotyrosines in the late third instar eye disc.

Late-third instar eye discs were stained with anti-phosphotyrosine antiserum.

Bars in (A) and (C) = 30 μm. Bars in (B) and (D) = 10 μm.

(A, B) Wild-type.

(C, D) Null allele sev^{P1}.

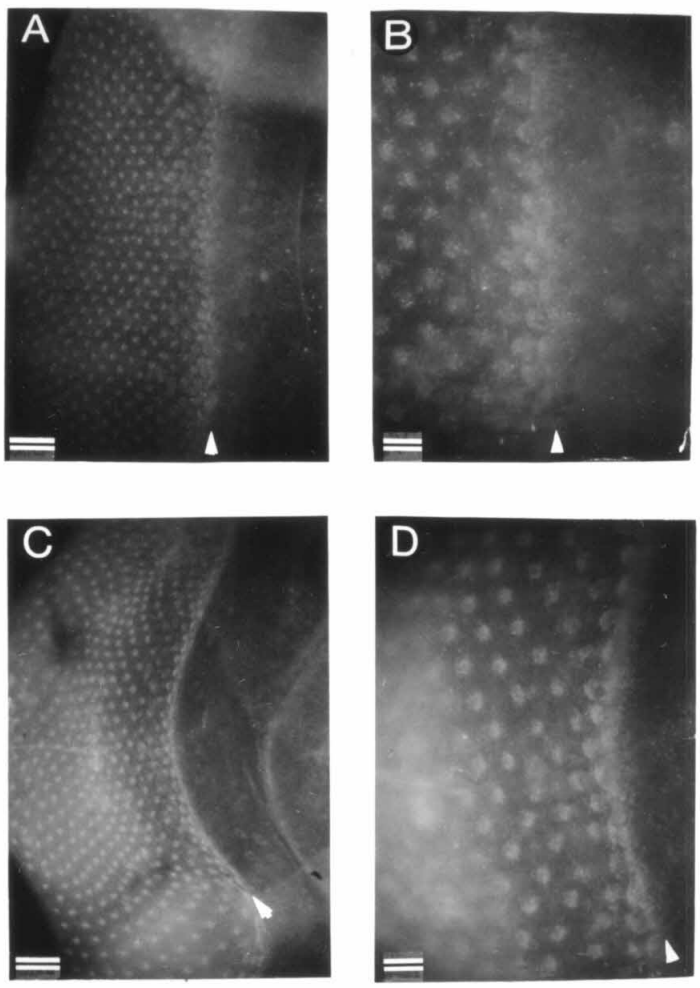
A
B
C
D

Table 1. Expression of the *sev* Gene Transcript and Protein in *sev* Alleles

	Transcript [Probe: c2(3)]		Protein expression [Probe: MAb 150C3]	
Allele	Head Northern	Eye disc *in situ*	Eye disc whole mount	Head Immunoblot
sev^+	+	+	+	+
E1	+	+	-	-
E2	+	+	+	+
E3	+/-	+/-	-	-
E4	+	+	+	+
E5	+	+	-	-
P1	-	-	-	-
P2	+	+	+	+*
P3	2	+/-	-	-**
LY3	+	+	+	+*
dr1	+/-	+/-	-	-
bb	?	nt	-	-
fig	+	-	-	+/-
elm	+	-	-	-
f1	+	+	-	-
d2	?	+	-	-
x1	?	+	-	-
x3	+/-	+	-	+/-
f3IE	2	nt	-	-

nt = not tested

* ratio of 250 kDa species to 60 kDa species greater in these alleles than in wild-type

** region encoding epitope deleted

Chapter IV

The *sevenless*$^{+}$ Protein Is Expressed Apically in Cell Membranes of Developing *Drosophila* Retina; It is Not Restricted to Cell R7

Introduction

The ultrastructural localization of the *sev*$^+$ protein is described in this chapter. The data were published in the following manuscript:

Banerjee, U., Renfranz, P.J., Hinton, D.R., Rabin, B.A., and Benzer, S. (1987). The *sevenless*$^+$ protein is expressed apically in cell membranes of developing *Drosophila* retina; it is not restricted to cell R7. *Cell* **51**, 151-158.

The chapter includes two major additions to the discussion section of the paper, in which our results are compared with those of Tomlinson et al. (1987), and also an additional proposal of R7 determination.

Study of a mutant lacking a single element of pattern could help in understanding the signals that lead to normal pattern formation. The *sev* gene was therefore cloned (Chapter II; Banerjee et al., 1987a), and it was shown to code for a single 8.2 kb transcript expressed at the apical surface of the eye disc epithelium, behind the morphogenetic furrow. The gene was independently cloned by Hafen et al. (1987), who showed that the conceptual translation of the sequence obtained from the 3' end of a *sev* cDNA gives a peptide sequence with marked homology to several protein tyrosine kinases, including the oncogenes v-*ros* and v-*src*, as well as to the kinase domain of the epidermal growth factor receptor.

To determine the cellular localization of the protein product of the *sev*$^+$ gene, we generated a fusion protein consisting of the C-terminal region of the *sev*$^+$ protein linked to bacterial β-galactosidase (see Chapters II and III). Mouse polyclonal antiserum made against this fusion protein stained the eye disc in a regular pattern associated with developing photoreceptor clusters (Chapter II; Banerjee et al., 1987a), and the staining was absent in a mutant lacking the *sev*$^+$ gene. In this chapter, the ultrastructural localization of the *sev*$^+$ protein is described, using a monoclonal antibody (MAb) raised

against the fusion protein.

Results

Eye disc immunohistochemistry by light microscopy

Figures 1A and B show MAb 150C3 staining of eye discs from wild-type and the EMS-induced mutant *sev*^{d2}. The specific staining in the wild-type eye disc begins immediately behind the furrow, in relatively diffuse patches. More posteriorly, the staining becomes more precisely localized over each cluster. The spacing between clusters is about 10 μm, but the stained crown on each cluster is approximately 3.5 μm wide. In the mutant *sev*^{d2} eye disc, this specific staining pattern is absent (Fig. 1B). Of the 18 *sev* alleles tested, 14 show no detectable staining pattern (see Chapter III). The other four alleles exhibit patterns similar to wild-type; these also show a normal-sized RNA band on Northern blots (Chapters II and III; Banerjee et al., 1987a; unpublished results).

In addition to the patterned staining, a weak background is also seen in the eye disc, possibly resulting from cross-reacting proteins (see Chapter III), since this staining persists in all *sev* mutants. The staining in larval brain (not shown) is also diffuse, and was not different in wild-type and *sev* mutant larval brains, even though protein immunoblot analysis (Chapter III) clearly shows that the *sev*$^{+}$ protein is present.

The MAb 150C3 staining is shown at higher magnification in Figures 2A and B. At the furrow (Fig. 2A), the diffuse patches on the apical surface initially look unpatterned. Later in development (more posteriorly) they collect into clusters of a few cells. Still more posteriorly (Fig. 2B), fibrillary, toroidal figures form.

In Figure 2C, a wild-type disc has been stained with a mixture of MAbs 150C3 and 22C10 to put their patterns in register. MAb 22C10, unrelated to *sev*, is used here as a marker for all neurons (Fujita et al., 1982); it is expressed early in the differentiation of the photoreceptor cells, shortly behind the furrow, first appearing intracellularly at their

apical tips. Tomlinson and Ready (1987a) showed that this antigen appears in a defined sequence among the photoreceptor cells, cell R8 being first. In the doubly stained normal disc, dots of 22C10 antigen are first found toward the rear of each sev^+ antigen patch; later they become central to the toroidal crowns. By changing the plane of focus, it was established that the *sev* antibody staining is more apical than the 22C10 apical tips staining.

The apical localization of the *sev* protein was striking, being limited to about a micron from the surface of an epithelium some 50 μm thick. Since the discs were stained as whole structures, this raised the question of the extent of penetration of the antibody into the tissue. Therefore, frozen sections of eye discs were stained with MAb 150C3. Figure 2D shows that staining of sections is also limited to the apical surface.

While most of the *sev* alleles failed to show staining with the MAb against sev^+ protein, some did express proteins that bind the antibody. These proteins must still be defective, since cell R7 does not form. Remarkably, the staining patterns in these mutants, which lack cell R7, were not very different from the wild-type pattern. This was an indication that the expression of sev^+ protein is not restricted to cell R7. To determine which cells express the protein, we studied the localization at the electron microscopic level.

Ultrastructural localization

Figures 3A and B compare the transmission EM images of a wild-type eye disc and of a disc from mutant sev^{P1} in which the *sev* gene has been deleted (Chapter II; Banerjee et al., 1987a). These were stained with MAb 150C3 and sectioned perpendicular to the furrow. In the wild-type disc, staining is limited to the apical edge of the disc, commencing at the furrow. Immediately behind the furrow the staining is at first fairly continuous; further posteriorly, where mature clusters form, the staining becomes largely restricted to a tuft at the top of each cluster. In the sev^{P1} disc (Fig. 3B), this specific

staining is absent.

Figure 4 shows a section of the furrow region at a somewhat oblique angle. In the central part of the figure, the section cuts through a mass of microvilli within the furrow. The earliest staining appears at the anterior edge of the furrow (at the right of the figure). This expression occurs focally in the membranes of microvilli of cells not yet organized into clusters. Along the posterior edge (at the left of the figure, corresponding to a slightly later stage of development) dark staining appears in a continuous fashion along the epithelium, on the apical cell membranes and the membranes of the microvilli.

Toward the posterior end of the disc, where the 8-cell clusters are fully formed, the staining becomes localized into the pattern of tufts that was shown in Figure 4. Figure 5 shows sections perpendicular to the surface at progressively higher magnifications. Staining is localized to the plasma membranes of the microvilli that form the tuft at the apex of each cluster and to a region about a micron thick along the apical cell membranes.

Figure 6 shows a set of sections tangential to the disc. At the highest level (Fig. 6A), the regular array of tufts of stained microvilli is visible. The plane of section also cuts into the curved disc surface somewhat, and stained outlines of clusters of cell membranes within the disc can be seen. Figure 6B shows two tufts at higher magnification. In a deeper section (Fig. 6C) the membranes of not only the eight photoreceptor cells but also the four peripheral cone cells are clearly stained by the MAb. In some cases, staining can be seen also in membranes of the surrounding cells, which are possibly precursors of pigment cells. In Figure 6D, at a still deeper level, the same cluster clearly shows that the membranes of all eight photoreceptor cells are stained.

It is important to point out that because of the extreme apicality of expression of the antigen, in a slightly oblique cut it is not unusual to find clusters that appear to lack staining in some of the cells. However, our serial reconstructions revealed that the expression of the antigen is not restricted to particular cell types.

Morphology of the tufts

Figure 7A shows an EM section of a tuft in a wild-type eye disc, using conventional fixation and staining. With this treatment the ultrastructure of the cell and their microvilli are better preserved than in lightly fixed tissue used for the immuno-EM studies. The convergence of the apices of the cells in a cluster is seen, their prominent microvilli forming a tuft that projects into the extracellular matrix.

The surface of the eye disc can be visualized in the scanning EM in whole mounts with the peripodial membrane removed (Ready et al., 1976). The microvilli are ordinarily obscured by a fibrous extracellular matrix that overlies the epithelium. We found that mild treatment with collagenase largely removes this material, revealing the microvillar array behind the furrow shown in Figures 7B and C. While microvilli are present over the entire surface of the disc, the photoreceptor clusters have long, nested microvilli at their tips, forming the tufts that appear after the furrow. These correspond in size, morphology, and location to the toroidal structures highlighted by the antibody against the *sev*$^{+}$ protein.

Discussion

In Chapter II (also, Banerjee et al., 1987a), a polyclonal antiserum to the *sev*$^{+}$ protein revealed a striking pattern corresponding to the array of ommatidia. In this chapter, using a monoclonal antibody, the protein has been localized at the ultrastructural level. Expression of the *sev*$^{+}$ protein is not limited to the presumptive cell R7. It appears also in all the other photoreceptors, as well as the cone cells, and is apical in the disc from its first appearance. As has been previously reported, the *sev*$^{+}$ gene transcript, at the furrow, is expressed throughout the thickness of the epithelium, becoming apical later, as the clusters mature (Chapter II; Banerjee et al., 1987a; Hafen et al., 1987). This suggests the possibility that the *sev*$^{+}$ mRNA may be transported during development to the apical regions of the cell. Transcript localization has recently been noted also for certain

cytoskeletal proteins (Lawrence and Singer, 1986), as well as for an mRNA species of possible developmental relevance in the *Xenopus* oocyte (Melton, 1987). Transport of *sev*$^+$ mRNA might provide an interesting system for studying protein-sorting in the polarized epithelial cells.

The *sev*$^+$ protein shows marked homology to protein tyrosine kinases in its C-terminal intracellular domain, and may also have a large extracellular domain that functions as a receptor (Hafen et al., 1987; Basler and Hafen, 1988; Bowtell et al., 1988). This study shows that the protein is abundant in the membranes of apical tips of cells and their microvilli, consistent with the idea that it is a receptor molecule. However, it is not restricted to cell R7, but is expressed in other cells as well. There is also the intriguing observation that the *sev*$^+$ protein is expressed in the brain of the larva as well as in the adult head, even in mutants lacking photoreceptors, as well as the adult body (Chapter III). The *sev*$^+$ protein therefore could be involved in differentiation of several neuronal tissues. Certain similarities can be seen with the expression of another tyrosine kinase, c-*src*, which is expressed postmitotically at the onset of neuronal differentiation in Drosophila (Simon et al., 1985) as well as in vertebrate cerebellum and retina (Sorge et al., 1984; Fults et al., 1985).

Studies on genetically mosaic eyes (Harris et al., 1976; Campos-Ortega et al., 1979; Tomlinson and Ready, 1987b) have shown that the *sev* mutation is cell autonomous. The presence of *sev*$^+$ function in the presumptive cell R7 thus appears to be a necessary condition for the cell to mature; usually, a cell R7 of *sev*$^-$ genotype is never seen even when all the other photoreceptor cells in a cluster are *sev*$^+$. Furthermore, a *sev*$^+$ R7 cell can mature even if all its companion photoreceptor and pigment cells are genetically *sev*$^-$; the absence of the *sev*$^+$ gene product in surrounding mutant cells does not prevent the differentiation of a genetically normal cell R7. Conversely, the *sev*$^+$ function is unnecessary for the differentiation of the remaining seven photoreceptor cells, which manage to form a reasonable cluster in *sev* mutants.

The expression of the *sev*$^+$ gene in all the cells could be a mechanism for providing pluripotency during development. Experiments with mosaics show that there are no strict lineage relationships among the photoreceptor cells (Ready et al., 1976; Lawrence and Green, 1979). In a *sev*$^+$ eye, any cell can potentially become cell R7. Yet, only one cell is triggered to assume this fate. It has been suggested that this induction is mediated by cell-cell interactions in which large areas of membrane contact are shared between particular combinations of the presumptive photoreceptor cells (Ready et al., 1986). In this context, the highly localized expression of the *sev*$^+$ protein at the apical tips, away from the bulk of the cell-cell membrane contacts, is surprising. The localization suggests that the membranes of apical tips and their microvilli play an as yet undescribed, important role in the accurate organization of clusters.

The distribution of the *sev*$^+$ protein was also determined by Tomlinson et al. (1987), using a polyclonal serum directed against a synthetic C-terminal peptide. Certain discrepancies exist between their results and the results described herein. However, the major conclusions of the localization are similar: The expression of the protein is not specific to presumptive R7, and its distribution is apical. The contrasting results and techniques are as follows: Tomlinson et al. (1987) used a silver / gold intensification technique for HRP staining, whereas our group used an Avidin-Biotin Complex procedure. Although both groups localized the protein to apical membranes, Tomlinson et al. also found antibody reaction product in intracellular vesicular bodies. Based upon a lack of vesicular staining, they conclude that cells R2, R5 and R8 do not express the *sev*$^+$ protein; they did not examine closely the more apical microvilli. Also, in the presumptive photoreceptors that did express the epitope, the staining was localized to membranes at the cells' contact with presumptive R8. They also saw staining in the membranes of the cone cells and what they term "mystery cells," and the distribution of stain varied as the clusters matured. We found membrane staining above the level of the desmosomes, especially in the region of the microvilli, in all the presumptive photoreceptor cells as well

as cone cells, along all cell membrane surfaces. This stain was limited to the plasma membrane; intracellular staining was never seen.

Banerjee, Hinton and A. Tomlinson (U. Banerjee and D.R. Hinton, pers. comm.) have made an initial attempt to clarify these results. Firstly, Tomlinson did not find vesicular staining at the light microscope level when using the Benzer lab MAb 150C3. This would lead one to suspect that the differences may be due to epitope expression and / or availability to antibody. However, using the Rubin lab antibody and intensification procedure, Banerjee and Hinton failed to detect any *sev*$^{+}$-specific intracellular staining at the EM level, nor did they detect any unstained cells among the presumptive cells in a cluster.

If the distribution found by Tomlinson and colleagues is correct, independent of epitope, then the presumptive cells R2, R5 and R8 do not have the potential to assume the R7 fate. This conclusion contradicts the genetic mosaic data, which strongly suggest that any one cell in the developing epithelium has the potential to assume the R7 fate. Also, our results suggest that *sev*$^{+}$ protein expression is initiated on the anterior, leading edge of the morphogenetic furrow (Fig. 4), before the establishment of preclusters and perhaps therefore before the assumption of any cell identities. It is interesting that Campos-Ortega et al. (1979) described a perdurance effect of *sev*$^{+}$ activity. In clones made shortly before pupariation, *sev*$^{-}$ cell R7s, as labelled with a marker, could be identified. The perdurance effect could occur if there had been only one to three cell divisions before the recombination event. This result indicates that expression of the *sev*$^{+}$ gene occurs before the final round of cell division in the epithelium. If expression of *sev*$^{+}$ protein is initiated before the last division, which occurs at the posterior, trailing edge of the furrow, then perdurance could be explained by a continued presence of *sev*$^{+}$ protein on the cell membranes after the genotype of the cell has become *sev*$^{-}$. Together, these data suggest that *sev*$^{+}$ must indeed be expressed in all presumptive retina cells, in order to maintain pluripotency. Current models claim that cell position in the developing cluster determines

cell fate, so if expression is initiated before precluster formation, all unpatterned cells on the anterior furrow edge must express *sev*$^+$ protein. If this interpretation is correct, it contradicts the conclusions of Tomlinson et al. (1987); their data would indicate that presumptive R8, R2 and R5, not expressing the protein, have eliminated one possible fate before the establishment of the precluster, and before their identities as such have been established.

Another interesting point in this regard is the following: In both Hafen's and Rubin's laboratories, P-element transformation constructs have been made in which transcription of the *sev*$^+$ gene is driven by the heat shock protein 70 or actin 5C promoter rather than by the native *sev* gene promoter (described by the respective groups at the EMBO Workshop on Molecular and Developmental Biology of *Drosophila*, Crete, 1988). These promoters would support equal transcription in any of the presumptive retina cells. The results show that R7 is determined in the transformants just as it is in wild-type flies, in terms of structural and morphological characteristics. Therefore, even if the results of Tomlinson et al. could be reproduced, the lack of expression in certain R cells that they saw is not likely to be functionally significant in the determination of R7.

The question remains as to how the specific differentiation of cell R7 is determined. Hafen et al. (1987) proposed that while a *sev*$^+$ product could be expressed in many cells, the tyrosine kinase activity might be limited to the presumptive cell R7, the activity being triggered by positional information mediated through specific cell-cell contacts. It is important to note that the antibody staining shows only the presence of the antigen, not where it is active. Basler and Hafen (1988) have subsequently constructed a mutation in the *sev* gene in which the conserved lysine residue in the tyrosine kinase domain, the putative ATP-binding site, is replaced with an arginine residue. Unlike an unaltered construct, this construct, when transformed into a *sev* mutant, is not capable of rescuing the *sev* phenotype. Hence, it can be concluded that a functional tyrosine kinase is instrumental in R7 determination.

While cell-cell contacts at the apical tips could introduce positional specificity, the extensive staining seen in the microvilli suggests that diffusible factors are involved. The tufts of microvilli may allow developing cells to interact with all the cells in a cluster, not only their nearest neighbors. Activity of *sev*$^+$ protein could be triggered in cell R7 by ligands expressed on the microvilli of other cells. Since the presumptive cell R7 is the last to join a cluster, it could be most subject to influence by the ensemble of others.

In another possible mechanism, the microvilli containing the *sev*$^+$ protein would, instead, interact with components of the extracellular matrix into which they project. Constituents of the basal lamina and intercellular space have been reported to exert important effects on neuronal development (Adler et al., 1985; Blumberg et al., 1987; Grumet et al., 1985). Although the apical extracellular matrix has not been explored in detail, it is interesting to note that a MAb (3E1) stains the extracellular matrix of the eye disc, and that this staining disappears behind the furrow as it advances (Zipursky et al., 1984), indicating that the biochemical characteristics of the matrix change during development.

An alternate model could account for the localization of the *sev*$^+$ protein in the apical microvilli, its expression in all cells, and the requirement for its activity only in the last cell to assume a neuronal phenotype in the cluster. The assumptions are that 1) all cells in the retinal epithelium have the potential to assume the R7 fate, but that an inhibitory molecule, present in the extracellular matrix, limits the activity of the enzyme and therefore inhibits R7 differentiation, and 2) the inhibitor is removed by being bound up or otherwise inactivated by cells that express the *sev*$^+$ protein. The first seven cells to join and differentiate in the cluster are inhibited from assuming the R7 fate, but as they join and differentiate, they inactivate the inhibitor and bring the level of inhibitor down to the threshold for R7 fate activation. When the concentration of the inhibitor falls below this threshold value, a cell can differentiate into R7, and this threshold crossing occurs reproducibly in the wild type after seven cells have joined clusters. In eye mutants in

which the number of R cells in each ommatidium varies, this model would predict that ommatidia with fewer than the normal complement of eight R cells would be phenotypically sevenless, while ommatidia with more than the normal complement of eight R cells would have multiple R7-like neurons.

Another possibility is that the specificity of the developmental response of the presumptive cell R7 could be due, not to the *sev*$^+$ product, but to a substrate for the kinase that is contained only in that cell. Cell-specific protein kinase substrates have been reported (Greenberg et al., 1984). If that is the case, one would expect that other genes whose products are solely expressed in cell R7 could give rise to autonomous sevenless phenotypes. Non-autonomous mutations could indicate the ligands involved. Reinke and Zipursky (1988) have identified mutations in a different gene, *boss*, on the third chromosome, that exhibit a sevenless phenotype. Unlike the *sev*$^+$ gene product, *boss*$^+$ function is not required autonomously by presumptive R7. Rather, its function is required solely in R8 to support the development of an R7 in the ommatidia. Its function does appear to be required in an "ommatidial autonomous" fashion. At this time, the distribution and activity of the *boss*$^+$ gene product and its possible interaction with the *sev*$^+$ protein are unknown (see Epilogue).

Experimental Procedures

Strains

The *sev* mutant and wild-type strains have been described (Chapter II; Banerjee et al., 1987a).

Immunohistochemistry and electron microscopy

Immunofluorescent staining of late third instar eye discs was performed as described (Zipursky et al., 1984). For immunoperoxidase staining, the peripodial

membrane was removed and the discs were fixed with 4% paraformaldehyde, 0.1% glutaraldehyde in 100 mM phosphate buffer for 5 min. Discs were stained utilizing the ABC method (Vector Labs), modified by the addition of 0.01% saponin in the dilution and wash buffers. The reaction product was visualized using 0.05% diaminobenzidine (DAB) and 0.02% hydrogen peroxide.

For transmission EM, whole discs were lightly fixed and then stained by the ABC method, as for light microscopy, but subsequent to DAB development, the discs were stained with 2% OsO_4 for 45 min, washed, postfixed with 1% glutaraldehyde, 1% paraformaldehyde in 100 mM phosphate buffer (pH 7.5) for 15 min, dehydrated, and embedded in Polarbed. Serial thin sections were viewed on a Phillips 301 or Zeiss EM10 electron microscope. These sections were not stained with uranyl acetate, in order to minimize darkening of membranes by anything other than the antibody-antigen reaction product.

For EM without antibody staining, discs were fixed with 1% glutaraldehyde, 1% paraformaldehyde in 100 mM phosphate buffer (pH 7.5), washed in 100 mM phosphate buffer, osmicated, stained in uranyl acetate, dehydrated and embedded in Polarbed. These thin sections were poststained with 0.16% uranyl acetate in 33% ethanol.

For scanning EM, eye discs were placed in TBS and their peripodial membranes removed by microdissection. The extracellular matrix was removed by a 1 min treatment with 70 units/ml collagenase (Worthington). Discs were fixed overnight in 2.5% glutaraldehyde, 2% paraformaldehyde in 100 mM cacodylate buffer (pH 7.3), stained with 2% OsO_4 for 1-2 hr, dehydrated, critical-point dried, sputter-coated with 10 nm of gold, and viewed on a Hitachi S-570 scanning EM.

Figure 1. Immunofluorescent staining of whole mounts of eye discs with MAb 150C3. Anterior is to the right. Arrow: morphogenetic furrow. Bar = 25 μm.

(A) Wild-type (B) Mutant *sev*^{d2}

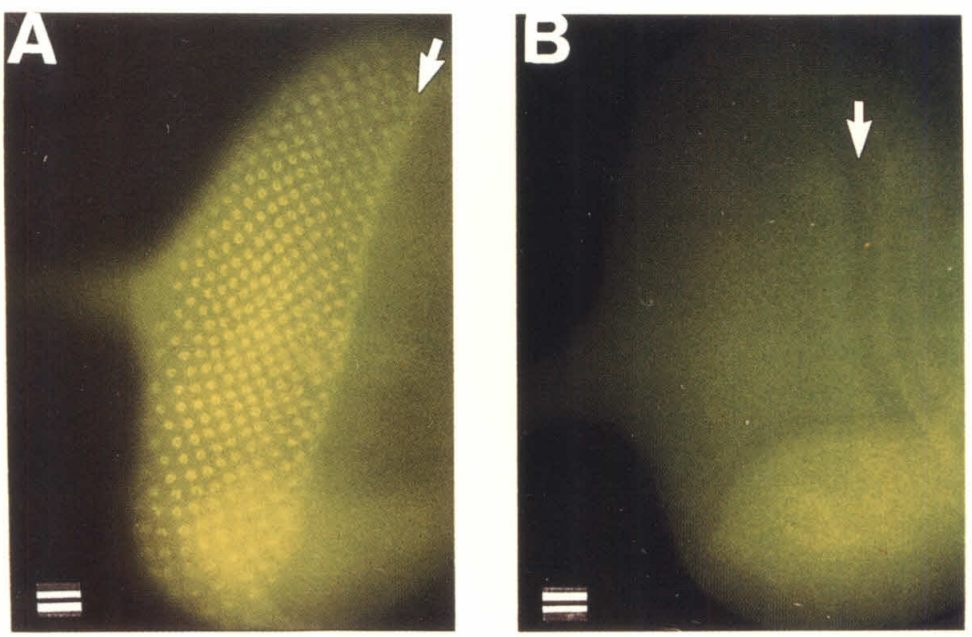
A
B

Figure 2. Localization of the *sev*$^+$ protein at the light microscope level.

(A) and (B) Wild-type eye disc stained with MAb 150C3, using ABC-peroxidase, and viewed with Nomarski optics.

(A) Furrow is marked by an arrow. Figure shows progression of staining from relatively unpatterned patches at the furrow to a well-defined region on each cluster. Anterior is to the right. Bar = 7 μm.

(B) Higher magnification view of the fibrillary staining on each cluster at the posterior end of the disc. Bar = 5 μm.

(C) Double immunofluorescence staining of a wild-type disc with a mixture of MAb 150C3 and MAb 22C10 (a general marker for neurons). Anterior is to the right.

Bar = 10 μm. Arrow: morphogenetic furrow.

The staining pattern for MAb 150C3 could be easily distinguished from that of MAb 22C10, as determined by comparing the pattern of the mixture to that for each MAb alone. In this figure, MAb 22C10, shows as fine dots corresponding to the apical tips of the developing photoreceptor neurons. These dots at first are in the posterior portions of the *sev*$^+$ patches. Later, i.e., more posteriorly, the tips become central to the toroidal *sev*$^+$ figures.

(D) Immunofluorescent staining with MAb 150C3 of a longitudinal section of a 7 to 9 hour prepupa. At this stage, the furrow has traversed the eye disc. The specific staining is apically localized. ed = eye disc, br = larval brain. Bar = 25 μm.

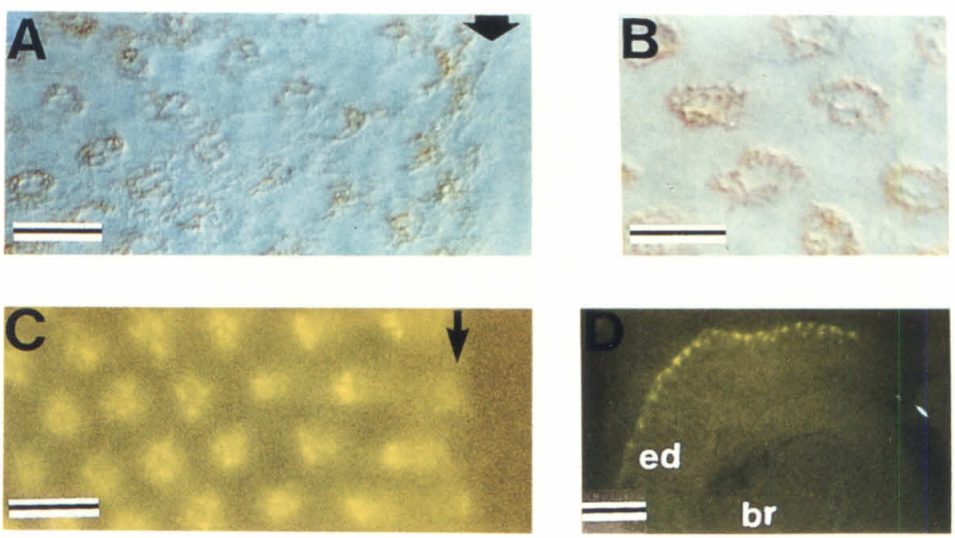
A
B
C
D
ed
br

Figure 3. Immuno-EM of eye discs, using MAb 150C3.

Stained discs were sectioned perpendicular to the furrow. Anterior is to the right. Large arrows mark the morphogenetic furrow. Bar = 10 μm.

(A) In wild-type, specific staining commences at the morphogenetic furrow and continues posteriorly. It is restricted to the apical surface of the disc. Arrowheads indicate a few of the stained apical tufts.

(B) Null allele sev^{P1} shows no staining.

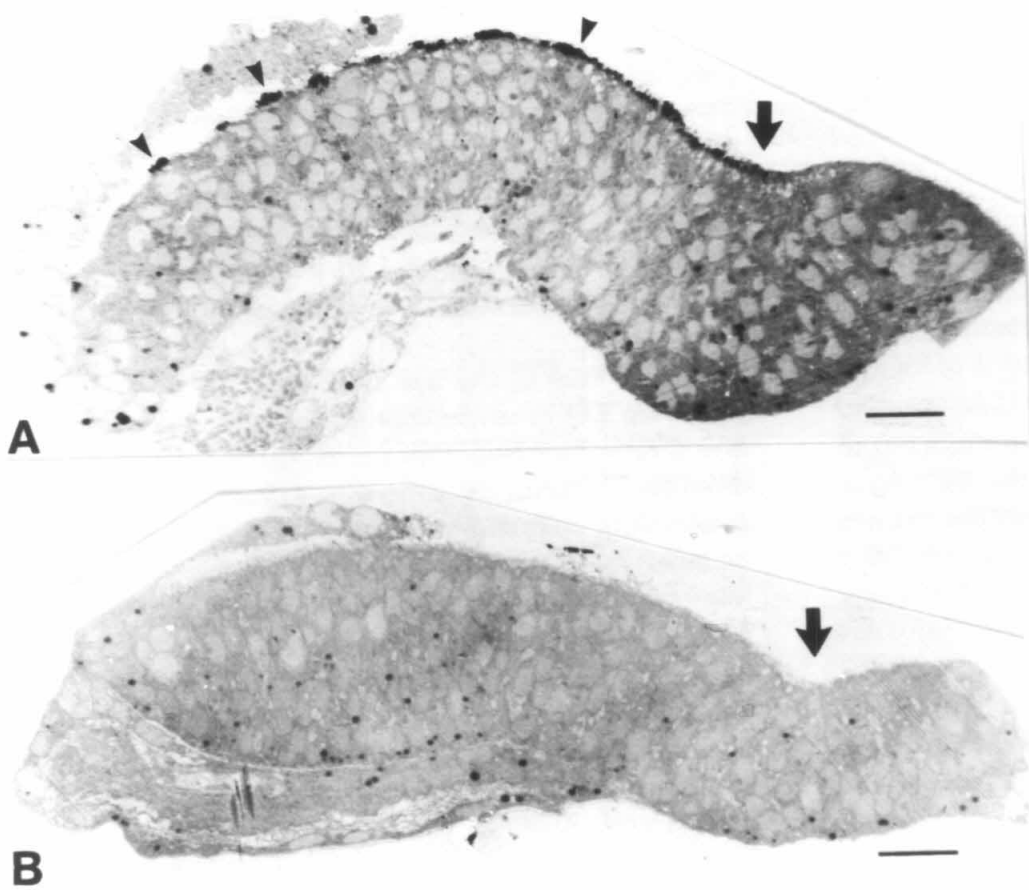
A
B

Figure 4. Immuno-EM of a wild-type eye disc, using MAb 150C3.

The figure shows a glancing section across the morphogenetic furrow (arrow). A = anterior edge of the furrow; P = posterior edge. Microvilli (M) line the apical surface. Staining appears at the anterior, leading edge of the furrow, on the cell membranes of a few microvilli (arrowheads). On the posterior edge, *sev*$^{+}$ protein is found in a continuous pattern on the membranes of the microvilli and the apical extremities of the cells.

Bar = 1 μm.

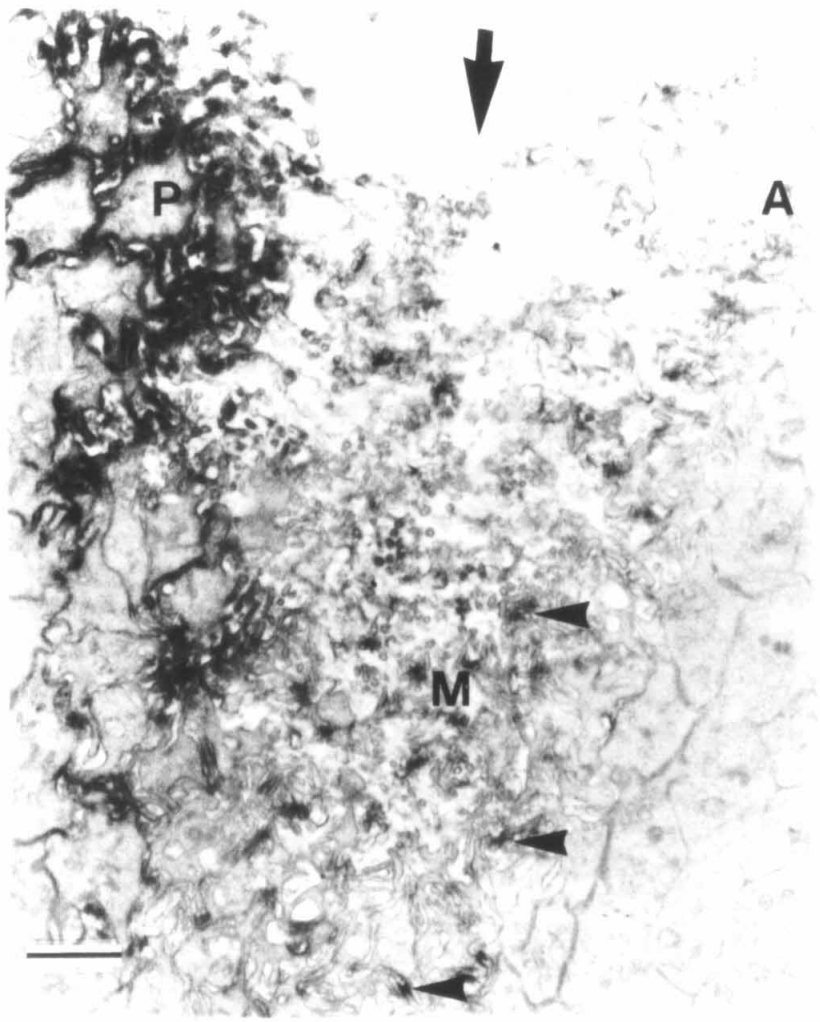
P
A
M

Figure 5. Transmission EM of wild-type discs stained with MAb 150C3.

Plane of section is perpendicular to the morphogenetic furrow. Anterior is to the right.

(A) At low magnification, *sev*$^{+}$ protein can be seen at the apical tuft of each cluster. Bar = 5 μm.

(B) At higher magnification, staining of the tuft overlying each cluster is specifically localized to the apical cell membranes and their microvilli. The cell membrane staining extends for a short distance below the surface of the disc, then stops. Bar = 1 μm.

(C) At still higher magnification, *sev*$^{+}$ protein is clearly associated with the plasma membranes of the cells and their microvilli. Bar = 0.3 μm.

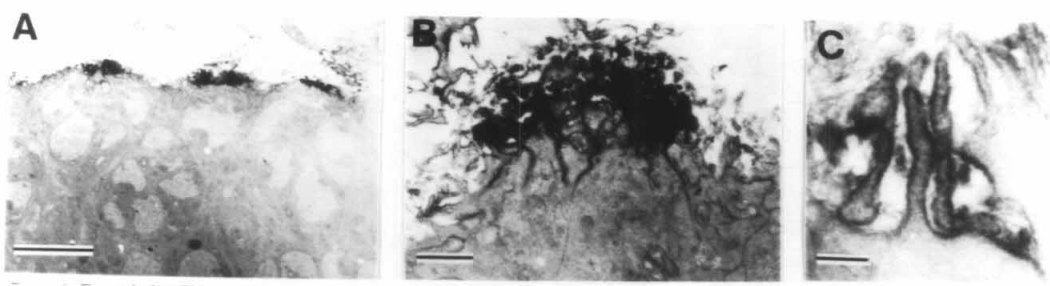
A
B
C

Figure 6. EM of a wild-type eye disc stained with MAb 150C3 in tangential sections parallel to the surface of the disc at different levels.

(A) By virtue of curvature of surface, one can see, in a section grazing the disc, staining at various levels. The most apical regions (lower area) show tufts of microvilli. More basally (upper center), outlines of clustered apical tips of cells can be seen in the tissue. Staining ranges from strong in the most apical microvilli, to fairly dark in the apical tips of cells in each cluster, to unstained regions at more basal levels. Bar = 5 μm.

(B) Section at higher magnification through two tufts.

(C) Section slightly below the surface showing staining in the membranes of the central cluster of eight photoreceptor cells as well as four surrounding cone cells (c). Staining can also be seen in microvilli extending from the upper cone cell. Bar = 0.5 μm.

(D) The same cluster as in (C), at a slightly lower level where the photoreceptor cells are larger in cross section. All eight neurons are clearly stained. Staining in the cone cells (c), however, is much reduced at this level. Bar = 0.4 μm.

In both (C) and (D), the staining is not of uniform intensity in all the cells. However, in successive sections, no particular cell type stood out as being much richer in staining at all levels.

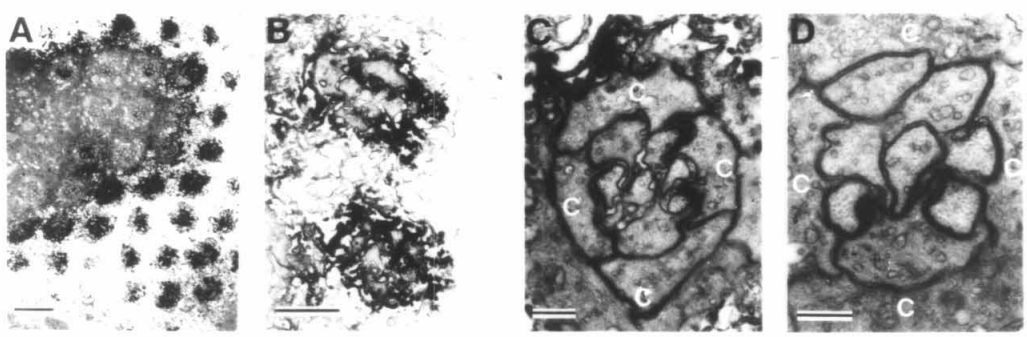
A
B
C
C
C
C
C
D
C
C
C

Figure 7. *Structure* of the apical tufts.

(A) Transmission EM of a section perpendicular to the surface of a conventionally fixed eye disc. The microvilli are seen projecting into the extracellular matrix, which lies between the disc surface and the peripodial membrane. Unlike the discs for immuno-EM, this disc stained in an uranyl acetate before and after sectioning. All the cell membranes are therefore dark. Bar = 2 μm.

(B) Scanning EM of a wild-type eye disc. Anterior is to the right. Arrow marks the furrow. The peripodial membrane of this disc was dissected off, and the extracellular matrix was removed by collagenase, revealing the array of microvillar tufts. Bar = 20 μm.

(C) At a higher magnification, each tuft can be seen to be composed of long, nested microvilli. Bar = 4 μm.

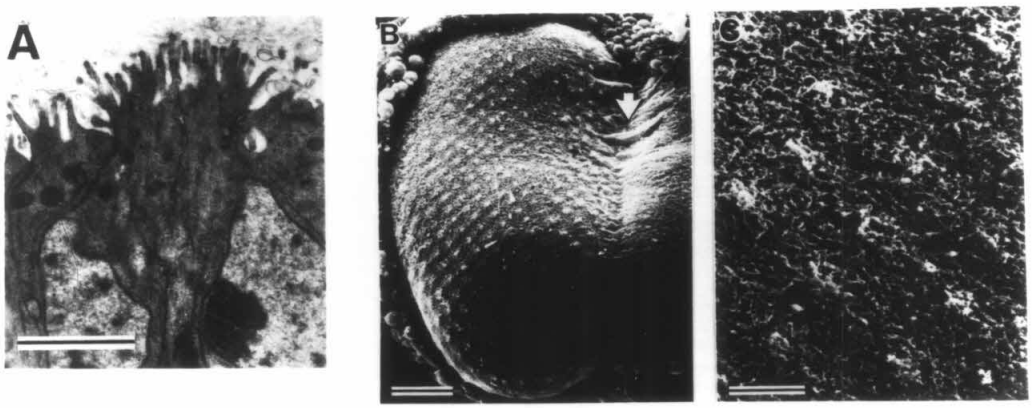
A
B
C

Chapter V

Characterization of Mutations Affecting the *Drosophila* Retina Using Monoclonal Antibody Staining of Late Third Instar Eye-Antennal Imaginal Discs

Introduction

During neural development, a program of diverse events must unfold in a temporally and spatially precise manner. These events include the generation of a precursor cell population, the control of precursor cell division, and the routing of daughter cells into developmental pathways. In many cases, in both vertebrates and invertebrates, daughter cell-type determination may occur independently of cell lineage (Ready et al., 1976; Lawrence and Green, 1979; Greenwald et al., 1983; Taghert et al., 1984; Turner and Cepko, 1987; Holt et al., 1988; Wetts and Fraser, 1988). These results imply that extracellular cues and interactions between cells function during cell-type determination. The characterization of mutations is a valuable means of studying neuronal patterns, as exemplified in studies of genes that have profound effects upon other aspects of pattern formation in *Drosophila* and in *C. elegans* (for reveiw, see Ingham, 1988; Sternberg and Horvitz, 1984).

The compound eye of *Drosophila* provides an attractive system for the study of neuronal development. Garcia-Bellido and Merriam (1969) estimated that about 23 precursor cells in a particular place in the blastoderm-stage embryo divide to generate the monolayer epithelium that will constitute the eye portion of the larval eye-antennal imaginal disc (for review, see Meinertzhagen, 1973; Kankel et al., 1980; Ready et al., 1986). These cells remain morphologically and antigenically undifferentiated until the middle of the third larval instar (see Zipursky et al., 1984). Genetic mosaic analysis indicates that these cells are multipotent until their final cell division (Ready et al., 1976; Lawrence and Green, 1979). The precursor cells for each of the cell types found in the adult eye thus do not constitute distinct populations.

During midthird instar, the cells begin to form the reiterative pattern associated with the ommatidia of the adult eye (Ready et al., 1976; Tomlinson, 1985). A morphogenetic furrow traverses the eye disc epithelium from posterior to anterior. Within the furrow, cells form into groups, first recognizable as clusters of five cells. These clusters are rather

evenly spaced at a distance of about 12-15 μm in each row. The five cells within each cluster soon begin to express neural antigens and to elongate axons (Zipursky et al., 1984; Tomlinson and Ready, 1987a). The five cells in each cluster have been traced through their subsequent development, and correspond to the adult photoreceptor cells R2, R3, R4, R5 and R8. The surrounding unpatterned cells undergo another round of cell division, and their daughters join the clusters, assuming the fates associated with the remaining elements of the pattern. Presumptive cells R1 and R6 are added, and finally R7, to complete the photoreceptor cell complement. The four presumptive accessory cone cells and the presumptive pigment cells are added radially to the eight-cell clusters. Prior to pupation, at least, pattern formation in the eye disc does not appear to be accompanied by substantial cell death (Fristrom, 1969; Spreij, 1971).

Terminal differentiation of the elements of the adult eye begins at the furrow during the middle of the third larval instar and continues throughout pupation, as described by Waddington and Perry (1960) and Perry (1968). Ommatidial morphogenesis includes the following: Early differentiation and movements place the bulk of the two primary pigment cells distal to the cone cells, and the four cone cells distal to the R cells. The sensory hair is secreted, and pigment granules are deposited in the pigment cells. Each ommatidium becomes covered with a cuticle layer, and the fibrous material of the corneal lens is laid down in a lamellar fashion, probably by the cone cells. The R cells elongate, and the light-collecting organelles, called the rhabdomeres, are formed. Expression of many genes associated with visual transduction begins after about 72 hours of pupal development (Montell et al., 1985; Zuker et al., 1985; Cowman et al., 1986; Fryxell and Meyerowitz, 1987; Montell et al., 1987; O'Tousa et al., 1985; Zuker et al., 1987).

Many different eye mutations have been identified, often based on external changes in the adult eye morphology or color, many of which are tabulated in Lindsley and Grell (1967). Examination of only the adult eye phenotypes of the different mutants does not allow specification of the time when the corresponding gene products are required.

However, mutations might be identified that disturb each step in the process, from precursor cell proliferation to maintenance and terminal form. Examination of the eye discs from these mutants should allow one to determine the stage of development at which each defect becomes manifest. This can, in turn, give some indication of the time when the corresponding genes function.

Monoclonal antibodies (MAbs) that stain various gene products sequentially expressed during development of the eye can be used to highlight various aspects of the array of presumptive ommatidia. This study employs a set of such MAbs in a comparative study of the developmental events in *Drosophila* eye mutants. Eye discs from twenty mutants were dissected from late third instar larvae and stained with the selected set of MAbs. The eye disc phenotype was then examined, to identify the stage at which the first morphological abnormalities occur in each mutation. In Table 1, a framework is established for identifying various classes of mutant phenotypes, including the probable time of gene action. At least one example from each class is presented in detail. Further characterization of these genes should allow the identification of proteins that function in the molecular interactions occurring during development of the neural pattern.

Results

To facilitate interpretation of our results, existing data on the development and differentiation of the wild-type adult compound eye are reviewed, as revealed by the visualization procedures we employed (Fig. 1).

Wild-type adult eye. The normal adult eye is characterized by the precision of the reiterative array of the ommatidia and the cells comprising each ommatidium. Briefly, each ommatidium is composed of eight photoreceptors (R1-R8), four accessory cone cells, three kinds of pigment cells and a four-cell hair-nerve group (Figs. 1A and B). The

rhabdomeres, the light-collecting organelles of the photoreceptor cells, are stained dark blue with toluidine, and provide a means of estimating the number of photoreceptor cells per ommatidium. The rhabdomeres of R7 and R8 lie on stalks that extend their rhabdomeres into the middle of the interretinular space. The R7 rhabdomere lies in the more distal half of the retina; the rhabdomere of R8 lies below in the proximal half. Hence, in any one plane of section, usually only seven rhabdomeres are visible per ommatidium.

Wild-type, late third instar, eye-antennal imaginal disc. The morphology of the eye-antennal imaginal disc and the staining patterns of the MAbs used in this study have been described elsewhere (Ready et al., 1976; Zipursky et al., 1984; Banerjee et al., 1987b), and are reviewed in Figure 1C-G. Midway through the formation of the complete array of ommatidial clusters, the posterior-anterior axis of the eye disc measures about 220 μm, with the morphogenetic furrow (MF) displaced about half of this distance from the posterior of the disc. The furrow progresses at a rate of about one column per two hours (Campos-Ortega and Hofbauer, 1977).

MAb 3E1 stains an extracellular matrix element that initially covers the entire epithelium of the eye disc, then disappears posteriorly as the furrow advances. MAb 22G8 highlights the furrow by its increased staining within the furrow groove (data not shown). MAb 6D6 identifies membrane elements ahead of and behind the furrow. Behind the furrow, the antigen appears especially concentrated on membranes of cells surrounding the photoreceptor cluster. This provides a "chicken-wire" pattern, which is an index of the regularity of the array, showing the linear arrangement of clusters and the consistent spacing between them. It is useful for picking up slight pattern defects.

The other MAbs used in this study identify antigens specific to cells that are undergoing differentiation. MAb 150C3 (Banerjee et al., 1987b) identifies the *sevenless*$^{+}$ protein, which is required for the proper differentiation of presumptive R7. This MAb

stains all the developing photoreceptor cells and accessory cone cells. It first appears on the anterior edge of the furrow, and is localized at the apical tips and microvillar tufts of the cells. Unlike the epitope identified by the anti-*sev* antibody isolated by Tomlinson et al. (1987), this *sev* protein epitope persists in all of the cells in the eye disc that express it, although the microvillar tufts appear to undergo morphogenetic changes as they mature (Fig. 1G). The 150C3 staining pattern yields very detailed information. Not only are pattern defects readily apparent, but the microvillar tufts reveal information of cluster maturation.

The MAb 22C10 antigen, which begins to appear in presumptive photoreceptor neurons just behind the furrow, is an early marker for neuronal differentiation (Fujita et al., 1982; Zipursky et al., 1984). The subcellular distribution of the antigen varies with the age of the neuron. At the furrow, it is concentrated in the apical tips of the photoreceptor cells. As development proceeds (as seen in more posterior regions of the disc), the stain spreads to the cell bodies and then to the axons of the photoreceptor neurons. After about 10-12 hours of photoreceptor cell development, the antigen is almost exclusively in axons.

The MAb 24B10 antigen is specific to photoreceptor cells and their axons. It appears on the membranes of the photoreceptor cells relatively late, after about 24 hours of neural development, i.e., some 12 columns behind the furrow (Zipursky et al., 1984). The antigen (encoded by the *chaoptic* gene) is necessary for the proper eleboration of the rhabdomeres (Van Vactor et al., 1988; Reinke et al., 1988).

Eye mutants. Most of the eye mutants studied are described in Lindsley and Grell (1967); references to others are cited. According to their external adult eye phenotypes, the mutants can be classified into two major categories: reduced eye and rough eye. Rough eyes result from any irregular arrangement of the facets. For some of the mutant strains, the number of photoreceptor rhabdomeres per plane of section was further characterized;

these results are summarized in Figure 2. For mutants within each of the categories, the severity of the adult eye phenotype varies. For this study the mutants were classified as in Table 1, based on their disc phenotypes and the time at which the phenotypes become apparent, as revealed by the MAbs. The results of detailed examination of the mutant phenotypes are summarized in Table 2; an example from each group is illustrated below in Figures 3-7.

Group I: Precursor cell defects. Six of the twenty mutations we examined fell into this class, exemplified by the eyeless mutant *eyes absent* (*eya*). The *eya* mutant arose spontaneouly in a wild population of *Drosophila melanogaster*, and was discovered by Sved (1986); it is being further characterized by W. Leiserson and R. Hackett in the Benzer lab. The defect is specific to the adult compound eye. In the fully penetrant allele, the mutant completely lacks the eye, whereas the dorsal ocelli and other head structures appear normal (Fig. 3A). This phenotype could result from retina-specific cell degeneration after establishment of the pattern, or from a developmental defect in the retina precursor cells of the eye disc. The results presented in Figure 3 indicate the latter.

In normal flies, the eye and antenna regions of eye-antennal disc grow in size. In the *eya* mutant, however, a defect in this process became apparent in the third instar larva. As shown in Figures 3B-E, the eye portion of the disc was reduced in size. The average anterior-posterior length is around 100 μm (n=4), as compared to about 220 μm for wild-type discs. No furrow is apparent. The antigen 3E1, which usually covers the unpatterned area of retinal precursor cells, appeared only as a wisp of stain, without discernible shape. There was no evidence of cluster formation. The anti-*sevenless* protein MAb 150C3 did not stain. MAbs 22C10 and 24B10 did not appear in the eye disc epithelium. However, these antibodies did stain the axon bundle from the larval photoreceptors (Bolwig's Organ), indicating that the mutation does not affect that organ. Thus, the developmental defect in *eya* is manifested before the initiation of cluster

formation.

The genes in this class appear to be required very early in development of the eye. They may affect the ability of the precursor cells to differentiate or to propagate differentiation.

Group II: Defects in pattern formation. Seven of the twenty were classified as having defects in formation of the cluster pattern. Eye discs from these mutants showed variations from the wild-type pattern at and posterior to the morphogenetic furrow. However, the disc phenotypes within this class vary somewhat from one another, so two examples are shown: the mutant *split* (*spl*) and the mutant *roughex* (rux^2) (Figs. 4 and 5).

The *spl* mutant, named for an eye bristle defect, also has a small, rough eye. It maps to the *Notch* (*N*) locus, at band 3C7 on the X chromosome. When *spl* is doubly heterozygous with other recessive members of the *N* locus, the eye is normal, but it shows the split phenotype when homozygous or when combined with dominant *N* mutations. Pilkington (1941) characterized the morphology of the *spl* eye, noting that there were often fewer R cells in *spl* ommatidia, and that there were empty sheaths of secondary and tertiary pigment cells. Molecular characterization of the *N* gene has shown that the *N* protein has repeats similar to epidermal growth factor (Wharton et al., 1985; Kidd et al., 1986) and that the defect in *spl* corresponds to a single amino acid change in one of the growth factor repeats (Hartley et al., 1987).

Examination of sections of *spl* eyes reveals that internally, the retina was irregular. As shown in Figure 4, the secondary and tertiary pigment cell borders, which insulate each ommatidium, appear to be thicker than in the wild-type retina. Regions with an excess of pigment were observed and the number of photoreceptor cells per ommatidium was irregular. The average number of rhabdomeres per ommatidium in any one plane of section was around 4-5, and the variation about this average was quite large, in contrast to the wild type, which almost always has seven (Fig. 2). In this eye, very few ommatidia

had the normal complement of 7 in any one tangential plane of section. In some facets, we were unable to count the number of rhabdomeres, because of their ramification or fusion. These data suggest that there might be a decrease in the number of neurons formed, an excess of non-neuronal cells, or cell degeneration in *spl* mutant eyes.

The eye discs we examined from *spl* were of normal size, with the furrow advanced the normal distance from the posterior end (Figs. 4B-D). However, the cluster arrangement showed marked irregularities, beginning just behind the morphogenetic furrow. MAb 6D6 staining revealed that the envelopes of the clusters had varying shapes and sizes. The microvillar tufts, as revealed by MAb 150C3, were also spaced at irregular intervals, and had irregular shapes. There seemed to be fewer tufts clearly highlighted than in normal controls, even at the furrow. MAbs 22C10 and 24B10 highlighted clusters that, unlike wild-type clusters, showed variable separation. Hence, the adult phenotype is the result of an early acting developmental defect. However, the defects occur later than in the *eya* mutant, since the disc grows normally and the elements of the array appear. There may be inadequate control of the spacing between clusters at the morphogenetic furrow. Also, there may be fewer presumptive clusters forming in the disc than in the wild type, while the ommatidia in the adult seem to have too few neurons and too many pigment cells.

Like *spl*, *rux* mutants also have severely roughened eyes. The *rux* gene maps to the X chromosome. The allele examined was rux^2; other alleles have defects in sterility and/or viability (Lindsley and Grell, 1967). In sections of the adult eye, the defects in the mutant were readily apparent (Fig. 5). The ommatidia had irregular shapes and sizes, and pigment granules between adjacent ommatidia were often missing, in contrast to *spl*. The number of rhabdomeres varied considerably between ommatidia (Fig. 2). Although the average number of rhabdomeres per ommatidium in a plane of section was only slightly less than seven, the distribution was broad; one was almost as likely to find ommatidia with five rhabdomeres as with nine. The rhabdomeres were often ramified, fused or

reduced in size, making them difficult to count. Even when there were seven, their arrangement was usually irregular.

As shown in Figures 5B-D, the defect in *rux*^{2} was apparent in differentiating eye discs. The area anterior to the furrow showed the normal staining with MAb 3E1. However, directly behind the furrow, the clusters, as revealed by the other antibodies, had abnormal shapes and sizes. As revealed by MAb 6D6, the clusters had a non-rectilinear arrangement. In some areas, the tufts shown by MAb 150C3 could appear crowded while in others, they appeared dispersed. The total number of tufts appeared normal, though.

Many possible mechanisms could account for the various defects seen in Group II. Pattern formation in *Rough Eye* is severely disrupted, and could be explained by defective recruitment of cells into different types or loss of control over cluster spacing at the furrow. Others, like *sevenless*, have a less obvious disc phenotype, which could result from more subtle defects in cell-type decision making.

Group III: Maintenance of the pattern in the eye disc. This group is characterized by defects that become apparent in the eye disc, but only some time subsequent to the passage of the morphogenetic furrow, and is typified by the mutation *Glued* (*Gl*). The *Gl* mutation is dominant, resulting in a rough and somewhat reduced eye, has a recessive lethal phenotype during embryogenesis, and is an essential locus (Harte and Kankel, 1982). Conceptual translation of the DNA sequence showed that the protein is similar to filamentous proteins, but its expression has not been characterized in the eye disc during differentiation (Swaroop et al., 1986, 1987).

Internally, the retina of the *Gl* adult was abnormal (Fig. 6A). The rhabdomeres were often fused, and had irregular profiles. In ommatidia where one could count the rhabdomeres, the average number was less than the normal complement of seven. Often there was a space enclosed by pigment cells that contained no rhabdomeres. The normally

hexagonal pigment cell architecture was irregular. The defect seemed to worsen in more proximal sections.

The phenotype first became apparent in the eye disc. However, it appears at a later stage of development (Figs. 6B-E) than do those discussed above. The disc size was about normal, as were the position of the furrow and the appearance of clusters immediately posterior to it. However, after about 10 hours (five columns) of development, the clusters began to look abnormal. The staining revealed by MAb 6D6 weakened. The microvillar tuft pattern, as seen with MAb 150C3, was most revealing. At the furrow, the antigen appeared in a normal pattern; there were no extra or abnormally shaped tufts at this time, and the morphogenetic changes of the tufts appear to proceed normally. However, in the posterior disc regions, the stain faded. Eventually, the stain was lost altogether, although not all of the tufts in a column were lost at one time. The axonal projections of the R cells into the optic lobes, revealed by MAb 22C10, were disarrayed and truncated (data not shown). Although antigen 24B10 was expressed, it appeared on cells and clusters that were rounded, and were perhaps dissociating from one another. This defect worsened in the older, more posterior regions.The data suggest that the Gl^{+} gene product is required for maintenance and / or differentiation of the R cells several hours after their determination.

The Group III gene products could function in morphogenetic events that occur as a consequence of differentiation, or to set up a framework on which later differentiation events, including axon outgrowth, R cell elongation, and rhabdomere elaboration, can occur.

Group IV: Terminal differentiation or maintenance of form. Group IV includes mutations that appear to affect terminal differentiation products in the pupa and / or products required for maintenance of form in the pupa. This group is exemplified by the rough eye mutant *rugose* (*rg*). The *rg* gene maps to the X chromosome, and mutations in it result in

a rough eye. A defect in the wings may also occur, although this varies from one allele to another. The internal architecture of the adult eye was extremely disrupted (Fig. 7A). There were large patches consisting solely of pigment granules. The number of rhabdomeres per ommatidium varied; often there was a "facet" of pigment cells within which no rhabdomeres were found. The rhabdomere number distribution is shown in Figure 2. The distribution was bimodal, with peaks at zero and seven. Although the average number of rhabdomeres was close to seven, their arrangement was often irregular.

The eye discs of *rg* were of normal size. The staining patterns revealed by all of the MAbs tested showed no obvious pattern defects, with large fields of developing ommatidia in straight columns and rows, and with appropriate morphogenetic changes (Figs. 7B-D). This is remarkable, considering the severity of the adult phenotype, and indicates that the gene product is required at a later stage of differentiation of the eye than the third instar.

Group IV contains mutations with rough eyes that appear to result from defects expressed after the larval stage. This group also includes genes that are known to function in photoreceptor cell terminal differentiation, e.g., *ninaE* and *chaoptic*.

Discussion

This study allows us to identify genes that appear to function at different stages in formation of the *Drosophila* compound eye. While the adult eye phenotypes of some mutants appear to be similar, their defects are seen to arise at quite different stages of development. With the disc phenotypes revealed by MAbs that stain various pattern elements, one can classify the mutants into the four main groups in Table 2.

Developmental events occuring anterior to the furrow. In order for the eye to develop, the prospective eye tissue must be capable of differentiation, and differentiation must be

initiated and propagated across the prospective retinal epithelium. Mutations that have been assigned to Group I may affect one of these steps.

In this regard, the developmental capacity of eye discs during the different larval stages has been investigated (Bodenstein 1943, 1962; Gateff and Schneiderman, 1975; Campos-Ortega and Gateff, 1976). Differently staged eye discs were transplanted into late third instar larvae, and allowed to develop, to find the stage at which adult eye facets would form despite the immaturity of the discs. Only discs older than midsecond instar were capable of generating ommatidia, although resulting eyes had relatively few facets. The differentiation of a retina cell seems not to be strictly a matter of temporal programming. Rather, it appears that competence to form retina may be determined at the midsecond instar. Once this state is attained, cells in the eye disc are able to respond to a midthird instar-specific differentiation "signal." Such a phenomenon has been described as occurring during development of the compound eye of the mosquito *Aedes aegypti*. In this case, the ability to differentiate appears to be accompanied by a morphologic change in the prospective retinal epithelium, the formation of the optic placode. The data suggest that formation of the optic placode passes as an inductive wave from posterior to anterior across the epithelium. In the *Drosophila* eye disc, it is possible that during midsecond instar the ability to differentiate, akin to formation of the optic placode in mosquito, passes across the developing disc.

The eyes that developed from transplanted immature discs, as described by Bodenstein (1939, 1962) and Gateff and Schneiderman (1975), are remarkably similar in appearance to the adult eye phenotypes of some of the Group I mutants, e.g., *B* and *bar-3* (reduced facet number, but the facets present are complete). It is possible that some of the Group I gene products function to make cells in the eye disc competent to form retina. Sturtevant (1927) noted that in mosaics of *B* and B^+ eyes, large patches of *B* mutant tissue could inhibit the differentiation of B^+ patches anterior to it. These results could be explained by the inability of *B* tissue to respond to and transmit an inductive signal for

competence, leaving wild-type cells anterior to the mutant cells without the ability to respond to developmental signals. Further study of these mutants could test the idea that competence is assumed by these cells in sequence across the disc, and might allow the identification of molecules involved.

Gene products from this group could also function in the initiation and propagation of differentiation. *Drosophila* eye discs grown *in vitro* do not differentiate unless cultured in the presence of the larval ring gland (for instance, see Bodenstein, 1962); humoral factors may therefore be involved in the initiation of differentiation. *Drosophila* mutants lacking compound eyes may be useful for identification of such a pathway. For instance, *eya* eye discs appear normal through the second larval instar and into the early third (R. Hackett, pers. comm.). However, the eye disc cells do not differentiate in the midthird instar larva. If development at this stage involves stimulation by humoral factor(s), *eya* cells may be unable to respond to or produce this factor. The reduced size of the eye field in the late third instar eye disc could be the result of cell degeneration, caused by a lack of alternate programs of differentiation. It is not known whether *eya* function is produced autonomously by eye disc cells; further work on this gene is currently in progress (W. Leiserson, R. Hackett, and S. Benzer, pers. comm.).

The control of cluster spacing at the furrow. In the *Drosophila* eye disc at the morphogenetic furrow, negative and positive feedback loops between neighboring cells could be in use to control the spacing between nascent ommatidia at the furrow. The disc culture experiments mentioned above indicated that an inducing factor may play a role in initiation of eye differentiation. Imposed upon the positive effect of this factor, an inhibitory mechanism could regulate the spacing, and therefore the number, of ommatidia in a row. In the alga *Anabaena* (Wilcox et al., 1973), an inhibitory mechanism seems to be used for regulating the number and spacing of the specialized heterocyst cells. In addtion, it has been suggested that the regular spacing of sensory bristles on insect cuticle

is the result of a graded inhibitory signal (Wigglesworth, 1940; Moscoso del Prado and Garcia-Bellido, 1984). In the differentiating eye disc, such a mechanism would likely involve the cells that form the "nucleation sites" at which the nascent ommatida condense. At the furrow, the presumptive ommatidia are regularly spaced at a center-to-center distance of about 12-15 μm. Once a cell, or group of cells, begins to differentiate, an inhibitor could be released, which would diffuse through the epithelium (perhaps via cell-to-cell contacts) or through the extracellular matrix. Given the structure of the apical extracellular matrix and the fact that the cells elaborate extensive microvilli into the space (Waddington and Perry, 1960; Perry, 1968; Banerjee et al., 1987b), this is a reasonable site for inhibitor release and action. The fibrous structure of the matrix limit the flow in certain directions, making the passage of macromolecules more a process of percolation than of free diffusion. Depending on the size of the inhibitor and its affinity for the stationary components of the matrix, its range of effectiveness could easily be limited to within a few microns laterally. Limiting inhibitor range to this short distance would otherwise require that it be quite short-lived, since a typical macromolecule will diffuse a distance of 10 μm in water in about 1 s, and a small molecule even faster (D.F. Blair, pers. comm.). Lateral inhibition could thus control the number of ommatidia seeded in a row. Also, if the number of cells at the furrow remains constant, this could influence the number of cells in each cluster.

In support of a lateral inhibition mechanism, development of the compound eye shares several gene products with neuroblast (NB) and epidermoblast (EB) segregation in the ventral neurectoderm of the *Drosophila* embryo, during which local cell interactions have been demonstrated to control cell type and number (reviewed by Campos- Ortega, 1988; Taghert et al., 1984; Doe and Goodman, 1985a,b). It appears that any cell in the neurectoderm is capable of differentiating into either type of progenitor cell, and that interactions between uncommitted cells play a role in the segregation process. Although a stochastic mechanism may bias a cell towards the NB fate, evidence suggests that an NB

cell then prevents neighboring cells from also assuming the NB fate. It may also promote the EB fate in neighboring cells, and positively reinforce its own NB fate. The neurogenic loci in *Drosophila* affect this pathway. In a mutant embryo with a loss of neurogenic function, all neurectoderm cells assume the NB fate. Six of the loci, e.g., *Notch* (*N*), have been shown to be non-autonomously required for EB differentiation, while one, *Enhancer of split* [*E(spl)*] is autonomously required for the EB fate.

Group II of Tables 1 and 2 includes mutants that may affect the initial spacing of nascent ommatidia at the furrow. In *spl* (a recessive, eye-specific *Notch* allele) eye discs, there does not appear to be cell degeneration in the anterior disc, and yet a reduced number of clusters seem to form at the furrow in the disc. Given the molecular genetic characteristics of the *Notch* protein that is altered in *spl*, our data suggest that there may be an inappropriate amount of neural induction postmitotically in these discs. In *Roi*, the size and spacing of clusters at the furrow seems random. D. Ballinger (pers. comm.) has noted that *Roi* increases the severity of the mutant *Star* (see below) by increasing the number of photoreceptor cells per ommatidium well beyond eight, with a concomitant decrease in the number of facets. The *Roi* disc defect is quite severe; it is surprising that the adult eye structure is as good as it is. Perhaps there is a mechanism that acts later in development that can in part correct for the increase in cluster number.

Cell-type determination. The second group also comprises mutants in which cell type determination within the ommatidium may be defective, such as *Star* (*S*), *roughex* (*rux*), *rough* (*ro*), and *sevenless* (*sev*). In most of these, there are patches where clusters appear slighlty too close to or too far from one another. Current models propose that cell-cell interactions among the neighboring cells in a cluster control the differentiation of cells in that cluster. If this is so, these gene products may act in this process. Once differentiation is initiated, the patterned cells may begin to express molecules that influence the fate of cells that join the cluster at a later time.

The *ro* gene has recently been investigated in greater detail (Saint et al., 1988; Tomlinson et al., 1988). Interestingly, both groups demonstrated that the *ro* gene contains sequences similar to the homeobox domain of other developmentally required loci. Saint et al. (1988) showed by *in situ* hybridization that the *ro* transcript is expressed in the eye disc strongly within the morphogenetic furrow, with levels decreasing posterior to it. Tomlinson et al. (1988) demonstrated by genetic mosaics that the *ro* gene product is required in R2 and R5 in order for an ommatidium to have the normal number of eight photoreceptor cells. Other Group II genes may have similar cell-type specific requirements.

Mutant groups III and IV. The gene products deficient in mutant groups III and IV presumably function in terminal differentiation of the retina. The phenotypes of Group III mutants appear before pupariation, while those of Group IV are presumed to function after that event.

Group III comprises mutants in which the initial formation of the array and the events preceding it appear normal, but the cells do not continue to develop and express antigens. Members of this group are *Gl* and *S* / ··*E(S)* ··. In these two mutants, the clusters degenerate after a few hours of development. Similarity between the putative *Gl* protein and filamentous proteins found in muscle fibers and intermediate filaments (Swaroop et al., 1987) suggests that *Gl* may be necessary for structural support and axon elongation, necessary for the cells to survive. It has not been possible to recover clones of homozygous *Gl* cells after making genetic mosaics (Meyerowitz and Kankel, 1978; Harte and Kankel, 1982). Since the dominant phenotype affects the eye so drastically, the elongated cells of the retina may be more sensitive to a defect in this protein than other cells in the fly. *S* alone has a phenotype that places it in Group II. In combination with the mutation *E(S)*, the disc defect is much more severe. Many cells in the eye disc with this genotype combination seem not to survive for more than 12 or so hours after their last

division. *E(S)* alone does not have a dominant phenotype. Therefore, it appears that *S* is required not only for correct formation of the pattern, but also, in combination with the *E(S)* gene product, for maintenance of the differentiated cells.

The final group we can describe contains mutants in which the eye discs appear normal through the third instar, despite the occasional similarity of adult phenotypes with members of other groups. Thus, these gene products may be used after pupariation. The *rg* gene product may be involved in maintenance requirements of cells of the retina and perhaps of the wing. Although not included in this study, mutants defective in genes encoding terminal differentiation products of photoreceptor cells, for instance, genes involved in phototransduction or eye color, would also be members of this group. These gene products seem not to play a role in development of the pattern, but encode proteins important for the function of the cells, once the pattern has been established.

Conclusion

This study describes an analysis using monoclonal antibodies as molecular probes for the events occurring during the formation of a neural pattern. The assignment of mutations to groups is intended as a guideline, since the functions of the different groups may overlap. Phenotypes for several of the mutations indicate that the corresponding wild-type gene products function in development at different steps in a series of necessary events. Cloning and sequencing of the genes, as well as identification of an allelic series for them, will provide a more detailed description of their temporal and spatial expression, and perhaps of their function. Such analysis may contribute towards understanding events, such as cell-to-cell interactions, required during development of the compound eye.

Experimental Procedures

Stocks. All *Drosophila* strains were obtained from the Pasadena Stock Facility at the

California Institute of Technology, and were maintained at 25 °C.

Eye disc immunohistochemisty. Late third instar eye discs were stained with monoclonal antibodies (MAbs) by a modification of the procedure of Zipursky et al. (1984). All steps were performed at room temperature. Discs were dissected from late third instar larvae in Tris-buffered saline (TBS: 100 mM Tris base pH 7.5, 130 mM NaCl, 5 mM KCl, 5 mM NaN_3, 1 mM EGTA), fixed for 30 min in 2% buffered formalin (pH 7.0), rinsed in TBS, and permeabilized for 30 min in 0.5% N-P40 (v:v) in TBS. Discs were then stained with the appropriate MAb supernatant, diluted 1:1 (v:v) in TBS for 60 min, then washed for 3X10 min in TBS. The MAb staining pattern was visualized by incubating the discs for 30 min in 1:50 (v:v) diluted goat antimouse IgG conjugated to FITC, and washed for 3X10 min in TBS. Discs were mounted in PDA glycerol [0.1% (w:v) phenylene diamine, 90% glycerol, in TBS] and viewed by epifluorescence.

Adult head sections. The tissue was prepared so that it could be analyzed at either the light- or electron-microscope level. Flies were decapitated and fixed in 1% paraformaldehyde, 1% glutaraldehyde for one hour at room temperature. They were rinsed for 1/2 hour in 0.1 M phosphate buffer, and postfixed with 1% osmium tetroxide for 1-2 hours. After rinsing in dH_2O for 10 minutes, the heads were stained in Kellenberger Uranyl acetate overnight. The heads were then washed in veronal acetate buffer for 30 minutes, then successively dehydrated in ethanol steps of 50%, 70%, 85%, and 95% for 5 minutes each, and two steps in 100% for 10 minutes. Final dehydration was completed in 100% propylene oxide 2 X 7 minutes. The tissue was infiltrated with 1:1 mixture of propylene oxide : Epon 812 for one hour. The tissue was then placed in pure Epon 812 in a vacuum dessicator for 3-4 hours. The tissue was embedded in pure Epon 812 in a capsule, and polymerization was allowed to occur overnight at 60 °C. For the light microscope, 1 micron-thick sections were made and stained with 1% toluidine

blue and 1% borax in water.

Figure 1. The wild-type eye and late third instar eye disc.

(A) Scanning electron micrograph of the adult head. The compound eye constitutes much of the external surface of the head and comprises about 800 facets. Anterior to the right. Bar = 10 μm.

(B) Light micrograph of a section tangential to the adult compound eye. In any one plane of section, seven rhabdomeres are visible. These are the blue-stained structures in the center of each ommatidium. Each cluster of photoreceptors is surrounded by pigment cells. Bar = 10 μm.

(C) Late third instar eye disc stained with MAb 3E1. This MAb stains anterior to the morphogenetic furrow (arrowhead) and demarcates the anterior, unpatterned region from the posterior, patterned region. Anterior to the right. Bar = 30 μm.

(D) Late third instar eye disc stained with MAb 6D6. This MAb highlights membranes both ahead of and behind the furrow (arrowhead). However, in the posterior region, it stains membranes of cells that surround each cluster, and reflects the reiterative composition of the developing eye. Anterior to the right. Bar = 30 μm.

(E) Late third instar eye disc stained with MAb 150C3. This MAb identifies the *sevenless* protein. Note the onset at the morphogenetic furrow (arrowhead), and the reiterative array of microvillar tufts. Anterior to the right. Bar = 30 μm.

(F) Late third instar eye disc stained with MAb 22C10. This MAb highlights peripheral nerves and their axons. Expression is initiated in the presumptive photoreceptor cells at the morphogenetic furrow (arrowhead). The axon from Bolwig's nerve also stains. Anterior to the right. Bar = 30 μm.

(G) Late third instar eye disc stained with MAb 24B10, specific for photoreceptor cells and their axons. Onset of expression occurs at least 12 hours after passage of the morphogenetic furrow. Anterior to the right. Bar = 30 μm.

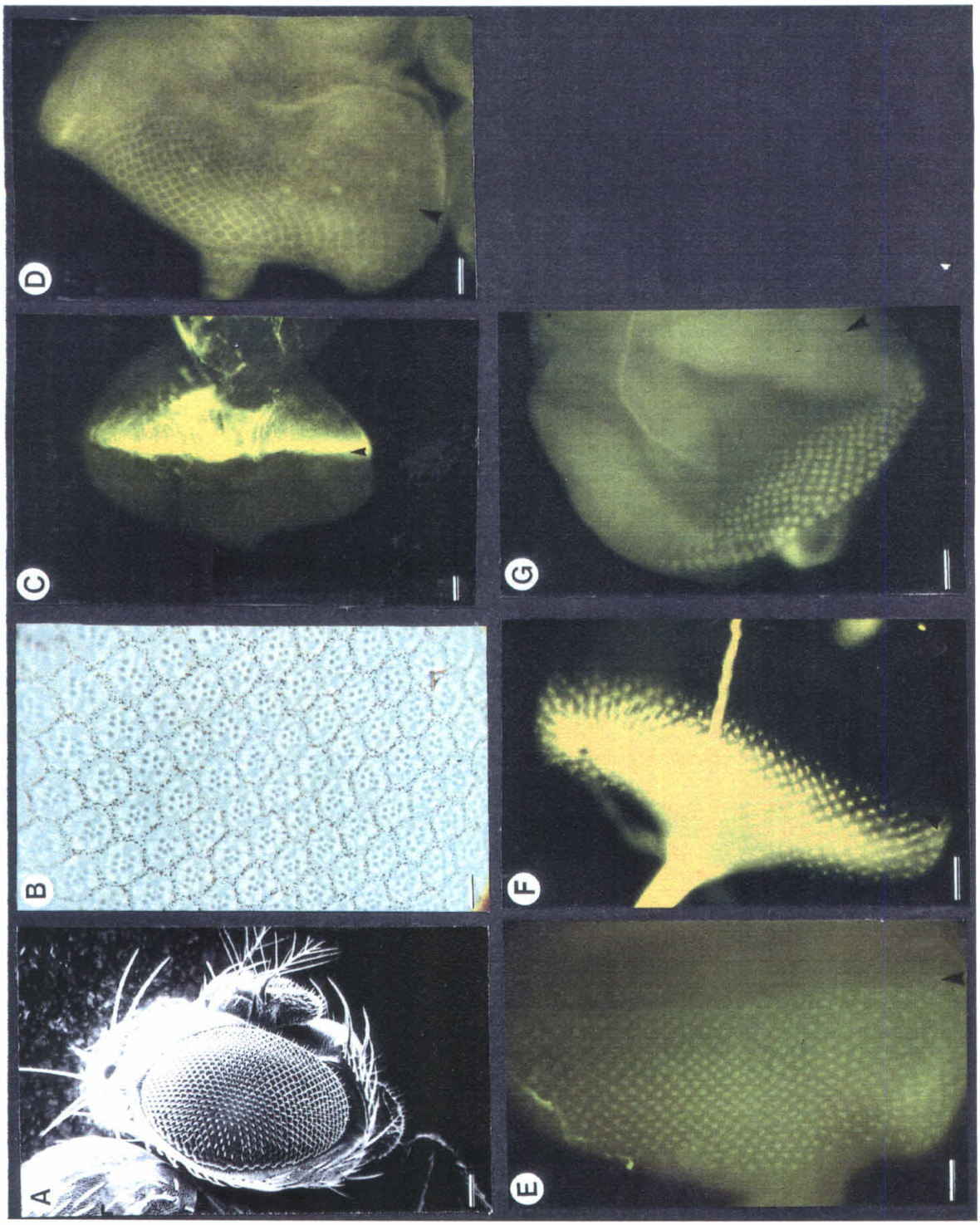
A
B
C
D
E
F
G

Figure 2. Different mutants with similar external phenotypes can have different internal phenotypes.

Eyes from wild-type and four different mutants with similar, rough-eyed phenotypes were sectioned, and the number of rhabdomeres per ommatidium per plane of section was compared. Plotted is the percent of ommatidia containing a given number of rhabdomeres versus the number of rhabdomeres.

In the wild-type retina, the vast majority of ommatidia contained seven rhabdomeres at any one level. In the mutant *rugose*, a bimodel distribution was seen. In *Rough Eye*, the mean is still close to seven, but the standard deviation is broader than in wild-type. In *split*, the mean has dropped to 4.3, and the standard deviation is broader than in wild-type. In *roughex*, the mean approximates seven, but the distribution is broader than wild-type or *Rough Eye*.

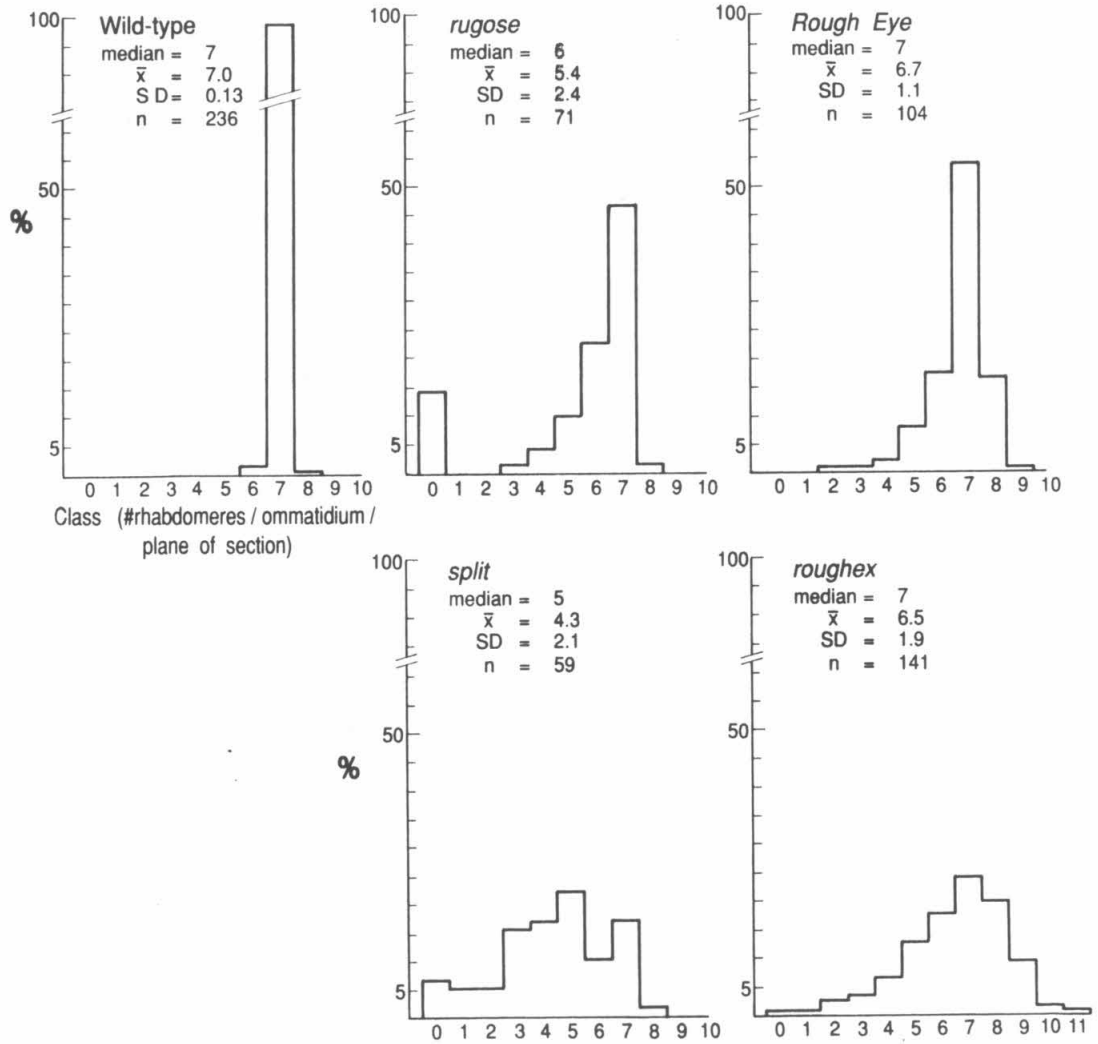
Wild-type
median = 7
x̄ = 7.0
S D = 0.13
n = 236
rugose
median = 6
x̄ = 5.4
SD = 2.4
n = 71
Rough Eye
median = 7
x̄ = 6.7
SD = 1.1
n = 104
split
median = 5
x̄ = 4.3
SD = 2.1
n = 59
roughex
median = 7
x̄ = 6.5
SD = 1.9
n = 141
100
50
5
%
0 1 2 3 4 5 6 7 8 9 10
0 1 2 3 4 5 6 7 8 9 10 11
Class (#rhabdomeres / ommatidium / plane of section)

Figure 3. The mutant *eyes absent*.

(A) Scanning electron micrograph of the adult head. This mutant lacks the compound eyes. Anterior is to the right. Bar = 10 μm.

(B) Late third instar eye disc stained with MAb 3E1. Anterior to the right. Bar = 30 μm. The stain is diffuse, and does not identify a furrow.

(C) Late third instar eye disc stained with MAb 150C3. The antennal disc (a), eye disc (e), and attached optic lobe (ol) are noted. Bar = 30 μm. The antigen is not present.

(D) Late third instar eye disc stained with MAb 22C10. Although the axon from Bolwig's nerve is stained, no neurons are identified in the eye disc. Anterior to the right. Bar = 30 μm.

(E) Late third instar eye disc stained with MAb 24B10. Bolwig's nerve is stained, but no photoreceptors in the eye disc. a = antenna disc, e = eye disc, ol = optic lobe. Anterior to the right. Bar = 30 μm.

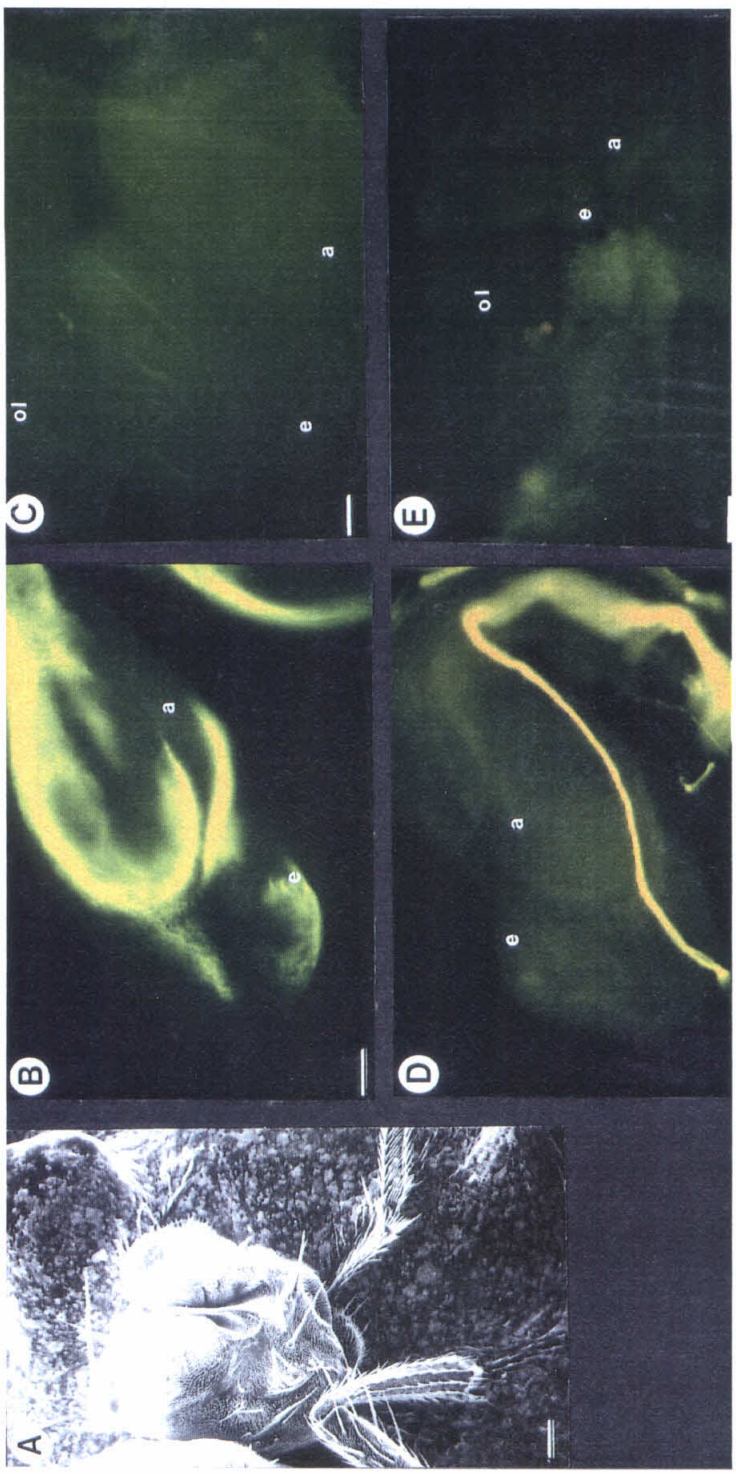
A
B
a
e
C
ol
e
a
D
e
a
E
ol
e
a

Figure 4. The *split* mutant.

(A) Section tangential to the adult eye. The number of rhabdomeres per ommatidium is highly variable (most often less than seven), and the pigment cell layer encircling each one appear thicker than in wild-type. Bar = 10 μm.

(B) Late third instar eye disc stained with MAb 3E1. Arrowhead = morphogenetic furrow. Anterior to the right. Bar = 30 μm.

(C) Late third instar eye disc stained with MAb 6D6. Immediately posterior to the furrow (arrowhead), the staining pattern is irregular. Anterior to the right. Bar = 30 μm.

(D) Late third instar eye disc stained with MAb 150C3. At the morphogenetic furrow (arrowhead), the array of microvillar tufts is abnormal. The number of tufts appears reduced. Anterior to the right. Bar = 30 μm.

(E) Late third instar eye disc stained with MAb 22C10. Expression begins in neurons at the morphogenetic furrow (arrowhead); it is not severely affected. Anterior to the right. Bar = 30 μm.

(F) Late third instar eye disc stained with MAb 24B10. Only slight pattern defects are visible. Anterior to the right. Bar = 30 μm.

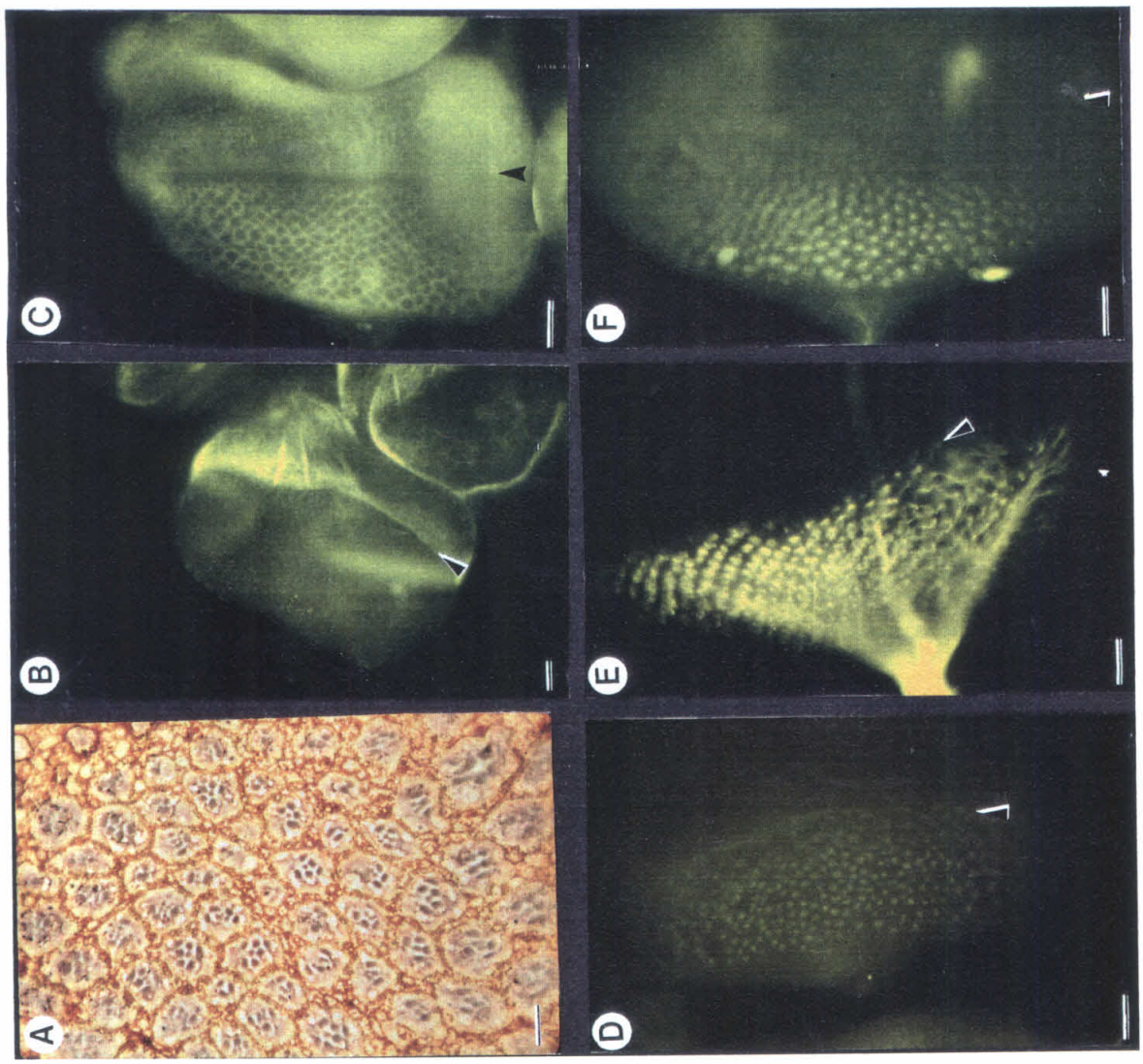
A
B
C
D
E
F

Figure 5. The *rough*^{ex2} mutant.

(A) Section tangential to the adult eye. The number of rhabdomeres per ommatidium is highly variable. Bar = 10 μm.

(B) Late third instar eye disc stained with MAb 3E1. Arrowhead = morphogenetic furrow. Anterior to the right. Bar = 30 μm.

(C) Late third instar eye disc stained with MAb 6D6. Immediately posterior to the furrow (arrowhead), the staining pattern is irregular. Anterior to the right. Bar = 30 μm.

(D) Late third instar eye disc stained with MAb 150C3. The array of microvillar tufts is abnormal, beginning at the morphogenetic furrow (arrowhead), with variable spacing and morphology. Anterior to the right. Bar = 30 μm.

(E) Late third instar eye disc stained with MAb 22C10. Slight pattern defects are seen posterior to the furrow (arrowhead). Anterior to the right. Bar = 30 μm.

(F) Late third instar eye disc stained with MAb 24B10. Anterior to the right. Bar = 30 μm.

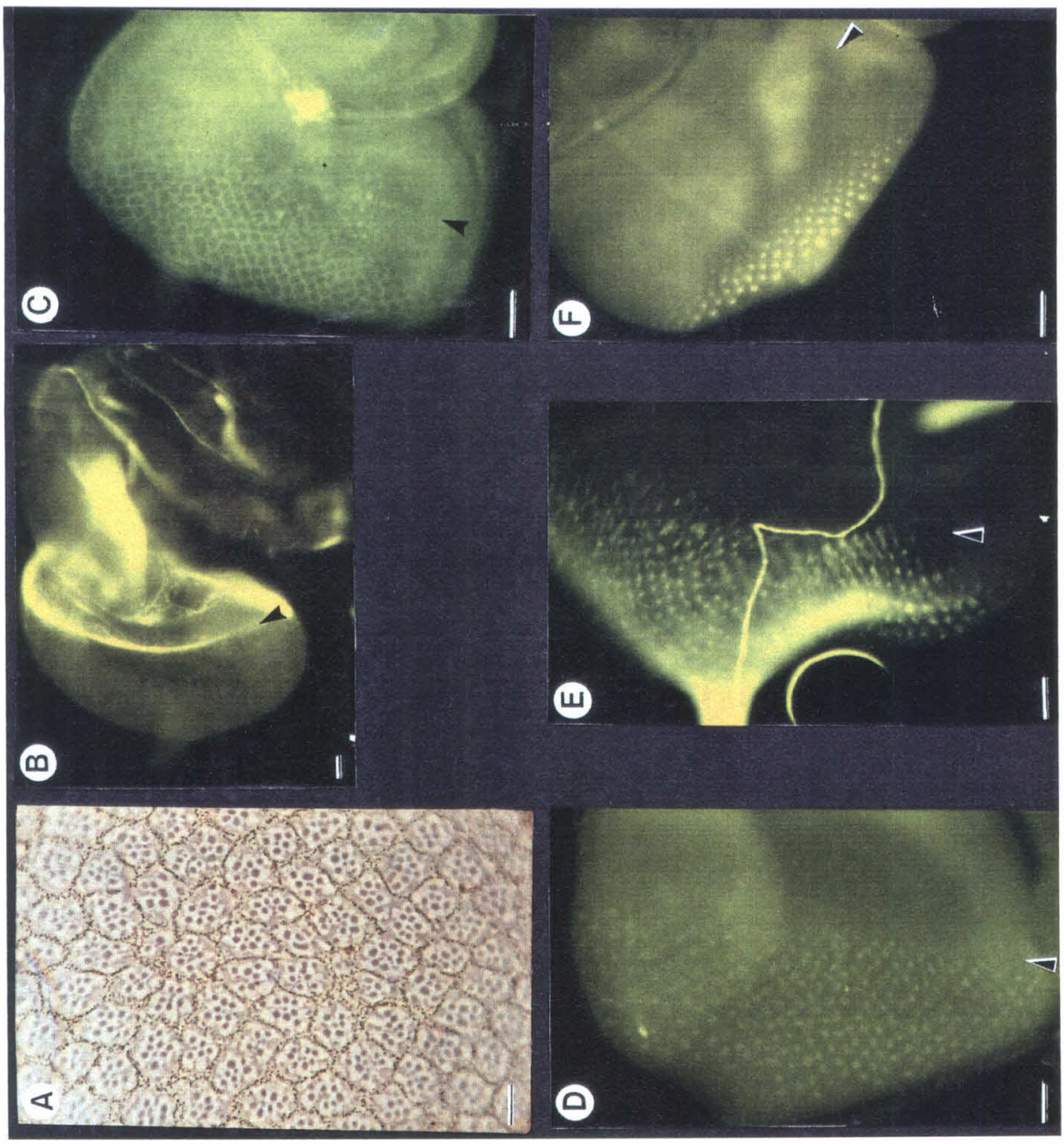
A
B
C
D
E
F

Figure 6. The *Glued* mutant.

(A) Section tangential to the adult eye. The number of rhabdomeres per ommatidium is varied; there can be facets that contain no rhabdomeres. Bar = 10 μm.

(B) Late third instar eye disc stained with MAb 3E1. Arrowhead = morphogenetic furrow. Anterior to the right. Bar = 30 μm.

(C) Late third instar eye disc stained with MAb 6D6. The pattern appears normal immediately behind the furrow (arrowhead). In the posteriormost regions of the disc, pattern defects become apparent. Anterior to the right. Bar = 30 μm.

(D) Late third instar eye disc stained with MAb 150C3. The array of microvillar tufts at the furrow (arrowhead) appears normal. However, after about 8-10 rows (16-20 hours of development), the tufts begin to lose the antigen. In the very posterior, the stain is often lost altogether. Anterior to the right. Bar = 30 μm.

(E) Late third instar eye disc stained with MAb 22C10. Expression begins in neurons at the morphogenetic furrow (arrowhead). In the posterior of the disc, the staining pattern begins to look somewhat abnormal. Anterior to the right. Bar = 30 μm.

(F) Late third instar eye disc stained with MAb 24B10. By the time the *chaoptic* gene is expressed, the photoreceptor cells look abnormal, as if the clusters are dissociating. Anterior to the right. Bar = 30 μm.

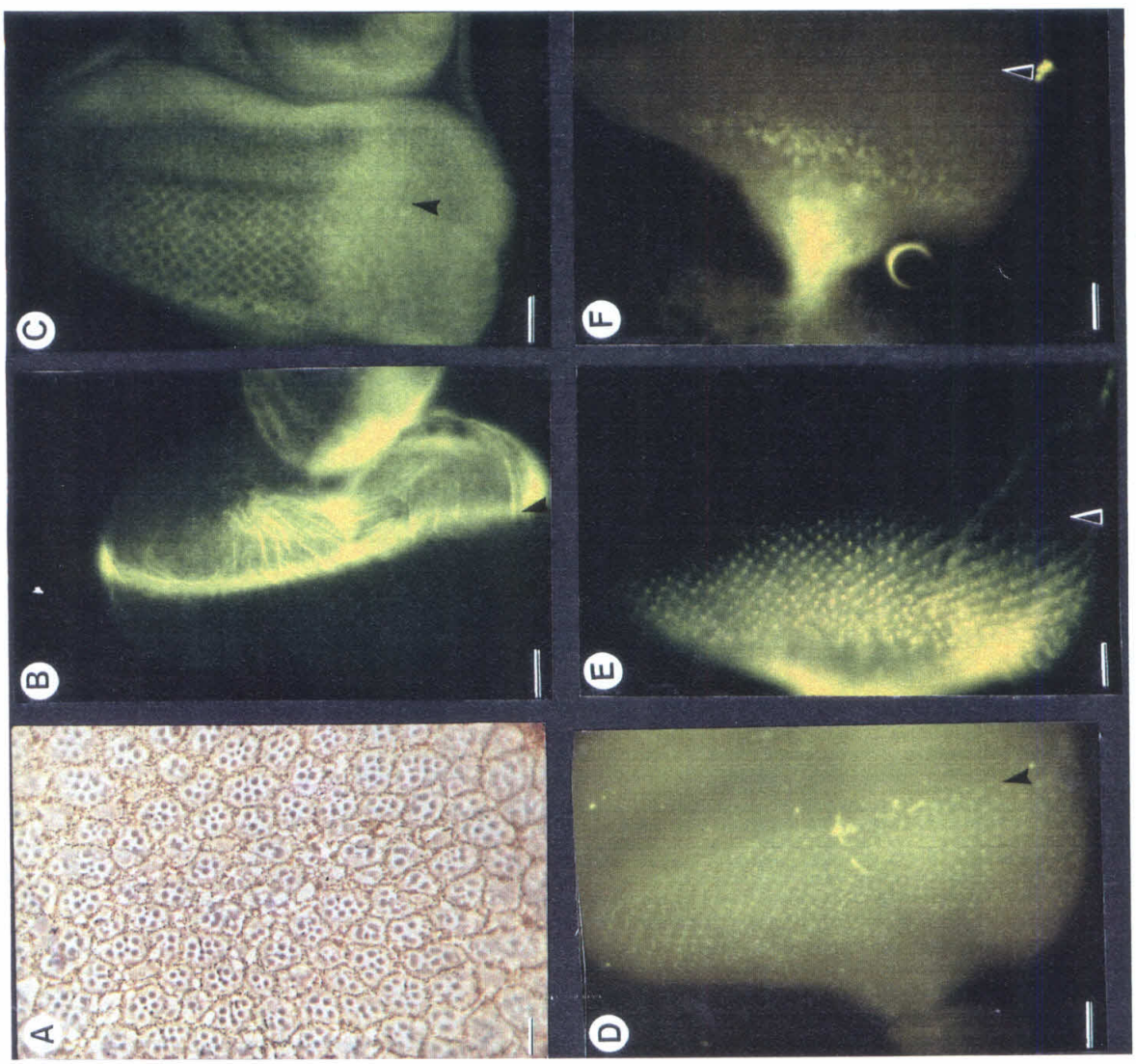
A
B
C
D
E
F

Figure 7. The *rugose* mutant.

(A) Section tangential to the adult eye. The number of rhabdomeres per ommatidium is highly variable, often being zero. Bar = 10 μm.

(B) Late third instar eye disc stained with MAb 3E1. Arrowhead = morphogenetic furrow. Anterior to the right. Bar = 30 μm.

(C) Late third instar eye disc stained with MAb 6D6. Anterior to the right. Bar = 30 μm.

(D) Late third instar eye disc stained with MAb 150C3. Anterior to the right. Bar = 30 μm.

(E) Late third instar eye disc stained with MAb 22C10. Anterior to the right. Bar = 30 μm.

(F) Late third instar eye disc stained with MAb 24B10. Anterior to the right. Bar = 30 μm.

The expression of the antigens and the patterns revealed in the eye disc all look like that in wild-type.

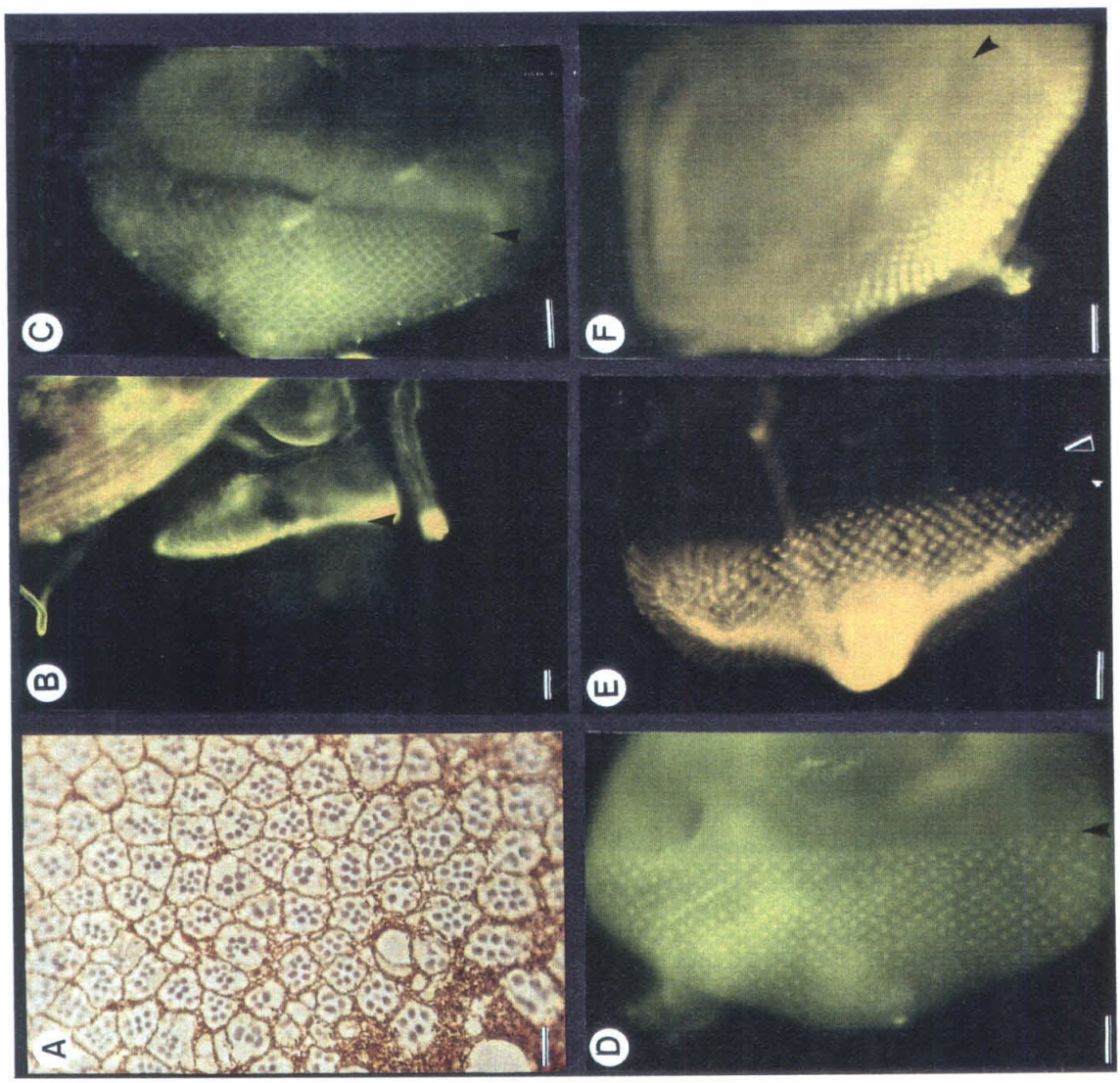
A
B
C
D
E
F

Table 1. Mutations Affecting Different Steps in Development of the Compound Eye

Group / Event	Adult phenotype	Eye disc phenotype	Mutants
I: Precursor cell proliferation, viability, capacity	no eye, or reduced eye	disc small, with no or few clusters apparent	*Bar*, *bar-3*, *Dr*^{Mio}, *eyeless*, ***eyes absent*** *Irregular Facets*
II: Pattern formation	rough eye; abnormal arrangement of facets, number of cells per facet	abnormal number or spacing of clusters at the furrow, defects in cluster size or shape	*glass*, *rough*, ***roughex***, *Rough Eye*, *sevenless*, ***split***, *Star*
III: Maintenance of pattern	rough eye; abnormal number of cells per facet	defect arises after initial array formation	***Glued***, *lozenge*, *Star + Enhancer of Star*
IV: Terminal differentiation	rough eye; abnormal cell morphology; non-functional eye	no defects evident in disc	*loboid*, ***rugose***, *roughened eye*, *roughoid*

The mutants were classified into groups by the adult eye phenotype and the late third instar eye disc phenotype, presented in Table 2. The staining patterns of the MAbs and the adult eye are shown for mutants listed in bold face in Figures 3-7.

Table 2. Summary of Eye Mutant Phenotypes

Additional references to and the external adult eye phenotypes of most of the mutations are described in Lindsley and Grell (1967), except where noted in the text. Further information regarding the structure of the adult optic lobes is available for many of these mutations in Meyerowitz and Kankel (1978). The internal adult eye phenotypes and the late third instar eye disc phenotype as revealed by monoclonal antibodies are from this study.

Table 2. Summary of Eye Mutant Phenotypes

Mutation	Genotype	Adult Eye: External	Adult Eye: Internal	Late Third Instar Disc
Group I: Precursor Cell Defect				
Bar	*B* ♂s	Small, narrow; facet #≈150.	Reduced facet #, but most ommatidia normal. Usually 7 rhabdomeres per ommatidium section.	Disc size reduced. MF absent; deep cleft at anterior margin of clusters. Only 4-5 rows of clusters. Those at cleft edge look mature.
	f BB ♂s	Anterior notch; facet #≈20-30.	Nick in anterior margin. Ommatidial arrangement, composition irregular. Most have 7 rhabdomeres but in abnormal arrangement.	Disc size reduced. Deep cleft. Clusters at cleft look mature.
bar-3	*bar-3*	Small, narrow; facet #≈150.	Most ommatidia sections have 7 rhabdomeres. Arrangement normal. Vestige of equator.	Disc size reduced. Deep cleft at anterior edge; clusters at cleft look mature.

Drop^{Mio}	*Dr^{Mio}/ TM6, UBX^{+}* (recessive lethal allele)	Very reduced, rough eye; facet #≈30.	5-7 rhabdomeres per ommatidium section Some rhabdomeres fused.	Disc size reduced. MF uneven. Weak antigen expression. Few clusters visible. Arrangement disturbed. Microvillar caps blurred, diffuse.
eyeless	*ci^{D}/ey^{D}* (late larval/pupal recessive lethal)	Eyes vary in size from none to full.	(not tested)	Variable, from rudimentary disc with no antigen expression, to full-sized disc, with normal antigen expression.
	ci^{D}/ey^{R}	"	"	"
eyes absent	*eya*	Adult compound eye lacking.	None	Disc size reduced. No furrow. No expression of differentiation antigens.
Irregular facets	*apx or/If*	Eye ~ 1/2 normal size; ventral half more prone to irregularities.	(not tested)	Fairly large number of clusters, but arrangement irregular, especially in ventral half.
	or If; st	Very narrow eye; ventral	Extreme reduction ~20 ommatidia;	Disc size reduced. Few clusters high-

		half can be devoid of facets.	rhabdomeres fused, irregular.	lighted. Difficult to see a furrow. Microvillar caps irregular: wispy dots. Anterior clusters mature.
Group II: Pattern Formation Defect				
glass	*gl*^{3}	Rough eye, somewhat reduced. Glassy texture.	Very irregular: gaps, no clear separation between ommatidia. No rhabdomeres. Masses of pigment granules. Architecture of pigment cells present.	Irregularities in sizes and shapes of clusters from the MF. No 24B10 antigen. Microvillar tufts over- and undercrowded. Tufts have irregular shapes, not well resolved. Excess of membranes stained at MF with MAb 150C3.
rough	*ro*	Eyes rough; facets irregular in size, shape.	Irregular sizes and shapes. Many fused, ramified rhabdomeres. Inappropriate pigment cell formations. Usually 5-7 rhabdomeres per ommatidium.	Cluster spacing varies subtly. Maturation of microvillar tufts irregular; regions of non-linearity.

roughex	*rux*^{2}	Eyes rough, somewhat reduced.	Variable shapes, sizes and composition of ommatidia. Rhabdomeres ramified, varying in size. If 7, often arrangement is irregular.	Variable size, shape of clusters. Regions of non-linear arrangement. Extra clusters, sloppy array. Poor resolution of membranes.
Rough Eye	*vg*$^{\mu}$/In(2L)*t*, *Roi*, In(2R) *Cy*, *bw sp*^{2} *or* (recessive lethal)	Eyes extremely rough. Irregular round, bulging facets.	Variable numbers of rhabdomeres per ommatidium. Fused facets and rhabdomeres. Even if 7 rhabdomeres, present, arrangement is often abnormal. Rhabdomeres ramified, varying in size.	Defect obvious at MF furrow. Highly variable sizes and shapes of clusters. Over- and under-crowded areas. Excess of microvillar caps in some areas. Severe defects.
sevenless	*sev*^{P1}	Very slightly rough.	R7 missing from each ommatidium of the eye.	Mostly normal, except that MAb 150C3 does not stain.
split	*sp1*	Eyes rough, slightly reduced. Irregu-	Highly irregular size, shape, composition of	Defect obvious at MF. Distance between nascent ommatidia

		lar facets. Multiple setae.	ommatidia. 2° and 3° pigment cell borders thickend. Rhabdomere defects: fused, ramified elongated. Fewer than normal rhabdomeres per ommatidium.	appears greater than in wild-type. Pattern shapes, sizes are irregular, sloppy. Microvillar caps vary: smaller, fuzzier.
Star	S^{db123} (recessive lethal)	Eyes rough, somewhat smaller.	Variable sizes and composition of ommatidia. Often less than 7 rhabdomeres per ommatidium section. Thickened pigment cell borders.	Clusters vary in size. Areas of distortion in rows and columns.
Group III: Post-pattern Formation Defects in the Disc				
Glued	*Gl* (recessive lethal)	Facets irregular, rough eye somewhat reduced.	Rhabdomeres highly irregular: bifurcated, fused, odd profiles. Rhabdomere number variable, occasionally none in a facet.	Pattern normal for several rows behind furrow; antigen expression then becomes irregular: clusters dissociating? Tufts lose *sev* protein. Axon projections abnormal.

lozenge	lz^{36}♂ strong allele	Smooth, pink eye surface.	Eye smooth. No lens, no cone cell cup. Masses of pigment granules. Pigment cell architecture missing. Rhabdomeres face outwards?	Pattern normal until time of 24B10 expression, then clusters became difficult to identify.
	lz^{K} weak allele	Slightly rough eye.	Irregular facet shapes. Usually 7 rhabdomeres per ommatidium. Pigment cell architecture often incomplete, ragged. Holes in retina.	Looks normal.
Star + *Enhancer of Star*	*S*/In(2L+2R) *Cy, Cy E(S);* *K-pn*	(see *S*) Eye reduced, very rough.	Variable number of rhabdomeres. Size reduced; varying shapes, orientations of rhabdomeres: some fused, some on long stalks. Usually <7 per ommatidium.	Looks approximately normal at furrow, except for subtle *Star* defects. After several rows, shapes become irregular. Antigen 22C10 and *sev* can be lost altogether. Microvillar tuft shape resolution rarely occurs.

	lm/In(2L+2R)*Cy*, *Cy* S^2 dp^{lv2} *E(S)*	Eyes rough, but not as reduced.	Mixture of normal and disarranged ommatidia.	Areas of unusual shapes of sizes, but no antigen fading.
Group IV: Later Occurring Defects				
loboid	*ld*	Very weakly rough.	(not tested)	Pattern normal.
rugose	*rg*	Very rough eye, variable facet shape.	Highly variable number of rhabdomeres per ommatidium. Irregular pigment cell architecture. Masses of pigment. Some facets lack rhabdomeres.	Pattern normal.
roughened eye	*roe* p^p	Eye rough, slightly reduced.	Almost normal. One out of every 10-20 ommatidia has irregular number of rhabdomeres. Rhabdomeres occasionally fused, bifurcated.	Pattern normal. Perhaps rare cases of crowding?

roughoid	*ru*	Eyes rough, somewhat reduced.	Photoreceptors usually normal, except that 1 out of 10-20 has irregular number of rhabdomeres. Pigment cell defects: too many or too few forming boundary between ommatidia.	Pattern normal.

Epilogue

One of the most compelling problems in biology is elucidation of the mechanisms by which a cell assumes its unique identity during development. The *Drosophila* compound eye has been touted as a system in which this problem can be studied in a thorough manner, given its various attributes, primary among these the availability of both classical and molecular genetic techniques. Also, the exquisite precision of the compound eye lends itself well to the identification of mutations that affect its morphology. Study of compound eye development has only begun to reveal its developmental mechanisms. This chapter is not meant to review the data, but rather to discuss what has yet to be done, including areas of research that have been neglected, in order to further our understanding of development of the compound eye.

1. Cells that will form the eye-antennal disc are first set aside in the embryo. These cells actively divide to generate the epithelium. An interesting question yet to be addressed is whether, even at this early stage, development, in the form of controlled proliferation, traverses the epithelium from posterior to anterior. Experimental results in both *Drosophila* and other insects suggest that this may be the case. In organisms in which the eye develops externally on the head epidermis, mitotic figures can be found in a band immediately anterior to an advancing wave of differentiation. The patterns generated by genetic mosaics and by position-effect variegation look as if they could result from waves of proliferation, as well as indicate that the clone of daughter cells expands towards the anterior.

One could test this idea by several methods. Young discs could be pulse-labelled with bromodeoxyuridine or other markers of DNA replication, and examined soon after the pulse to determine if cells are labelled in a band, indicative of a wave, or if the labelled cells are dispersed across the posterior-anterior axis. First instar eye discs are difficult to identify upon dissection, though; examination of clones of eye-color markers generated

by recombination, if generated at precise times during the different instars, could be more indicative of both waves of proliferation and direction of daughter cell migration. Results indicating that proliferation does occur in a wave would be important for models regarding the initiation of differentiation in the posterior of the eye disc (see below).

2. The next question concerns the time at which cells in the eye disc become capable of responding to signals for differentiation. Do cells in the eye disc, as discussed in the introductory chapter, assume a genuine competent state? If so, does this state cross the epithelium as a wave, and does the passage of the wave rely on induction? Results from heterochronic *Drosophila* eye disc transplantations and from invasive experiments on the mosquito eye suggest such questions.

These questions could be investigated using several methods. First, one could examine discs at the ultrastructural level from progressively more mature larvae, to see if cells exhibit morphological changes during mid- to late- second instar. Although not necessarily expected, a positive result would correlate nicely with optic placode formation on the mosquito retinal epithelium. Secondly, in mosquito, transplanted patches of non-prospective retina arrest optic placode formation, and therefore differentiation of the eye, anterior to them. A similar experiment can be performed genetically in *Drosophila*. In the homeotic mutant *cephalotergite* (Schardin, 1983), patches of tergite tissue replace parts of the compound eye. The patches vary considerably in size from fly to fly, and can be identified in the third instar eye disc by a lack of staining with MAbs highlighting neural differentiation of the eye. Even the axons from developing clusters in the eye disc do not pass through this foreign tissue (Leiserson and Benzer, unpubl.). It could prove interesting to determine whether tergite-committed tissue is able to propagate an eye-specific inductive signal. One could examinine differentiation on eye discs from the *cephalotergite* mutant. Presumably, in some cases the patch of tergite would extend across the dorsal-ventral axis of the disc. One could examine such cases closely, to see if retinal

differentiation could occur on the anterior side of such a patch. One would also examine the different patterns of tergite versus retina patches in the adult eye. A consistent lack of differentiation on the anterior side of tergite tissue would suggest that at some stage, an inductive signal passes from cell to cell across the eye disc. Since differentiation *per se* of cells in the eye disc does not appear to require contact with previously differentiating cells, this result would indicate that competence, as in the mosquito, is a state acquired by cells at an earlier stage of development, and that this state is assumed by induction.

Once there is some indication that this event is real, the study of genes that, when mutant, result in a missing or severely reduced compound eye, could lead to molecular explanations of the process. Some mutations with this phenotype are described in Chapter V. The gene products involved in such a phenomenon would be expected to be those required during the mid- to late- second instar; temperature-sensitive alleles would aid in describing the temporal requirements.

3. During the midthird instar, differentiation of the retina is initiated in the posterior of the eye disc. Since the furrow itself does not appear to be causal, the question of how differentiation is initiated remains. The product of the decapentaplegic gene complex (DPP-C) of *Drosophila* is required at different times in development, including in all the imaginal discs during their differentiation (for review, see Gelbart et al., 1985). Molecular characterization of DPP-C (Padgett et al., 1987) has shown similarity between its product and transforming growth factor -β (TGF-β), a factor that can both promote and inhibit cell division (it does not appear to function solely as a mitogen, see Sporn and Roberts, 1988, for review). The eye-specific *blink* allele of DPP-C has a severely reduced eye, a phenotype suggesting that diffusible factors may be required for differentiation in the eye disc. By using a gene fusion between the promoter of the DPP gene and bacterial β-galactosidase, Gelbart and colleagues (R.K. Blackman and W.M. Gelbart, pers. comm.) have shown that in the eye disc, DPP is expressed within the morphogenetic

furrow. Iniatiation of differentiation in the posterior of the eye disc could result from posterior cells' being able to respond to such a factor at an earlier time than more anterior cells.

Other mutations in which the eye does not develop, such as *eyes absent*, could prove useful in defining the pathway involved in initiation of differentiation. It is possible that these gene products, like DPP, serve a more general function. Therefore, study of late larval or pupal lethal loci may be necessary.

4. Once differentiation is initiated, the cells form clusters at the appropriate distance from each other, resulting in a precise and reproducible number of cells. One question concerns whether the control of cluster spacing can be separated from the control of cluster composition.

Genes that function in embryonic neurogenesis in the fly may have a similar function in the developing retina; both *Notch* and *Enhancer of split* have alleles with eye phenotypes, suggesting that their gene products are required. In Chapter V, data concerning the eye disc phenotype of the *split* allele of the *Notch* locus were presented. Preliminary data of Ballinger (D. Ballinger and S. Benzer, pers. comm.) suggest the the *Rough Eye* phenotype can be enhanced by a mutation in *Delta*, another neurogenic locus. The identification of mutations that affect the spacing of clusters in the eye disc, perhaps including *spl* and *Roi*, could allow the elucidation of a mechanism similar to the one controlling neuroblast (NB) versus epidermoblast (EB) number and spacing in the ventral neurectoderm of the embryo. The control of the spacing of clusters could be exerted via neural and non-neural cell type segregation. In this model, a cell which is responsive to a positive factor begins to assume the neural fate. One of the first steps it takes is to express an inhibitor to prevent neighbors within a defined range from assuming the same fate. This cell also begins to express a molecule that negates the effect of the inhibitor but that disperses less readily than the inhibitor. As suggested in Chapter V, the extracellular

matrix may furnish a means of fine-tuning the mobilities of diffusible factors. These overlapping patterns would in effect give an inhibitor concentration profile resembling that shown in Figure 1; the effective distribution of inhibitor would have an approximately sinusoidal distribution, with clusters nucleating about the minima. Below a certain threshold of effective inhibitor concentration, neural cells differentiate; above it, the non-neuronal fate is assumed. In a mutant in which the distribution of, or the susceptibility to, the inhibitor is disturbed, more or fewer clusters could form at the furrow, with variable numbers of cells in them; the adult eye would be roughened. The identification, and the structural and molecular characterization of mutants with rough eyes, such as those discussed in Chapter V, could lead to tests of this hypothesis. If the relevant genes can be cloned and fused to regulatable promoters, one should be able to vary cluster size in a systematic and predictable fashion.

5. Cell-type determination within the ommatidium is an area of intense study. The *sevenless*$^+$ (*sev*$^+$) gene, which functions in the pathway of photoreceptor cell R7 determination, has been discussed at length in this thesis. When the gene is defective, the phenotype is the lack of R7 from every ommatidium of the adult eye. Data described herein as well as those obtained by Hafen, Rubin and co-workers, indicate that the *sev*$^+$ gene product is a membrane-associated receptor expressed in all the potential R7s in the eye disc, perhaps before any cells have differentiated. Its activity, strongly suggested to be that of a protein tyrosine kinase, is required autonomously in presumptive R7. Recessive mutants at the *bride of sevenless* (*boss*) locus also lack R7 in every ommatidium. However, mosaic data suggest that the *boss*$^+$ gene activity is required in R8. In Figure 2, a model for the interaction between the *sev*$^+$ gene product and the *boss*$^+$ gene product is proposed. The *sev*$^+$ receptor protein is expressed on all cells, but the enzyme is not active. One of the steps of R8 differentiation is the expression of the *boss*$^+$ protein, which may activate the tyrosine kinase of *sev*$^+$, thereby promoting differentiation

into an R7 photoreceptor. Several different mechanisms could explain why only the cell in the position of presumptive R7 receives this cue. Either temporal or spatial control of *boss*$^+$ expression could limit its presence to the niche occupied by the presumptive R7. For example, the *boss*$^+$ gene product could be expressed only after all the other cells in the cluster have begun to differentiate, or its expression could be limited to the surface of R8, which contacts the presumptive R7. Equally likely is that *boss*$^+$ is released from R8 into the apical extracellular matrix, that may have structural features which can direct the flow of the gene product in the direction of presumptive R7. Molecular analysis of the *boss*$^+$ gene and gene product are in progress in the laboratory of S.L. Zipursky, and the results should be quite exciting.

6. An interesting question raised by this thesis concerns the role of other protein tyrosine kinases during development of the retina. Both biochemical and immunohistochemical data indicate that other tyrosine kinases are active during differentiation. Although unfortunate for me, the anti-*sev* MAbs cross-react with at least one other protein tyrosine kinase. Perhaps this cross-reaction will allow identification of the corresponding gene(s) after immunopurification. Perhaps more straightforward would be screening a late third instar, eye-antennal disc cDNA library with the 3' region of a *sev*$^+$ cDNA clone at varying stringencies. By using such a probe with extensive homology to protein tyrosine kinases, one should be able to identify other such species expressed in the eye disc. Once such genes have been identified and characterized, it will be interesting to see if lack of function at any one of these loci has as specific a phenotype as *sev*.

The staining pattern of the antiphosphotyrosine polyclonal serum showed a striking apical localization, similar to that of the *sev*$^+$ protein. At the light microscope level, the patterns of wild-type and *sev*^{P1} were similar, suggesting that the activity of another protein tyrosine kinase may be localized apically, perhaps also on the microvilli extending into the extracellular matrix. An antiphosphotyrosine antibody might allow the

identification of substrates in the eye disc, by protein immunoblot analysis. The apical localization of phosphotyrosine staining further implicates the apical microvilli and the extracellular matrix as containing differentiation cues.

7. Lastly, the *sevenless* characterization project revealed that the gene product is also expressed in the optic lobes at a time when photoreceptor axons are innervating them, and in the adult brain, and possibly in the ventral ganglion in the adult body. Its ultrastructural localization and its function have yet to be determined. Non-cross-reacting anti-sev^{+} antibodies will be useful for determining its localization. Further characterization of the *Photophobe* mutant, which exhibits allele-specific interactions with *sev*, may reveal the functional requirements of sev^{+} in the adult brain. Morphologic characterization of the *sev* mutant brain, as well as detailed behavioral analysis on *sev* mutants, such as activity, life-span, learning, optomotor response, taste and smell perception, and biological rhythm, may further clarify its function.

In conclusion, it is hoped that this thesis will contribute to future investigations and models in developmental neurobiology. In some ways it is difficult to stop, now that the most exciting work can be done; in other ways, it is not difficult at all.

The End

Figure Legends

Figure 1. A gradient of effective inhibitor concentration could affect cluster spacing as well as cell number and identity per cluster.

(A) In the wild-type eye disc at the morphogenetic furrow, there could exist a gradient of effective concentration of an inhibitor (see text). Below a certain threshold, neurons (photoreceptors) will differentiate, while above it, non-neural cell types (cone cells, pigment cells) will differentiate. The cell at the minimum differentiates into a neuron first, and will become R8. A similar pattern of inhibitor expression could control the spacing of the nascent clusters, as well as the ratio of neurons to non-neurons in each cluster.

(B) In a mutant in which the gradient is disturbed, both the spacing and composition of the clusters would be abnormal.

A. Wild-Type

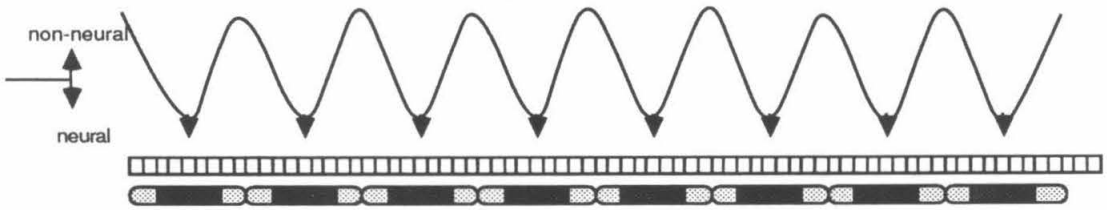

B. mutant (rough adult eye)

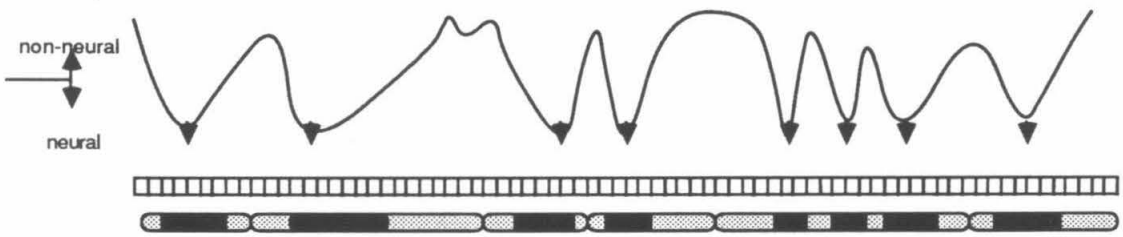

□ undifferentiated cells at the morphogenetic furrow

▼ nucleation site of cluster

presumptive neural cells in a cluster

presumptive non-neural cells in a cluster

Figure 2. The *boss*$^+$ protein could interact directly with the *sevenless*$^+$ protein. In this model, all cells in the differentiating epithelium express the *sevenless*$^+$ protein. A cell assuming the R8 fate begins to express the *boss*$^+$ protein. Somehow (see text), *boss*$^+$ activity is directed towards a cell in the position of presumptive R7. Interaction between the two proteins results in activation of the *sev*$^+$ kinase, which in turn directs a cell down the R7 pathway.

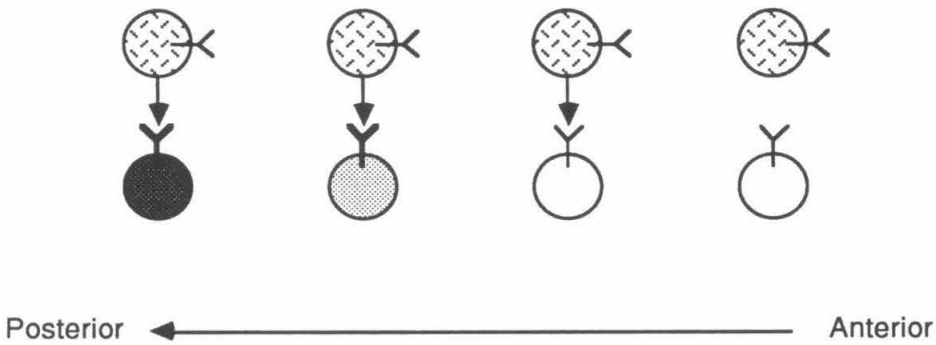
Posterior
Anterior

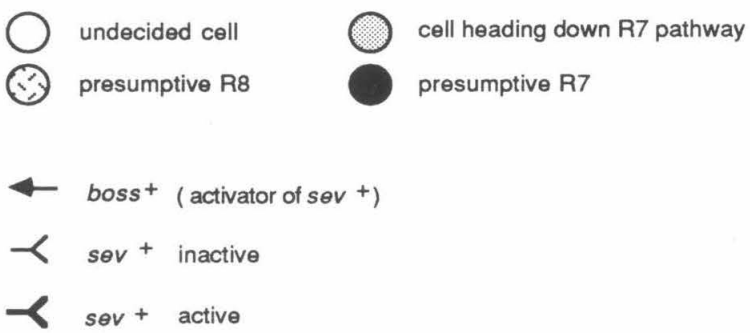
undecided cell
cell heading down R7 pathway
presumptive R8
presumptive R7
boss+ (activator of sev +)
sev + inactive
sev + active

References

Adler, R., Jerdan, J. and Hewitt, A. T. (1985). Responses of cultured neural retinal cells to substratum-bound laminin and other extracellular matrix molecules. *Dev. Biol.* **112**, 110-114.

Baker, W.K. (1978). A clonal analysis reveals early developmental restrictions in the *Drosophila* head. *Dev. Biol.* **62**, 447-463.

Baker, W.K., Marcey, D.J., and McElwain, M.C. (1985). On the development of ectopic eyes in *Drosophila melanogaster* produced by the mutation *extra eye* (*ee*). *Genetics* **111**, 67-88.

Ballinger, D.B. and Benzer, S. (1988). *Photophobe* (*Ppb*), a *Drosophila* mutant with a reversed sign of phototaxis; the mutation shows an allele-specific interaction with *sevenless*. *P.N.A.S. USA* **85**, 3960-3964.

Banerjee, U. Renfranz, P.J., Pollock, J.A., and Benzer, S. (1987a). Molecular characterization of *sevenless*, a gene involved in neuronal pattern formation in the *Drosophila* eye. *Cell* **49**, 281-291.

Banerjee, U., Renfranz, P.J., Hinton, D.R., Rabin, B.A., and Benzer, S. (1987b) The *sevenless*$^+$ protein is expressed apically in cell membranes of developing *Drosophila* retina; it is not restricted to cell R7. *Cell* **51**, 151-158.

Barbacid, M. (1987). *ras* genes. *Ann. Rev. Biochem.* **56**, 779-827.

Basler, K. and Hafen, E. (1988). Control of photoreceptor cell fate by the *sevenless*

protein requires a functional tyrosine kinase domain. *Cell* **54**, 299-311.

Bautch, V.L., Toda, S., Hassell, J.A., and Hanahan, D. (1987). Endothelial cell tumors develop in transgenic mice carrying polyoma virus middle T oncogene. *Cell* **51**, 529-538.

Bingham, P.M., Kidwell, M.G., and Rubin, G.M. (1982). The molecular basis of P-M hybrid dysgenesis: The role of the P element, a P-strain-specific transposon family. *Cell* **29**, 995-1004.

Bishop, J.G. III and Corces, V.G. (1988). Expression of an activated *ras* gene causes developmental abnormalities in transgenic *Drosophila melanogaster*. *Genes and Dev.* **2**, 567-577.

Blumberg, B., MacKrell, A. J., Olson, P. F., Kurkinen, M., Monson, J. M., Natzle, J. E. and Fessler, J. H. (1987). Basement membrane procollagen IV and its specialized carboxyl domain are conserved in *Drosophila*, mouse, and human. *J. Biol. Chem.* **262**, 5947-5950.

Bodenstein, D. (1939). Investigations on the problem of metamorphosis. V. Some factors determining the facet number in the *Drosophila* mutant *Bar*. *Genetics* **24**, 494-508.

Bodenstein, D. (1943). Hormones and tissue competence in the development of *Drosophila*. *Biol. Bull.* **84**, 34-59.

Bodenstein, D. (1962). Humoral conditions and cellular interactions in the development of the insect eye. In Insect Physiology. (Oregon State University Press: Corvallis).

Bolwig, N. (1946). Sense and sense organs of the anterior end of the house fly larvae. *Vidensk. Medd. fra Dansk naturh. Foren. Bd.* **109**, 80-212.

Bowtell, D.D.L., Simon, M.A., and Rubin, G.M. (1988). Nucleotide sequence and structure of the *sevenless* gene of *Drosophila melanogaster*. *Genes and Dev.* **2**, 620-634.

Braitenberg, V. (1967). Patterns of projection in the visual system of the fly. I. Retina-lamina projections. *Exp. Brain Res.* **3**, 271-298.

Campos-Ortega, J.A. (1988). Cellular interactions during early neurogenesis of *Drosophila melanogaster*. *Trends Neurosci.* **11**, 400-405.

Campos-Ortega, J.A. and Gateff, E.A. (1976). The development of ommatidial patterning in metamorphosed eye imaginal disc implants of *Drosophila melangaster*. *Roux's Arch. Dev. Biol.* **179**, 373-392.

Campos-Ortega, J.A. and Hofbauer, A. (1977). Cell clones and pattern formation: On the lineage of photoreceptor cells in the compound eye of *Drosophila*. *Roux's Arch. Dev. Biol.* **181**, 227-245.

Campos-Ortega, J.A., Jurgens, G., and Hofbauer, A. (1979). Cell clones and pattern formation: studies on *sevenless*, a mutant of *Drosophila melanogaster*. *Roux's Arch. Dev. Biol.* **186**, 27-50.

Cooper, J.A. and Hunter, T. (1982). Discrete primary locations of a tyrosine protein kinase and of three proteins that contain phosphotyrosine in virally transformed chick

fibroblasts. *J. Cell Biol.* **94**, 287-296.

Cowan, W.M., Fawcett, J.W., O'Leary, D.D.M., and Stanfield, B.B. (1984). Regressive events in neurogenesis. *Science* **225**, 1258-1265.

Cowman, A.F., Zuker, C.S., Rubin, G.M. (1986). An opsin gene expressed in only one photoreceptor cell type of the *Drosophila* eye. *Cell* **44**, 705-710.

Desplan, C., Theis, J., and O'Farrell, P.H. (1985). The *Drosophila* developmental gene, *engrailed*, encodes a sequence-specific DNA binding activity. *Nature* **318**, 630-635.

DiCicco-Bloom, E. and Black, I.B. (1988). Insulin growth factors regulate the mitotic cycle in cultured rat sympathetic neuroblasts. *Proc. Natl. Acad. Sci. USA* **85**, 4066-4070.

Doe, C.Q. and Goodman, C.S. (1985a). Early events in insect neurogenesis. I. Development and segmental differences in the pattern of neuronal precursor cells. *Dev. Biol.* **111**, 193-205.

Doe, C.Q. and Goodman, C.S. (1985b). Early events in insect neurogenesis. II. The role of cell interactions and cell lineage in the determination of neuronal precursor cells. *Dev. Biol.* **111**, 206-219.

Ebina, Y., Ellis, L., Jarnagin, K., Edery, M., Graf, L. et al. (1985). The human insulin receptor cDNA: the structural basis for hormone-activated transmembrane signalling. *Cell* **40**, 747-758.

Eisen, J.S. and Youssef, N.N. (1980). Fine structural aspects of the developing compound eye of the honey bee, *Apis melliifera L.*. *J. Ultra. Res.* **71**, 79-94.

Engels, W.R. and Preston, C.R. (1979). Hybrid dysgenesis in *Drosophila melanogaster*: the biology of female and male sterility. *Genetics* **92**, 161-174.

Eugene, O., Yund, M.A., and Fristrom, F.W. (1979). Preparative isolation and short-term organ culture of imaginal discs of *Drosophila melangaster*. *Tissue Culture Association Manual* **5**, 1055-1062.

Fischbach, K.F. (1983). Neural cell types surviving congenital sensory deprivation in the optic lobes of *Drosophila melanogaster*. *Dev. Biol.* **95**, 1-18.

Fischbach, K.-F. and Technau, G. (1984). Cell degeneration in the developing optic lobes of the *sine oculis* and *small-optic-lobes* mutants of *Drosophila melanogaster*. *Dev. Biol.* **104**, 219-239.

Franceschini, N. and Kirschfeld, K. (1971a). *In vivo* optical study of photoreceptor elements in the compound eye of *Drosophila*. *Kybernetik.* **8**, 1-13.

Franceschini, N. and Kirschfeld, K. (1971b). Pseudopupil phenomena in the compound eye of *Drosophila*. *Kybernetik.* **9**, 159-182.

Fristrom, D. (1969). Cellular degeneration in the production of some mutant phenotypes in *Drosophila melanogaster*. *Molec. Gen. Genetics* **103**, 363-379.

Fryxell, K.J. and Meyerowitz, E.M. (1987). An opsin gene that is expressed only in the

R7 photoreceptor cell of *Drosophila*. *EMBO* **6**, 443-451.

Fujita, S.C., Zipursky, S.L., Benzer, S., Ferrus, A., and Shotwell, S.L. (1982). Monoclonal antibodies against the *Drosophila* nervous system. *Proc. Natl. Acad. Sci. USA*. **79**, 7929-7933.

Fults, D. W., Towle, A. C., Lauder, J. M. and Maness, P. F. (1985). $pp60^{c\text{-}src}$ in the developing cerebellum. *Mol. Cell. Biol.* **5**, 27-32.

Gall, J. G. and Pardue, M. L., (1971). Nucleic acid hybridization in cytological preparation. *Meth. Enzymol.* **21**, 470-480.

Garcia-Bellido, A. and Merriam, J.R. (1969). Cell lineage of the imaginal discs in *Drosophila* gynandromorphs. *J. Expt. Zool.* **170**, 61-76.

Garcia-Bellido, A. and Merriam, J.R. (1971). Genetic analysis of cell heredity in imaginal discs of *Drosophila melanogaster*. *Proc. Natl. Acad. Sci. USA* **68**, 2222-2226.

Gateff, E. and Schneiderman, H.A. (1975). Developmental capacities of immature eye-antennal imaginal discs of *Drosophila melanogaster*. *Roux's Arch. EntwMech. Org.* **176**, 171-189.

Gelbart, W.M., Irish, V.F., St. Johnston, R.D., Hoffman, F.M., Blackman, R.K., Segal, D., Posakony, L.M., and Grimaila, R. (1985). The decapentaplegic gene complex in *Drosophila melanogaster*. *CSH Sym. Quant. Biol.* **L**, 119-125.

Gerresheim, F. (1981). Isolation and characterization of mutants with altered phototactic

reaction to monochromatic light in *Drosophila melanogaster*. Ph.D. thesis, Munich University, Munich, Federal Republic of Germany.

Green, S. and Lawrence, P.A. (1975). Recruitment of epidermal cells by the developing eye of *Oncopeltus* (Hemiptera). *Roux's Arch. Dev. Biol.* **177**, 61-65.

Greenberg, M. E., Brackenbury, R. and Edelman, G. M. (1984). Changes in the distribution of the 34-Kdalton tyrosine kinase substrate during differentiation and maturation of chicken tissues. *J. Cell Biol.* **98**, 473-486.

Greenwald, I. (1985). *lin-12*, A nematode homeotic gene, is homologous to a set of mammalian proteins that includes epidermal growth factor. *Cell* **43**, 583-590.

Greenwald, I., Sternberg, P.W., and Horvitz, H.R. (1983). The *lin-12* locus specifies cell fates in *Caenorhabditis elegans*. *Cell* **34**, 435-444.

Grumet, M., Hoffman, S., Crossin, K. L. and Edelman, G. M. (1985). Cytotactin, an extracellular matrix protein of neural and non-neural tissues that mediates glia-neuron interaction. *Proc. Natl. Acad. Sci. USA* **82**, 8075-8079.

Hafen, E., Basler, K., Edstroem, J.-E., and Rubin, G.M. (1987). *sevenless*, a cell-specific homoetic gene of *Drosophila*, encodes a putative transmembrane receptor with a tyrosine kinase domain. *Science* **236**, 55-63.

Hafen, E., Levine, M., Garber, R.L., and Gehring, W.J. (1983). An improved *in situ* hybridization method for the detection of cellular RNA's in *Drosophila* tissue sections and its application for localizing transcripts of the homeotic Antennapedia gene complex.

EMBO J. **2**, 617-623.

Hanley, M.R. (1988). Proto-oncogenes in the nervous system. *Neuron* **1**, 175-182.

Harris, W.A., Stark, W.S., and Walker, J.A. (1976). Genetic dissection of the photoreceptor system in the compound eye of *Drosophila melanogaster*. *J. Physiol.* **256**, 415-439.

Harte, P.J. and Kankel, D.R. (1982). Genetic analysis of mutations at the *glued* locus and interacting loci in *Drosophila melanogaster*. *Genetics* **101**, 477-501.

Hartley, D.A., Xu, T., and Artavonis-Tsakonas, S. (1987). The embryonic expression of the *Notch* locus of *Drosophila melanogaster* and the implications of point mutations in the extracellular EGF-like domain of the predicted protein. *EMBO J.* **6**, 3407-3417.

Hazelrigg, T., Levis, R., and Rubin, G.M. (1984). Transformation of *white* locus DNA in *Drosophila*: Dosage compensation, *zeste* interactions, and position effects. *Cell* **36**, 469-481.

Heisenberg, M. and Buchner, E. (1977). The role of retinula cell types in visual behavior of *Drosophila melanogaster*. *J. Comp. Physiol.* **117**, 127-162.

Henkemeyer, M.J., Bennett, R.L., Gertler, F.B., and Hoffman, F.M. (1988). DNA sequence, structure, and tyrosine kinase activity of the *Drosophila melanogaster* Abelson proto-oncogene homolog. *Mol. Cell. Biol.* **8**, 843-853.

Hinke, W. (1961). Das relative postembryonale Wachstum der Hirnteile von *Culex*

pipiens, Drosophila melanogaster und *Drosophila*-Mutanten. *Z. Morph. und Ökol. der Tiere* **50**, 81-118.

Holt, C.E., Bertsch, T.W., Ellis, H.M., and Harris, W.A. (1988). Cellular determination in the *Xenopus* retina is independent of lineage and birth date. *Neuron* **1**, 15-26.

Honegger, A.M., Dull, T.J., Felder, S., Van Obberghen, E., Bellot, F., Szapary, D., Schmidt, A., Ullrich, A., and Schlessinger, J. (1987). Point mutation at the ATP binding site of EGF receptor abolishes protein-tyrosine kinase activity and alters cellular routing. *Cell* **51**, 199-209.

Hyde, C.A.T. (1972). Regeneration, post-embryonic induction and cellular interaction in the eye of *Periplaneta americana. J. Embryol. Exp. Morph.* **27**, 367-369.

Ingham, P.W. (1988). The molecular genetics of embryonic pattern formation in *Drosophila. Nature* **335**, 25-34.

Itoh, N., Slemmon, J.R., Hawke, D.H., Williamson, R., Morita, E., Itakura, K., Roberts, E., Shively, J.E., Crawford, G.D., and Salvaterra, P.M. (1986). Cloning of *Drosophila melanogaster* choline acetyltransferase complementary DNA. *Proc. Natl. Acad. Sci. USA.* **83**, 4081- 4085.

Kankel, D.R., Ferrús, A., Garen, S.H., Harte, P.J., and Lewis, P.E. (1980). The structure and development of the nervous system. In The Genetics and Biology of *Drosophila*. Vol. 2d. Ashburner, M. and Wright, T.R.F., eds. (Academic Press: London), pp. 295-368.

Kidd, S., Kelley, M.R., and Young, M. (1986). Sequence of the *Notch* locus of *Drosophila melanogaster*: relationship of the encoded protein to mammalian clotting and growth factors. *Mol. Cell Biol.* **6**, 3094-3108.

Kimble, J., Sulston, J., and White, J. (1979). In Cell Lineages, Stem Cells and Differentiation LeDuoarin, N., ed. (Elsevier: Amsterdam), pp. 59-68.

Kipreos, E.T., Lee, G.J., and Wang, J.Y.J. (1987). Isolation of temperature- sensitive tyrosine kinase mutants of v-*abl* oncogene by screening with antibodies for phosphotyrosine. *P.N.A.S. USA* **84**, 1345-1349.

Kornberg, A. (1980). In DNA Replication. (W.H. Freeman and Co.: San Francisco).

Kornberg, T., Siden, I., O'Farrell, P., and Simon, M. (1985). The engrailed locus of *Drosophila*: *in situ* localization of transcripts reveals compartment-specific expression. *Cell* **40**, 45-53.

Laemmli, U.K. (1970). Cleavage of structural proteins during the assembly of the head of bacteriophage T4. *Nature* **227**, 680-685.

Lawrence, J. B. and Singer, R. H. (1986). Intracellular localization of messenger RNAs for cytoskeletal proteins. *Cell* **45**, 407-415.

Lawrence, P.A. and Green, S.M. (1979). Cell lineage in the developing retina of *Drosophila*. *Dev. Biol.* **71**, 142-152.

Lebovitz, R.M. and Ready, D.F. (1986). Ommatidial development in *Drosophila* eye disc fragments. *Dev. Biol.* **117**, 663-671.

Levis, R., Hazelrigg, T., and Rubin, G.M. (1985). Effects of genomic position on the expression of transduced copies of the *white* gene of *Drosophila. Science* **229**, 558-561.

Levy, L.S. and Manning, J.E. (1981). Messenger RNA sequence complexity and homology in developmental stages of *Drosophila. Dev. Biol.* **85**, 141-149.

Lewis, E. B. and Bacher, F. (1968). Method of feeding ethyl methane sulfonate to *Drosophila* males. *Dros. Inf. Serv.* **43**, 193-194.

Lindsley, D.L. and Grell, E.H. (1967). Genetic variations of *Drosophila melanogaster.* Carnegie Inst. of Wash. Publication No. 627.

Maniatis, T., Fritsch, E.F., and Sambrook, J. (1982). Molecular Cloning: A Laboratory Manual (Cold Spring Harbor Laboratory: Cold Spring Harbor).

Marcey, D.J. and Stark, W.S. (1985). The morphology, physiology, and neural projections of supernumerary compound eyes in *Drosophila melanogaster. Dev. Biol.* **107**, 180-197.

Meinertzhagen, I.A. (1973). Development of the compound eye and optic lobes of insects. In Developmental Neurobiology of Arthropods. Young, D., ed. (Cambridge University Press: Cambridge), pp. 51-104.

Melamed, J. and Trujillo-Cenóz, O. (1975) The fine structure of the eye imaginal discs in

muscoid flies. *J. Ultra. Res.* **51**, 79-93.

Melton, D.A. (1987). Translocation of a localized maternal mRNA to the vegetal pole of *Xenopus* oocytes. *Nature* **328**, 80-82.

Meyerowitz, E. M. and Kankel, D.R. (1978). A genetic analysis of visual system development in *Drosophila melanogaster*. *Dev. Biol.* **62**, 112-142.

Mitchell, H.K. and Petersen, N.S. (1982). Developmental abnormalities in *Drosophila* induced by heat shock. *Dev. Gen.* **3**, 91-102.

Montell, C. and Rubin, G.M. (1988). The *Drosophila ninaC* locus encodes two photoreceptor cell specific proteins with domains homologous to protein kinases and the mysoin heavy chain head. *Cell* **52**, 757-772.

Montell, C., Jones, K., Hafen, E., and Rubin, G.M. (1985). Rescue of the *Drosophila* phototransduction mutation *trp* by germline transformation. *Science* **230**, 1040-1043.

Montell, C., Jones, K., Zuker, C.S., and Rubin, G.M. (1987). A second opsin gene expressed in the ultraviolet sensitive R7 photoreceptor cells of *Drosophila melanogaster*. *J. Neurosci.* **7**, 1558-1566.

Morata, G. and Lawrence, P.A. (1979). Development of the eye-antennal imaginal disc of *Drosophila*. *Dev. Biol.* **70**, 355-371.

Morrison, R.S., Kornblum, H.I., Leslie, F.M., and Bradshaw, R.A. (1987). Trophic stimulation of cultured neurons from neonatal rat brain by epidermal growth factor.

Science **238**, 72-75.

Moscoso del Prado, J. and Garcia-Bellido, A. (1984). Cell interactions in the generation of chaetae pattern in *Drosophila*. *Roux's Arch. Dev. Biol.* **193**, 246-251.

Muller, J.H. (1947). The gene. *Proc. Roy. Soc. B* **134**, 1-37.

Nardi, J.B. (1977). The construction of the insect compound eye: the involvement of cell displacement and cell surface properties in the positioning of cells. *Dev. Biol.* **61**, 287-298.

Nowell, M.S. (1981). Postembryonic growth of the compound eye of the cockroach. *J. Embryol. Exp. Morph.* **62**, 259-275.

Nowell, M.S. and Shelton, P.M.J. (1980). The eye margin and compound-eye development in the cockroach: Evidence against recruitment. *J. Embryol. Expt. Morph.* **60**, 329-343.

O'Tousa, J.E., Baehr, E.W., Martin, R.L., Hirsh, J., Pak, W.L., and Applebury, M.L. (1985). The *Drosophila ninaE* gene encodes an opsin. *Cell* **40**, 839-850.

Padgett, R.W., St. Johnston, R.D., and Gelbart, W.M. (1987). A transcript from a *Drosophila* pattern gene predicts a protein homologous to the transforming growth factor-β family. *Nature* **325**, 81-84.

Palazzolo, M.J. and Meyerowitz, E.M. (1987). SWAJ: A family of lambda phage cDNA cloning vectors that allows the amplification of RNA sequences. *Gene* **XX**; 111-111.

Perry, M.M (1968). Further studies on the development of the eye of *Drosophila melanogaster*. I. The ommatidium. *J. Morph.* **124**, 227-248.

Pilkington, R.W. (1941). Facet mutants of *Drosophila*. *Zool. Soc. London Proc. Sec. A.* **111**, 199-222.

Piovant, M. and Léna, P. (1988). Membrane glycoproteins immunologically related to the human insulin receptor are associated with presumptive neuronal territories and developing neurones in *Drosophila melanogaster*. *Development* **103**, 145-156.

Poodry, C.A., Hall, L., and Suzuki, D.T. (1973). Developmental properties of *shibire*. A pleiotropic mutation affecting larval and adult locomotion and development. *Dev. Biol.* **32**, 373-386.

Ready, D.F., Hanson, T.E., and Benzer, S. (1976). Development of the *Drosophila* retina, a neurocrystalline lattice. *Dev. Biol.* **53**, 217-240.

Ready, D. F, Tomlinson, A., and Lebovitz, R. M. (1986). Building an ommatidium: Geometry and genes. In Cell and Developmental Biology of the Eye. Hilfer, S. R. and Sheffield, J. B., eds. (Springer-Verlag: New York), pp. 97-125.

Reinke, R. and Zipursky, S.L. (1988). Cell-cell interaction in the *Drosophila* retina: The *bride of sevenless* gene is required in photoreceptor cell R8 for R7 development. *Cell* **55**, 321-330.

Reinke, R., Krantz, D.E., Yen, D., and Zipursky, S.L. (1988). *chaoptin*, a cell surface

glycoprotein required for *Drosophila* photoreceptor cell morphogenesis, contains a repeat motif found in yeast and human. *Cell* **52**, 291-301.

Rubin, G.M., Kidwell, M.G., and Bingham, P.M. (1982). The molecular basis of P-M hybrid dysgenesis: The nature of induced mutations. *Cell* **29**, 987-994.

Saint, R., Kalionis, B., Lockett, T.J., and Elizur, A. (1988). Pattern formation in the developing eye of *Drosophiila melanogaster* is regulated by the homeo box gene, *rough*. Nature, in press.

Schardin, M. (1983). *Cephalotergite*: An unusual mutant in the Bithorax gene complex. *Cal. Inst. Tech. Biology Ann. Report* Abstract No. 216, 170-171.

Shelton, P.M.J. and Lawrence, P.A. (1974). Structure and development of ommatidia in *Oncopeltus fasciatus*. *J. Embryol. Exp. Morph.* **32**, 337-353.

Simon, M.A., Drees, B., Kornberg, T., and Bishop, J.M. (1985). The nucleotide sequence and the tissue-specific expression of *Drosophila* c-*src*. *Cell* **42**, 831-840.

Sorge, L. K., Levy, B. T. and Maness, P. F. (1984). $pp60^{c\text{-}src}$ is developmentally regulated in the neural retina. *Cell* **36**, 249-257.

Sporn, M.B. and Roberts, A.B. (1988). Peptide growth factors are multifunctional. *Nature* **332**, 217-219.

Spreij, T.E. (1971). Cell death during the development of the imaginal discs of *Calliphora erythrocephala*. *Netherlands J. Zool.* **21**, 221-264.

Steinberg, A.G. (1943). The development of the wild type and *Bar* eyes of *Drosophila melanogaster*. *Can. J. Res.* **21**, 277-283.

Steller, H., Fischbach, K.-F., and Rubin, G.M. (1987). *disconnected*: A locus required for neuronal pathway formation in the visual system of *Drosophila*. *Cell* **50**, 1139-1153.

Sternberg, P.W. (1988a). Control of cell fates within equivalence groups in *C. elegans*. *Trends Neurosci.* **11**, 259-264.

Sternberg, P.W. (1988b). Lateral inhibition during vulval induction in *Caenorhabditis elegans*. *Nature* **335**, 551-554.

Sternberg, P.W. and Horvitz, H.R. (1984). The genetic control of cell lineage during nematode development. *Ann. Rev. Genet.* **18**, 489-524.

Sternberg, P.W. and Horvitz, H.R. (1986). Pattern formation during vulval development in *C. elegans*. *Cell* **44**, 761-772.

Strausfeld, N.J. (1976). Atlas of an Insect Brain. (Springer-Verlag: Heidelberg).

Stryer, L. (1986). Cyclic GMP cascade of vision. *Ann. Rev. Neurosci.* **9**, 87-119.

Sturtevant, A.H. (1927). The effects of the *Bar* gene of *Drosophila* in mosaic eyes. *J. Expt. Zool.* **46**, 493-498.

Sulston, J. and Horvitz, R. (1977). Postembryonic cell lineages of the nematode

Caenorhabditis elegans. *Dev. Biol.* **56**, 110-156.

Sved, J. (1986). *eyes absent*. *Dros. Inf. Serv.* **63**, 169.

Swaroop, A., Sun, J.W., Paco-Larson, M.L., and Garen, A. (1986). Molecular organization and expression of the genetic locus *glued* in *Drosophila melanogaster*. *Mol. Cell. Biol.* **6**, 833-841.

Swaroop, A., Swaroop, M., and Garen, A. (1987). Sequence analysis of the complete cDNA and encoded polypeptide for the *Glued* gene of *Drosophila melanogaster*. *Proc. Natl. Acad. Sci. USA* **84**, 6501-6505.

Taghert, P.H., Doe, C.Q., and Goodman, C.S. (1984). Cell determination and regulation during development of neuroblasts and neurones in grasshopper embryo. *Nature* **307**, 163-165.

Tomlinson, A. (1985). The cellular dynamics of pattern formation in the eye of *Drosophila*. *J. Embryol. Exp. Morphol.* **89**, 313-331.

Tomlinson, A., Bowtell, D.D.L., Hafen, E., and Rubin, G.M. (1987). Localization of the *sevenless* protein, a putative receptor for positional information, in the eye imaginal disc of *Drosophila*. *Cell* **51**, 143-150.

Tomlinson, A. and Ready, D.F. (1986). *sevenless*, a cell- specific homeotic mutation of the *Drosophila* eye. *Science* **231**, 400-402.

Tomlinson, A. and Ready, D. F. (1987a). Neuronal differentiation in the *Drosophila*

ommatidium. *Dev. Biol.* **120**, 366-376.

Tomlinson, A. and Ready, D.F. (1987b). Cell fate in the *Drosophila* ommatidium. *Dev. Biol.* **123**, 264-275.

Tomlinson, A., Kimmel, B.E., and Rubin, G.M. (1988). *rough*, a *Drosophila* homeobox gene required in photoreceptors R2 and R5 for inductive interactions in the developing eye. *Cell* **55**, 771-784.

Trujillo-Cenóz, O. and Bernard, G.D. (1972). Some aspects of the retinal organization of *Sympycnus lineatus* Loew (Diptera, Dolidiopodidae). *J. Ultra. Res.* **38**, 149-160.

Trujillo-Cenóz, O. and Melamed, J. (1973). The development of the retina-lamina complex in muscoid flies. *J. Ultra. Res.* **42**, 554-581.

Turner, D.L. and Cepko. C.L. (1987). A common progenitor for neurons and glia persists in rat retina late in development. *Nature* **328**, 131-136.

Ullrich, A., Bell, J.R., Chen, E.Y., Herrera, R., Petruzzelli, L.M., Dull, T.J., Gray, A., Coussens, L., Liao, Y.C., Tsubokawa, M., et al., (1985). Human insulin receptor and its reletionship to the tyrosine kinase family of oncogenes. *Nature* **313**, 756-761.

Van Vactor, D. Jr., Krantz, D.E., Reinke, R.L., and Zipursky, S.L. (1988). Analysis of mutants in *chaoptin*, a photoreceptor cell-specific glycoprotein in *Drosophila*, reveals its role in cellular morphogenesis. *Cell* **52**, 281-290.

Vässin, H., Vielmetter, J., and Campos-Ortega, J.A. (1985). Genetic interactions in early

neurogenesis of *Drosophila malnogaster*. *J. Neurogen.* **2**, 291-308.

Venkatesh, T.R., Zipursky, S.L., and Benzer, S., (1985). Molecular analysis of the development of the compound eye in *Drosophila*. *Trends Neurosci.* **8**, 251-257.

Waddington, C.H. and Perry, M.M (1960). The ultra-structure of the developing eye of *Drosophila*. *Proc. Roy. Soc. B.* **153**, 155-178.

Walicke, P.A. (1988). Basic and acidic fibroblast growth factors have trophic effects on neurons from multiple CNS regions. *J. Neurosci.* **8**, 2618-2627.

Wang, J.Y.J. and Baltimore, D. (1983). Characterization of the Abelson murine leukemia virus- encoded tyrosine-specific protein kinase. *Meth. Enzymol.* **99**, 373-378.

Wang, J.Y.J. and Baltimore, D. (1985). Localization of tyrosine kinase-coding region in v-*abl* oncogene by the expression of v-*abl*-encoded proteins in bacteria. *J. Biol. Chem.* **260**, 64-71.

Wang, J.Y.J., Queen, C., and Baltimore, D. (1982). Expression of an Abelson murine leukemia virus-encoded protein in *Escherichia coli* causes extensive phosphorylation of tyrosine residues. *J. Biol. Chem.* **257**, 13181-13184.

Wetts, R. and Fraser, S.E. (1988). Multipotent precursors can give rise to all major cell types of the frog retina. *Science* **239**, 1142-1145.

Wharton, K.A., Johansen, K.M., Xu, T., and Artavanis-Tsakonas, S. (1985). Nucleotide sequence from the neurogenic locus *Notch* implies a gene product that shares

homology with proteins containing EGF-like repeats. *Cell* **43**, 567-581.

White, R.H. (1961). Analysis of the development of the compound eye in the mosquito, *Aedes aegypti*. *J. Expt. Zool.* **148**, 223-239.

White, R.H. (1963) Evidence for the existence of a differentiation center in the developing eye of the mosquito. *J. Expt. Zool.* **152**, 139-148.

Wigglesworth, V.B. (1940). Local and general factors in the development of "pattern" in *Rhodnius prolixus* (Hemiptera). *J. Expt. Biol.* **17**, 180-200.

Wilcox, M., Mitchison, G.J., and R.J. Smith (1973). Pattern formation in the blue-green alga, *Anabaena*. I. Basic mechanisms. *J. Cell Sci.* **12**, 707-723.

Yarden, Y. and Ullrich, A. (1988). Growth factor receptor tyrosine kinases. *Ann. Rev. Biochem.* **57**, 443-478.

Yochem, J., Weston, K., and Greenwald, I. (1988). The *Caenorhabditis elegans lin-12* gene encodes a transmembrane protein with overall similarity to *Drosophila Notch*. *Nature* **335**, 547-550.

Young, R.A. and Davis, R.W. (1983). Efficient isolation of genes by using antibody probes. *Proc. Natl. Acad. Sci. USA* **80**, 1194-1198.

Zhimulev, I.F., Pokholkova, G.V., Bgatov, A.V., Semeshin, V.F., and Belayaeva, E.S. (1981). Fine cytogenetical analysis of the band 10A1-2 and the adjoining regions in the *Drosophila melanogaster* X chromosome. *Chromosoma* **82**, 25-40.

Zipursky, S.L., Venkatesh, T.R., and Benzer, S. (1985). From monoclonal antibody to gene for a neuron-specific glycoprotein in *Drosophila*. *Proc. Natl. Acad. Sci. USA* **82**, 1855-1859.

Zipursky, S.L., Venkatesh, T.R., Teplow, D.B., and Benzer, S. (1984). Neuronal development in the *Drosophila* retina: monoclonal antibodies as molecular probes. *Cell* **36**, 15-26.

Zipursky, S.L., Venkatesh, T.R., and Benzer, S. (1985). From monoclonal antibody to gene for a neuron-specific glycoprotein in *Drosophila*. *Proc. Natl. Acad. Sci. USA* **82**, 1855-1859.

Zuker, C.S., Cowman, A.F. and Rubin, G.M. (1985). Isolation and structure of a rhodopsin gene from *D. melanogaster*. *Cell* **40**, 851- 858.

Zuker, C.S., Montell, C., Jones, K.R., Laverty, T. and Rubin, G.M. (1987). A rhodopsin gene expressed in photoreceptor cell R7 of the *Drosophila* eye: homologies with other signal transducing molecules. *J. Neurosci.* **7**, 1550-1557.